Protrusion-retraction switches and traction forces in spontaneous cell polarization

THÈSE N^{O} 7006 (2016)

PRÉSENTÉE LE 29 AVRIL 2016

À LA FACULTÉ DES SCIENCES DE BASE
LABORATOIRE DE BIOPHYSIQUE CELLULAIRE
PROGRAMME DOCTORAL EN BIOTECHNOLOGIE ET GÉNIE BIOLOGIQUE

ÉCOLE POLYTECHNIQUE FÉDÉRALE DE LAUSANNE

POUR L'OBTENTION DU GRADE DE DOCTEUR ÈS SCIENCES

PAR

Alicia Carine BORNERT

acceptée sur proposition du jury:

Prof. F. G. van der Goot Grunberg, présidente du jury
Dr A. Verkhovskiy, directeur de thèse
Dr A. Asnacios, rapporteur
Prof. B. Wehrle-Haller, rapporteur
Prof. A. Radenovic, rapporteuse

ÉCOLE POLYTECHNIQUE
FÉDÉRALE DE LAUSANNE

Suisse
2016

Remerciements

Je tiens avant tout à remercier ma famille pour leur soutien inconditionnel, leur confiance et leurs encouragements durant toutes mes années d'étude et de thèse. Je remercie également mes ami(e)s qui ont toujours été là pour moi durant toutes ces années, et ce malgré la distance qui nous sépare.

Je voudrais ensuite remercier mon directeur de thèse, Sasha Verkhovsky, pour sa confiance et son aide pour ce travail de thèse. Merci également au Prof. Meister de m'avoir offert la possibilité de travailler dans son laboratoire et pour son soutien. Enfin, je souhaite remercier le Prof. Dietler et tous les membres du LPMV pour leur accueil.

Je tiens également à remercier les membres du jury, Prof. Gisou van der Goot, Prof. Aleksandra Radenovic, Prof. Atef Asnacios et Prof. Bernhard Wehrle-Haller, d'avoir accepté de juger ma thèse ainsi que pour leur disponibilité et leur intérêt à l'égard de mon travail.

Pour finir, j'aimerais remercier mes collègues du laboratoire LCB pour leur accueil chaleureux et la bonne ambiance de travail ainsi que pour leur collaboration et leur soutien durant ma thèse.

Ce travail de recherche a bénéficié du soutien financier du Fonds National Suisse de la Recherche Scientifique.

Abstract

Cell migration is a fundamental property of all animal cells which is involved in processes such as embryogenesis, immune response, tissue regeneration and cancer metastasis. Directional migration requires cell polarization which could happen in response to external signals but also spontaneously. Polarization involves the change in the cell edge activities from random distribution of protrusion and retraction to their separation into two large regions corresponding to the leading and trailing edges of the cell. Many studies investigated cytoskeletal mechanisms of protrusions and retractions but it is still not well understood how the cell orchestrates protrusion and retraction along its edge and what triggers transitions between these two types of activity. These questions are essential to understand both cell polarization and cycles of protrusion and retraction which characterize exploratory edge dynamics before polarization.

This thesis focuses on the analysis of cell edge dynamics during the initiation of motion and on the mechanisms of transition (switches) between protrusion and retraction. We considered the cell polarization and protrusion-retraction cycles as two related phenomena and aimed to identify common mechanisms. Live cell imaging, cytoskeletal inhibitors, traction force microscopy, patterned substrates, micromanipulation, and computational analysis and modeling were used to examine cell polarization in the experimental model of fish epithelial keratocytes that are characterized by simple and regular shape and robust polarization and motion.

We found that protrusion-retraction switches happened at maximal distance from the cell center both during cell edge fluctuation and directional motion and did not depend on the edge orientation with respect to the cell motion direction. Computational model demonstrated that switches at a threshold distance were sufficient for self-organization of edge activity leading to spontaneous polarization and stable cell shape and motion suggesting that distance-sensing is a fundamental mechanism of cell symmetry breaking. Next we investigated the mechanisms of distance-sensing focusing on two hypotheses: traction forces and tridimensional cell shape. Traction force may increase with the distance from the cell center (e.g., due to a build-up of actomyosin network) leading to detachment of the edge and initiation of retraction. We discovered that traction forces indeed increased with the distance and that protrusion-retraction switches occurred near maximal forces. Local external force also induced protrusion-retraction switch. However, inhibition of contractility reduced traction forces and abolished the dependence of force on the distance, but did not prevent cell polarization. Taken together, these results suggest that traction forces are sufficient, but not necessary mediators of distance-dependent switch and cell polarization. In an alternative mechanism, tridimensional shape of the cell edge may depend on the distance from the cell center and affect the balance of forces at the edge, inducing switches. We have locally modified this tridimensional force balance by using substrates with topographic features and showed that switches preferentially happen near these features.

These results provide a novel framework to understand cell edge dynamics and symmetry breaking in terms of protrusion-retraction switches and physical force balance at the cell edge.

***Keyword**: cell motility, cell polarization, fish epithelial keratocytes, traction forces, cell edge dynamic, actin polymerization, myosin II contractility, membrane tension, contact angle.*

Résumé

La migration cellulaire est une propriété fondamentale de toutes les cellules animales qui est impliquée dans des processus tels que l'embryogénèse, la réponse immunitaire, la régénération tissulaire et les métastases cancéreuses. La migration directionnelle nécessite une polarisation de la cellule qui peut se produire en réponse à des signaux externes mais aussi spontanément. La polarisation implique un changement de l'activité du bord cellulaire passant d'une distribution aléatoire des protrusions et rétractions, à une séparation en deux larges régions correspondant aux bords avant et arrière de la cellule. Beaucoup d'études ont examiné les mécanismes de protrusions et rétractions du cytosquelette mais il n'est pas encore bien compris comment la cellule organise les protrusions et rétractions le long de son contour et ce qui déclenche les transitions entre les deux types d'activités. Ces questions sont essentielles pour comprendre aussi bien la polarisation cellulaire que les cycles de protrusion et rétraction qui caractérisent les dynamiques d'exploration du bord de la cellule avant la polarisation.

Cette thèse est centrée sur l'analyse de la dynamique du bord de la cellule durant l'initiation de la motilité et sur les mécanismes de transition (switches) entre protrusion et rétraction. Nous avons considéré la polarisation cellulaire et les cycles de protrusion-rétraction comme étant deux phénomènes liés et nous visons à identifier des mécanismes communs. L'imagerie cellulaire en temps réelle, des inhibiteurs du cytosquelette, la microscopie de force de traction, des substrats agencés en motifs, la micromanipulation, ainsi que l'analyse et la modélisation informatique ont été utilisés pour examiner la polarisation cellulaire sur un modèle expérimental de kératocytes de l'épithélium de poissons, cellules caractérisées par une forme simple et régulière ainsi qu'une polarisation et migration robuste.

Nous avons découvert que les switches de protrusion-rétraction se produisaient à distance maximale du centre de la cellule durant la fluctuation du bord cellulaire et la migration directionnelle et qu'ils ne dépendaient pas de l'orientation de bord par rapport à la direction du mouvement de la cellule. Le modèle informatique a démontré que des switches à une distance-seuil étaient suffisants pour une organisation spontanée du bord cellulaire tout comme pour une forme et une migration cellulaire stables suggérant que la détection de la distance est un mécanisme fondamental de l'acquisition de la polarité cellulaire. Ensuite, nous avons étudié les mécanismes de détection de la distance en se focalisant sur deux hypothèses : les forces de traction et la forme tridimensionnelle de la cellule. La force de traction pourrait augmenter avec la distance par rapport au centre de la cellule (par exemple, dû à la mise en place du réseau d'actomyosine) aboutissant au détachement du bord et à l'initiation de la rétraction. Nous avons découvert que les forces de traction augmentaient effectivement avec la distance et que les switches de protrusion-rétraction avaient lieu à proximité des forces maximales. Une force locale externe a induit également un switch de protrusion-rétraction. Cependant, l'inhibition de la contractilité a réduit les forces de traction et a abolit la dépendance de la force sur la distance, mais n'a pas empêché la polarisation cellulaire. Pris dans leur ensemble, ces résultats suggèrent que les forces de traction sont suffisantes, mais pas nécessairement les médiateurs de la dépendance des switches à la distance, ni de la polarisation cellulaire. Selon un mécanisme alternatif, la forme tridimensionnelle du bord de la cellule pourrait dépendre de la distance par rapport au centre de la cellule et ainsi affecter la balance des forces à cet endroit, induisant des switches. Nous avons localement modifié cette balance des forces tridimensionnelles en utilisant des substrats ayant des caractéristiques topographiques définies et nous avons montré que les switches se produisaient préférentiellement à proximité de ces structures.

Ces résultats fournissent une nouvelle perspective pour comprendre les dynamiques du bord de la cellule et l'acquisition de la polarité en termes de switches de protrusion-rétraction et de balance physique de force au bord de la cellule.

Mots clés: *migration cellulaire, polarisation cellulaire, keratocytes de l'épithélium de poisson, forces de traction, dynamique du bord de la cellule, polymérisation de l'actine, contractilité de la myosine II, tension de membrane, angle de contact.*

Contents

REMERCIEMENTS I

ABSTRACT III

RÉSUMÉ V

CONTENTS VII

1) INTRODUCTION 1

1.1 GENERAL CONTEXT 1
1.2 CONTENT OF THE THESIS 2

2) BIOPHYSICAL BACKGROUND 5

2.1 THE CYTOSKELETON 5
2.2 ACTIN 7
2.2.1 Actin microfilaments 7
2.2.2. Actin associated proteins 9
2.3 CYTOSKELETAL MOTORS 12
2.3.1 Microtubule motors 13
2.3.2. Actin motors 13
2.3.2.1. Myosin II 14
2.4 THE CELL MEMBRANE 16
2.5 THE CRAWLING MOTION 17
2.5.1 Fish keratocyte as a model for crawling motion 18
2.5.2 Polarized organization of the cytoskeleton during motion in keratocytes 19
2.6 CELL PROTRUSION 20
2.6.1 The dendritic nucleation 20
2.6.2 Protrusive forces 22
2.6.2.1 Brownian ratchet model 22
2.7 CELL RETRACTION 23
2.7.1 Dynamic network contraction 24
2.8 CELL ADHESION 25
2.9 FORCE GENERATION DURING CELL MIGRATION 26
2.9.1 Traction forces 26
2.9.2 Cell traction forces measurement methods 27
2.9.2.1 Cell-populated collagen gel 27
2.9.2.2 Thin silicon membrane 27
2.9.2.3 Force sensor array 28
2.9.2.4 Traction force microscopy 29
2.10 MEMBRANE TENSION 30
2.11 CELL POLARIZATION 31
2.11.1 Signaling networks 32
2.11.2 Actin flow 33
2.11.3 Membrane tension and cell shape 34

3) MATERIALS AND METHODS 35

3.1 CELL CULTURE 35
3.2 MICROSCOPY 35
3.2.1 Phase-contrast and fluorescence microscopy 35

3.2.2 Scanning electron microscopy *36*
3.3 CELL TREATMENT 36
3.3.1 Cytoskeleton inhibitors *36*
3.3.2 Hypo-osmotic treatment *37*
3.4 IMMUNOSTAINING 37
3.5 POLYACRYLAMIDE GEL FABRICATION 38
3.6 TRACTION FORCE MICROSCOPY 39
3.6.1 Analysis of force map *39*
3.7 COMPUTATIONAL MODEL OF CELL EDGE DYNAMIC 40
3.7.1 Mapping protrusion-retraction switches *40*
3.7.2 Model parameters *42*
3.7.3 CELL CENTER, LOOP ELIMINATION AND CONTOUR RE-SAMPLING 42
3.8 ACTIN MICROINJECTION 43
3.8.1 Microinjection *43*
3.8.2 Phalloidin solution *43*
3.9 TOPOGRAPHIC SUBSTRATE 43
3.9.1 Fabrication of features *43*
3.9.2 Switch frequency measurement near the feature *44*
3.10 FLUORESCENCE DISPLACEMENT METHOD 45
3.11 CONTRIBUTION TO CITED PAPERS 45
3.12 GLOSSARY 45

4) CELL EDGE DYNAMICS DURING THE PROCESS OF MOTILITY INITIATION 47

4.1 EXPERIMENTAL CELL EDGE DYNAMICS 47
4.1.1 Cell fluctuation *47*
4.1.2 Myosin II inhibition *49*
4.1.3 Actin polymerization inhibition *51*
4.2 PROTRUSION-RETRACTION TRANSITIONS IN CELL POLARIZATION 53
4.2.1 Distribution of protrusion/retraction switches during cell polarization *53*
4.2.2 Induced cell shape perturbation *55*
4.2.3 Computational model of cell edge dynamic *57*
4.2.4 Actin dynamics during protrusion-retraction fluctuations *58*
4.3 CELL EDGE DYNAMICS ON FLEXIBLE GEL SUBSTRATE 59
4.3.1 Cell detachment methods *60*
4.3.2 Polyacrylamide gel rigidity *61*
4.4 CONCLUSION 63

5) RELATION BETWEEN TRACTION FORCES AND PROTRUSION- RETRACTION SWITCHES 65

5.1 TRACTION FORCES MICROSCOPY 65
5.2 TRACTION FORCES DURING CELL POLARIZATION ON SOFT GEL 66
5.2.1 Two distinct pathways to initiate motility *67*
5.2.2 Distribution of traction forces on soft gel *69*
5.2.3 Force-distance relationship on soft gel *70*
5.3 TRACTION FORCES AND SWITCHES DURING CELL POLARIZATION ON RIGID GEL 72
5.3.1 Force-distance relationship *73*
5.3.2 Induced cell shape perturbation *74*
5.3.3 Correlative mapping of switches and traction forces *75*
5.4 CELL CONTRACTILITY INHIBITION ON RIGID GEL 77
5.4.1 Distribution of traction forces in contractility-inhibited cells *77*
5.4.2 Mapping of switches in contractility-inhibited cells *78*

5.5 MANIPULATION OF EDGE DYNAMICS WITH EXTERNAL FORCES 79
5.5.1 External forces during cell fluctuation 79
5.5.2 External forces on contractility-inhibited cells 80

6) CONTACT ANGLE AT THE LEADING EDGE CONTROLS SWITCHING PROCESS 83

6.1 SHAPE OF THE PROTRUDING EDGE 83
6.2 MODIFICATION OF CONTACT ANGLE USING SUBSTRATE TOPOGRAPHY 86
6.3 EFFECT OF SUBSTRATE TOPOGRAPHY ON CELL BEHAVIOR AND SWITCH DISTRIBUTION 87
6.4 CONCLUSION 89

7) CONCLUSIONS AND PERSPECTIVES 91

BIBLIOGRAPHY 95

CV 103

1) Introduction

1.1 General context

The ability to migrate is a fundamental property of all animal cells. Cell motion has a crucial role in important physiological and pathological processes such as embryonic development, immune response, tissue regeneration and cancer metastasis. For these reasons, the cell motion is an important topic of research.

Directional migration requires cell polarization which could happen in response to external signals but also spontaneously in the absence of any special cues. Polarization involves the change in the cell edge activities from random distribution of protrusion and retraction to their separation into two large regions corresponding to the leading and trailing edges of the cell. Many studies investigated cytoskeletal mechanisms of protrusions and retractions but it is still not well understood how the cell orchestrates protrusion and retraction along its edge and what triggers transitions between these two types of activity. These questions are essential to understand both cell polarization and cycles of protrusion and retraction which characterize exploratory edge dynamics before polarization.

Current hypothetical mechanisms of polarization and edge oscillation suggest two types of feedback relationships leading to the segregation of cell activities and components: reaction-diffusion feedback between signaling molecules, and mechanical feedback within the cytoskeletal machinery itself. Signaling network are believed to be largely responsible for polarization of chemotactic cells, but more and more studies suggest that this chemical feedback mechanisms are not sufficient and physical forces have to be taken into account. Indeed, dynamics of the cell edges, protrusion and retraction are ultimately the result of physical forces such as those generated by actin polymerization and actomyosin contractility in balance against membrane tension and adhesion, so investigating how these forces are arranged in relation to the dynamics and shape of the cell may provide essential clues.

A prominent emerging concept about mechanical feedback in cell polarization is the idea of the feedback from the motion itself that works through actin flow that brings the polarization cue, most likely the contractile force generator myosin II, to the back of the cell, thereby promoting contraction at the back and reinforcing polarity. This concept is however limited in that in order for this feedback to work the cell should have already started moving, and therefore this idea has difficulty explaining initial steps of polarization and relating them to the preceding oscillatory edge dynamics.

In this thesis, we consider the cell polarization and protrusion-retraction cycles as two related phenomena and aim to identify and analyze common mechanisms in cell edge dynamics controlling the transitions (switches) between protrusion and retraction. We have found that protrusion-retraction switches universally happen at the maximal distance from the cell center independently of the orientation with respect to the overall motion direction during cell oscillation, polarization and directional motion. We have demonstrated, with the aid of a computational model, that this distance sensitivity is sufficient for spontaneous emergence of cell polarity, motion and stable shape in the absence of any external directional cues. Actin dynamics during protrusion-retraction cycles suggested that initiation of retraction happens via sudden change of actin flow velocity suggesting partial detachment and subsequent collapse of the protruding cell edge. Consistent with these observations, we focused on testing two physical hypotheses to explain protrusion-retraction switches and their distance sensitivity. The first one is based on traction forces between the cell and the substrate that could increase with distance from the cell center, leading to detachment of the edge and initiation of retraction at a critical force level. We have observed the correlation between maximal forces and switches, partial disorganization of switches upon inhibition of contractility and induction of switches by external force, suggesting that traction forces are indeed sufficient for distance-dependent switching, but are likely not the only mechanism. The second hypothesis takes into account the tridimensional shape of the protruding edge: increasing the length of the protrusion is expected to change locally its shape resulting in the change of the force-balance at the triple interface between membrane, substrate and extracellular medium and may result in a switch from protrusion to retraction. In the way of testing this hypothesis, we have demonstrated that edge shape changes in a predicted manner during protrusion-retraction cycles and that manipulating the force balance at the edge via substrate topography affects the edge dynamics and the distribution of switches.

1.2 Content of the thesis

We first describe the biophysical background necessary to study and understand cell motion. We define the most important cytoskeletal components involved in cell motility, describe the mechanisms underlying crawling motion and explain the phases of protrusion, retraction and adhesion constituting the crawling motion cycle. We also consider the tension of the plasma membrane and the forces exerted by the cell to the substrate and describe different ways to measure these traction forces. We conclude the background with the description of cell polarization and an overview of different studies focusing on the mechanisms of symmetry breaking and initiation of motion.

Secondly, we present the materials and methods used during this work. We explain our experimental approaches and data treatment in order to facilitate the understanding and reproducing our experiments.

The next chapters contain the main results of this thesis work:

Chapter 1 describes the cell edge dynamics. In a first phase, we described the cell fluctuation and subsequent polarization and the organization of the actomyosin cytoskeleton in these processes. Then, we analyzed more precisely the edge dynamics and in particular the switches between protrusion and retraction and their link with the distance from the cell center (published in Nature Physics (Raynaud et al., 2016)). At the end of the chapter, we investigate the cell fluctuation behavior on flexible gel substrate to find the best conditions to study cell edge dynamic and traction forces (described in the next chapter).

Chapter 2 presents the results of the analyses of traction forces, on soft and rigid gel substrate. We describe two distinct pathways leading to initiation of motility and study the link between distance of the edge from the cell center and traction forces. We demonstrate correlation between traction forces and switches and investigate what happens when generation of traction forces is inhibited. Finally, we apply external forces to cells to induce switches on both control and contractility-inhibited cells.

Chapter 3 demonstrates the importance of protrusion shape for switches. Based on a theory developed in our laboratory and published in Current Biology (Gabella et al.), we study the dynamics of the contact angle at the interface between membrane, substrate and extracellular medium and its role in the mechanism of switches. We are able to change the contact angle at the cell edge and induce switches using tridimensional patterned substrate.

Finally, we conclude and discuss the results and outline the main perspectives of this thesis work which we see as investigation of the cytoskeletal bases of the force-distance relationship, generalization of the concept for other types of cells, and combining three-dimensional patterns with traction force study to uncover possible relationship between the two mechanisms of protrusion-retraction switches.

2) Biophysical background

The cell: unit of life

The cell is the basic structural, functional and biological unit of life. It is often called the “building block of life”. The existence of cells was discovered in 1665 by Robert Hooke. A scientific theory, the “cell theory” which describes the properties of cells, was developed in 1839 by Matthias Schleiden and Theodor Schwann. It states that the cell is the fundamental unit of structure and function for life, that all organisms are composed of one or more cells, and that all cells arise from pre-existing living cells (Mazzarello, 1999).

An individual cell is constituted of a fluid membrane which separates the inside from the outside. Inside this plasma membrane, there are several organelles such as the nucleus which contains the genetic information, the Golgi apparatus, mitochondria, endoplasmic reticulum, lysosomes and vacuoles. These organelles are surrounded by a cytoplasm, composed of water with biomolecules such as proteins.

Cells exist in various shapes and sizes, from 1um bacteria to 100 µm plant cells and 10 µm animal cells. In animal cell body, there are more than 200 types of cells that are organized to form the 4 basic types of tissues: epithelial, muscle, connective and nervous. Then, these tissues are joined in structural units called organs, to serve a specific function.

2.1 The cytoskeleton

The cytoskeleton is an intracellular matrix, composed of organized biological polymers, which supports cell shape and gives to cell its mechanical properties. The proteins of the cytoskeleton form a network of filaments, which constitutes a dynamic structure that is capable of rapid assembly or disassembly by constant polymerization/depolymerization. This organization of dynamic polymers allows the cell reorganize in function of the cell’s requirements. There is a multitude of functions attributed to the cytoskeleton: cell signaling pathways, intracellular transport and cellular division. One of the major functions of the cytoskeleton is to allow the cell to migrate.

The cytoskeleton is composed of three main proteins networks. The intermediate filaments are the most stable structure of the cytoskeleton. They have an average diameter of 10 nanometer and are composed of several fibrillar proteins (fig 2.1). They have mainly structural functions and take part in the adhesion and cellular cohesion. The microtubules are a second type of cytoskeleton components, they are tubular structures of 25 nm outer diameter and 12 nm inner diameter. It is a highly dynamic structure, formed by the polymerization of a dimer of α- and β-tubulin, two globular proteins (fig 2.1). They are present in cellular structures such as cilia and flagella and participate in important biological processes like mitosis by forming the mitotic spindle to segregate the chromosomes during the cell division. The third component of the cytoskeleton is the actin filaments. They are the smallest filaments with a diameter of 6nm (fig 2.1). Actin is the major component of the cytoskeleton and the most abundant protein in eukaryotic cells. These filaments are important in several processes, in particular in cell motility (Alberts B., 2002).

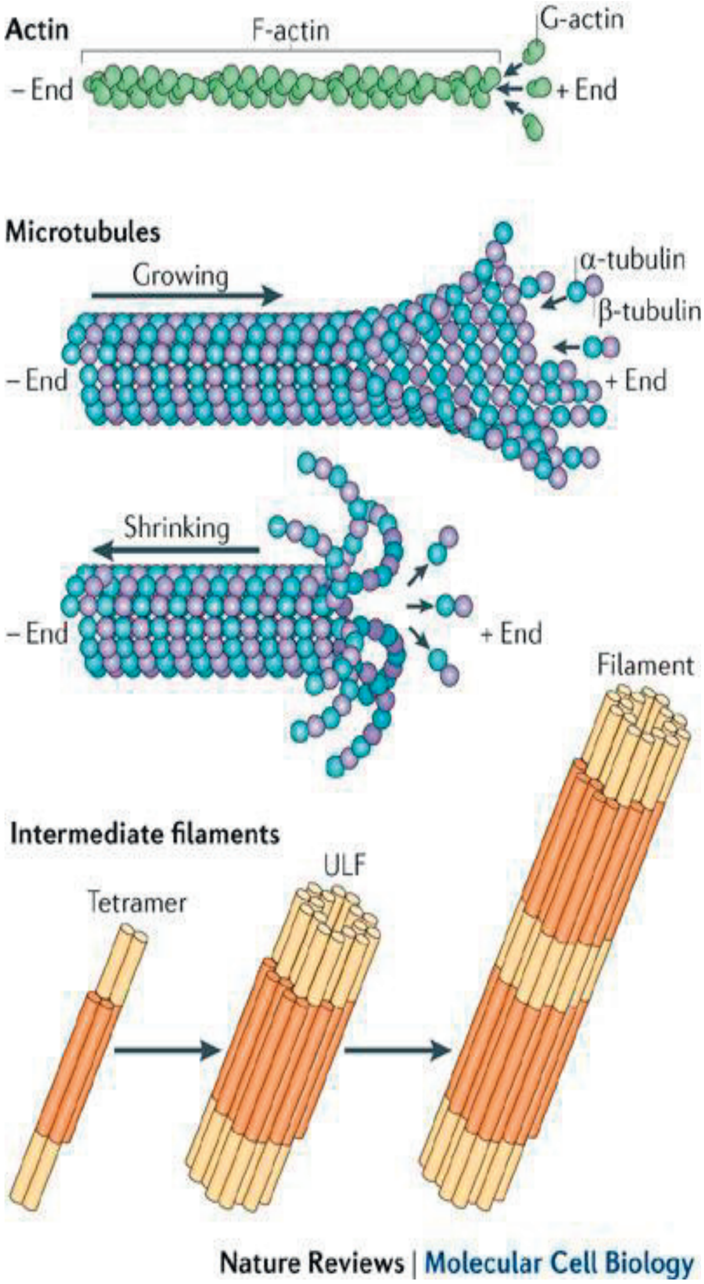
Actin
F-actin
G-actin
– End
+ End
Microtubules
Growing
α-tubulin
β-tubulin
– End
+ End
Shrinking
– End
+ End
Filament
Intermediate filaments
ULF
Tetramer
Nature Reviews | Molecular Cell Biology

Figure 2.1: Composition and structure of the three main components of the cytoskeleton (Mostowy and Cossart, 2012).

2.2 Actin

Actin is a 43kDa ubiquitous protein that is highly conserved between species. It exist as a free monomer called G-actin (globular) or as a linear polymer called F-actin (filamentous). The G-actin is made of 375 amino acids and is associated to a bivalent cation (calcium or magnesium ion) and an ATP/ADP nucleotide. In vertebrates, it exist three main groups of actins: α-actins are present in muscles tissues and the β- and γ-actins are prominent in non-muscles cells, as components of the cytoskeleton. In mammals, actin isoforms are encoded by six different gens, which shows the importance of this protein for many cellular processes. By the ability of the cell to dynamically form actin microfilaments, it can rapidly remodel itself in response to external stimuli given by the environment and to the internal cell signaling. For example, actin filaments can transport vesicles or organelles through the cell with the help of specific motor proteins, have a crucial role during cytokinesis or else participate into structures such as microvilli that are involved in process like cell absorption/secretion or cellular adhesion.

2.2.1 Actin microfilaments

Actin filament structure resembles a double helix, formed by two helical strands with a diameter of the fiber about 6 to 9 nm depending on the twist. The helix is repeated every 37 nm and the persistence length of a filament is around 17 µm which correspond to the typical diameter of cells. The actin microfilament is a polar structure (Alberts B., 2002) with two structurally and functionally distinct ends: a fast growing plus-end and a slow growing minus-end. As decoration with myosin heads reveals a distinct arrowhead appearance along the actin filament, the plus end is also referred to as the barbed end and the minus-end as the pointed end (fig 2.2.A). The possibility to grow at one direction end and to shorten at the opposite end is given by polymerization rate which is different at the two ends of the actin filament: monomer addition is approximately 10 times faster at the plus-end than at the minus-end (fig 2.2.B). The polymerization speed depends on the critical concentration (K) which correspond to the concentration of free monomers at which net polymerization equals net depolymerization. If the cytosolic concentration of actin free subunits is above the respective critical concentration of each ends, new subunits will be added: if it is below the critical concentration, subunits will be removed.

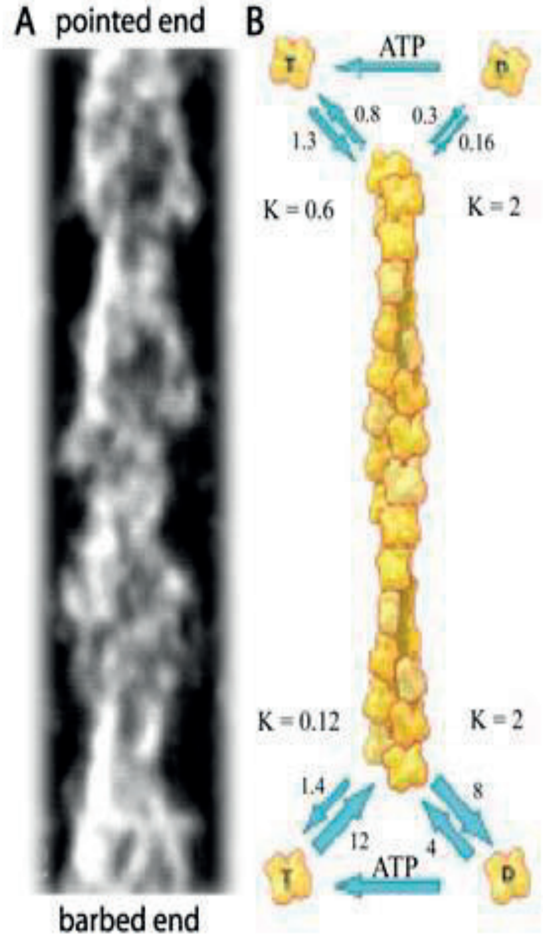

Figure 2.2: Structure and dynamics of actin filament. (A) Arrowhead features of actin filament decorated with myosin head. (Verkhovsky et al., 1997) (B) Association ($\mu M^{-1}.s^{-1}$) and dissociation (s-1) rate constants for ATP/ADP at filaments ends, with K the critical concentration (μM). (Pollard and Borisy, 2003)

The first step of actin assembly process is known as "nucleation". It correspond to the formation of an actin nucleus composed of three actin monomers (fig 2.3.A). Free actin monomer spontaneously oligomerizes in solution. This actin nucleus is a highly unstable structure and requires additional proteins to stabilize and form it. The main protein which play this role of "actin nucleator" is the Arp2/3 complex.

When the actin nucleus is formed, the filament can elongate. Only ATP-actin monomers are likely to participate in polymerization. When the actin monomer binds to the barbed end of the growing filament, the associated ATP is irreversibly hydrolyzed (fig 2.3.B). The γ-phosphate is released and the resulting ADP is trapped into the polymer (Carlier, 1986). At the other end, monomers leave the filament end, a process that occurs at a constant rate independently of the free monomers concentration (fig 2.3.A).

During this elongation process, proteins of formin family play important role by translocating themselves along the growing filament and simultaneously catalyzing the addition of monomers.

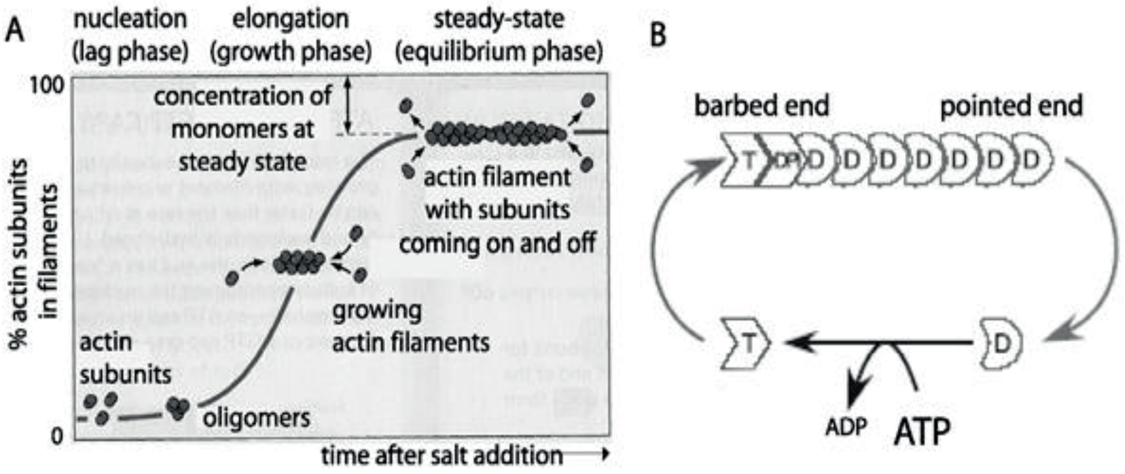
A
nucleation (lag phase)
elongation (growth phase)
steady-state (equilibrium phase)
100
0
% actin subunits in filaments
concentration of monomers at steady state
actin filament with subunits coming on and off
growing actin filaments
actin subunits
oligomers
time after salt addition
B
barbed end
pointed end
T
DP
D
D
D
D
D
D
D
T
D
ADP
ATP

Figure 2.3: Time course of actin polymerization and treadmilling in vitro. (A) Step of polymerization mechanism, after addition of salt in a pure solution of actin. (Alberts B., 2002) (B) Equilibrium phase is characterized by actin treadmilling. (Carlier et al., 2003)

After the growing step, the filament reaches a steady-state phase (fig 2.3.A), where the net rate of actin assembly matches the net rate of actin disassembly, and the actin filament maintains thus a constant length, leading to a net flux of subunits from the barbed end to the pointed end. This phenomenon is known as treadmilling and has been observed in solution (Wegner, 1976) and directly on a single actin filament (Fujiwara et al., 2002).

All these events to form actin filament happen spontaneously inside the cell, ant are regulated by additional molecules.

2.2.2. Actin associated proteins

Nucleation proteins

The first step of the formation of microfilament requires accessories proteins, known as “nucleation proteins”, to stabilize the actin nucleus.

- Arp2/3 complex: this protein complex was discovered by Machesky and co-workers in 1994 (Machesky et al., 1994). It is formed by seven subunits with two of them, Arp2 and Arp3 (Actin Related Proteins), have a similar structure to the actin monomer and serve as nucleation site for new actin filaments formation. Arp2/3 forms a nucleation core to promote actin filament growth by binding to the side of pre-existing filaments (fig 2.4.a). This process allows the formation of a complex network of nascent actin filaments. The Arp2/3 complex requires an activation by Nucleation Promoting Factors (NPFs) such as WASp (Wiskott - Aldrich Syndrome protein) (Derry et al., 1994) (Symons et al., 1996), N-WASp (Miki et al., 1996), Scar (suppressor of cAMP receptor) (Bear et al., 1998) or WAVE (Wiskott - Aldrich Syndrome Protein Verprolin-homologous) (Miki et al., 1998). Members of this familly proteins share similar binding sequences for Arp2/3 complex and monomeric actin, and both are required and sufficient to activate Arp2/3. They are regulated by signaling pathways arising from membrane receptors (Ma et al., 1998) (Mullins and Pollard, 1999), involving the GTPase Cdc42 for WASP and N-WASP or the GTPase Rac in the case of Scar/WAVE (Machesky and Insall, 1999).

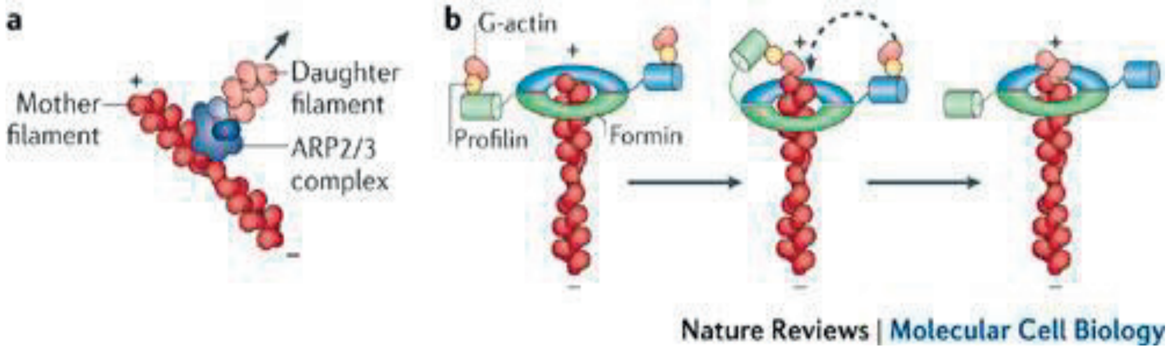

Figure 2.4: Actin nucleation proteins. (a) ARP2/3 complex binds to the side of a pre-existing actin filament to nucleate actin polymerization. (b) Formins is associated to actin filament to promote rapid insertion of actin subunits while protecting the end from capping proteins. (Ratheesh and Yap, 2012)

- Formins: this group of proteins was discovered in 1994 by Castrillon and Wasserman (Castrillon and Wasserman, 1994) and all the members are characterized by the presence of formin homology (FH) domains. The FH2 domain is the most important and is involved in actin nucleation. Formins bind to the actin-ATP at the barbed end, removing the capping protein and preventing re-capping to allow growth of filaments (fig 2.4.b). As formin-capped filaments are still able to polymerize, formins are thus called *leaky cappers (Zigmond et al., 2003)*. The proline-rich FH1 domain helps this process by mediating interaction with a variety of proteins such as the actin-binding protein profilin, which helps the delivery of actin monomers at the growing barbed end. The formins are activated by Rho GTPases and phosphorylation (Higgs, 2005) (Chesarone et al., 2010).

Capping proteins

Proteins called "F-actin capping proteins" bind to the ends of the filaments (Isenberg et al., 1980) to inhibit addition or loss of actin subunits. For example, CapZ binds to the barbed (+)-end, inhibiting polymerization (Casella et al., 1986). This process is regulated by various intracellular localized signals, in particular the inositol phospholipid PIP2. In response to signaling pathways arising from cell surface receptors, the PIP2 concentration increases in the cytosol which leads to uncapping of filaments ends. There are also proteins that bind to the pointed (-)-end to prevent monomer dissociation such as tropomodulin (Weber et al., 1994).

Depolymerizing proteins

To favor the dynamics of assembly and disassembly, there exist actin-binding proteins that depolymerize and cut the microfilaments.

- Gelsolin: It is an actin-severing protein composed of six subdomains. Gelsolin is able to bind to the actin monomer localized at the (+)-end and also to induce the breaking of the filament in the middle. Once gelsolin has severed an actin filament, it remains bound to the barbed end and plays the role of an effective capping protein. Gelsolin is activated by Ca^{2+} (Gremm and Wegner, 2000) and is regulated by PIP2.

- ADF/cofilin: Cofilin is a member of the ADF (Actin Depolymerizing Factor) family and can bind to actin monomers or filaments (Mabuchi, 1983). By attaching along the length of the filament, it induces more twist in the filament which causes a mechanical stress leading to the severing of the filament. Cofilin binds preferentially to ADP-actin monomers (Maciver, 1998) on the filament rather than to ATP-containing filament. In the cell, the new actin filaments contain mostly ATP and by consequence are more resistant to depolymerization by cofilin. The severing of actin filaments allows the formation of new filaments by creating new active ends.

Actin monomer sequestering proteins

Actin monomers, present in the cytosol to enable the elongation of actin filaments, can be sequestered by some proteins.

- Thymosin β4: it was isolated by Safer and co-workers from human platelets in 1990 (Safer et al., 1990). It is the principal and most abundant of the actin sequestering proteins. Thymosin β4 forms a 1:1 complex with the G-actins present in the cytosol, which makes the actin monomer unable to associate with either the plus or minus ends of actin filament and to hydrolyze or exchange ADP/ATP (Carlier et al., 1993).

- Profilin: it is a small protein which plays the role of actin sequestering and can spatially and temporally control growth of actin microfilaments (Markey et al., 1978). Profilin can form a 1:1 complex with G-actin. This complex can bind to the (+)-end, but not to the (-)-end of actin filament (Carlier et al., 2013). Profilin enhances actin growth: it catalyzes the exchange of ADP to ATP (Mockrin and Korn, 1980), which facilitates the elongation of the filament at the (+)-end side.

Cross-linking proteins

Actin cytoskeleton is important in many mechanical functions, this is why it is organized into a dynamic and complex subcellular scaffolds. For that, actin-crosslinking proteins organize the actin filaments network in mainly three different structure types: parallel bundles, contractile bundles and gel-like networks. *"Parallel bundles"* are defined by filaments oriented in the same direction (with the same polarity), and with a short distance between them (typically 10-20 nm). These structures are found for example in filopodia. *"Contractile bundles"* are filaments oriented with alternate polarity and separated by a greater distance (between 30-60 nm). Contractile ring which divides the cell in two equal parts during mitosis is composed of contractile bundles. Stress fibers are also contractile bundles. *"Gel-like network"* is composed of cross-linked actin filaments which form a loose network. It composes the cortex of the cell.

- α-actinin: it is a homodimer with two actin binding sites that are 30 nm apart. This conformation allows the formation of a loosely packed actin bundles, useful to enable the insertion of other proteins such as myosin II (discussed below). α-actinin allows the formation of actin contractile bundles such as the stress fibers and contributes also to the maturation of cell adhesions.
- filamin: it is a V-shaped crosslinking protein with two actin binding sites. This conformation allows the formation of cross-linked actin filaments network, with filaments associated at almost right angle to each other.

2.3 Cytoskeletal motors

Motor proteins are able to move along cytoskeletal filaments using a force-generating mechanism driven by the ATP hydrolysis. These proteins convert chemical energy into mechanical work. They move unidirectionally along the oriented filaments. They can participate in intracellular trafficking by carrying cargos across the cell or can be responsible of force generation through the cytoskeleton.

Cytoskeletal motor proteins associate with the filament through a "head" region (or motor domain), being the active part which binds to the filament and hydrolyzes ATP. The head characterizes the track and the direction of movement along it. The second part of the protein is the "tail" which connects the motor to its cargo. The tail defines the biological function of the individual motor protein, by identifying the cargo, which can be vesicles, organelles or other filaments.

2.3.1 Microtubule motors

Microtubule motors move along microtubules. They could be divided in two categories, the plus-end motors and the minus-end motors, depending on the direction of the movement along the microtubule.

- Kinesins: some kinesins move along microtubule filaments from the minus-end to the plus-end. This anterograde movement allows the transport of cargos from the cell center towards the periphery. Other kinesins move from the plus-end to minus-end. The active movement of kinesins supports several cellular functions such as mitosis or meiosis by handling the movement of the chromosomes (Cross and McAinsh, 2014), or for transportation of cellular cargos in the axonal transport mechanism.
- Dyneins: their movement along microtubules is retrograde, from the plus to the minus-end. There is axonemal dyneins (Porter, 1996) involved in the sliding of microtubules inside the cilia and flagella to power their movement. And there are cytoplasmic dyneins (Kardon and Vale, 2009) which drive the transport of organelles to the cell center and also participate in mitosis and self-centering of microtubule arrays (Raaijmakers and Medema, 2014).

2.3.2. Actin motors

Myosins are motor proteins that move along actin filaments. Myosins are composed of one or two heavy chains containing the N-terminal “head” domain and the C-terminal coiled-coil “tail” domain and also several light chains (fig 2.5). The head is a conserved domain which binds to actin, hydrolyzes ATP and produces the power stroke (head displacement after ATP hydrolysis). The tail binds specific substrates or cargos, depending of the myosin type. In between, a “neck” region (or “lever arm”) transduces the force generated by the catalytic motor domain and binds to the light chains. E.g., myosin II has two light chains per head: the *regulatory light chain* which actively participates in the power-stroke and the *essential light chain* for which the function remains unclear, but is believed to contribute to the structural stability of the myosin. The length of the neck and the number of light chains influence the “step size” of different myosin types, which is the distance along actin filament traveled by a single myosin head for one ATP hydrolysis (Toyoshima et al., 1990).

The movement of myosin motors along actin filaments is directed towards the barbed end, expect for the myosin VI which moves to the pointed end. As the actin filaments are usually oriented from the center to the cell periphery, myosin VI walks in the direction of the cell center, acts as the major motor protein for import, while the other myosins such as myosin V have primarily the function of cargo export. All myosin types except myosin II are often called *unconventional myosin*. The *conventional myosin* is myosin II which is involved in muscle contraction and in the formation of contractile bundles in non-muscle cells.

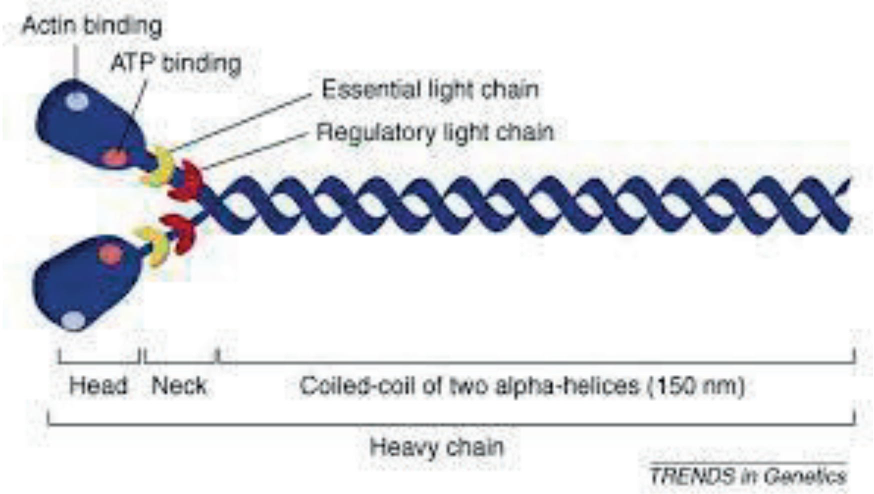

Figure 2.5: Schematic representation of the myosin II. It is composed of two heavy chains (*blue*) containing ATP- and actin-binding sites in their heads, two essential light chains (*red*) and two regulatory light chains (yellow). (Quintin et al., 2008)

2.3.2.1. Myosin II

Myosin II is a dimeric protein, composed of two heavy chains and two pairs of light chains (Dominguez et al., 1998). A long and thin tail is formed by the tails of the two heavy chains which wind around each other to form the "coiled-coil" rod. At one extremity of the rod, the two globular head are located side by side.

Several myosin II can form bipolar complexes through an antiparallel interaction of the coiled-coil tails resulting in the formation of myosin filaments. This filament structure can contain many myosin II molecules and are thus able to interact with multiple actin filaments, moving them with respect to each other.

The powerstroke mechanism of myosin II, similar as for other myosin motor proteins, acts in a cyclical manner with an ATPase activity which induces conformational changes in the protein. In the first step, nucleotide-free myosin is attached to a region of actin filament (fig 2.6 *attached*) in conformation known as the "rigor conformation". ATP binding to the myosin head leads to a conformational change that

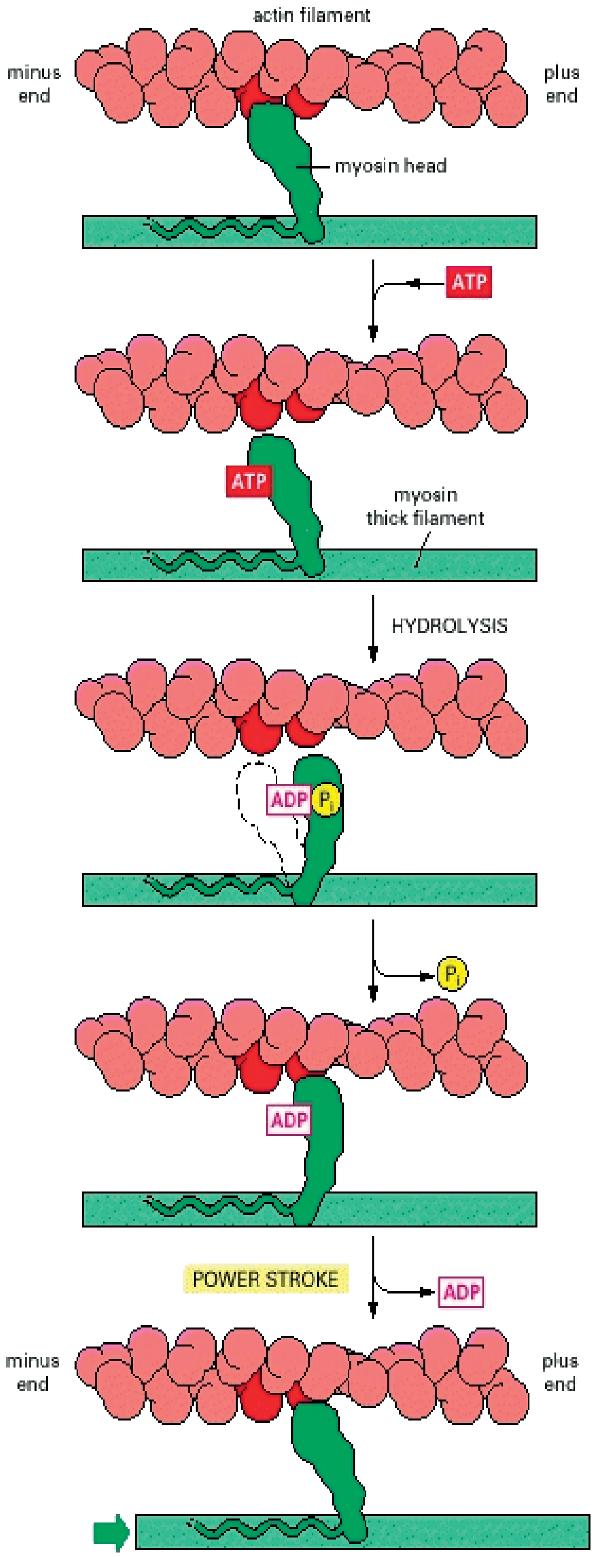

ATTACHED At the start of the cycle shown in this figure, a myosin head lacking a bound nucleotide is locked tightly onto an actin filament in a *rigor* configuration (so named because it is responsible for *rigor mortis*, the rigidity of death). In an actively contracting muscle, this state is very short-lived, being rapidly terminated by the binding of a molecule of ATP.

RELEASED A molecule of ATP binds to the large cleft on the "back" of the head (that is, on the side furthest from the actin filament) and immediately causes a slight change in the conformation of the domains that make up the actin-binding site. This reduces the affinity of the head for actin and allows it to move along the filament. (The space drawn here between the head and actin emphasizes this change, although in reality the head probably remains very close to the actin.)

COCKED The cleft closes like a clam shell around the ATP molecule, triggering a large shape change that causes the head to be displaced along the filament by a distance of about 5 nm. Hydrolysis of ATP occurs, but the ADP and inorganic phosphate (P_i) produced remain tightly bound to the protein.

FORCE-GENERATING A weak binding of the myosin head to a new site on the actin filament causes release of the inorganic phosphate produced by ATP hydrolysis, concomitantly with the tight binding of the head to actin. This release triggers the power stroke—the force-generating change in shape during which the head regains its original conformation. In the course of the power stroke, the head loses its bound ADP, thereby returning to the start of a new cycle.

ATTACHED At the end of the cycle, the myosin head is again locked tightly to the actin filament in a rigor configuration. Note that the head has moved to a new position on the actin filament.

Figure 2.6: Power stroke generation by myosin II on actin filament. (Alberts B., 2002)

reduces the actin-binding affinity of the myosin, allowing its displacement along the filament (fig 2.6 *released*). Then, ATP is hydrolyzed releasing an ADP and inorganic phosphate that stays attached to myosin (fig 2.6 *cocked*). The myosin head is cocked and the powerstroke can occur. The inorganic phosphate is then released, inducing a weak binding of the myosin at the new site of the actin filament (fig 2.6 *force-generating*). This triggers the force-generation of the powerstroke, by the return of the myosin head to its original conformation and release of the ADP. The myosin is now bound to the actin filament at the new position, in a rigor configuration, bringing the cycle back to the beginning and ready to be set off again.

Myosin II is essential for many biological processes. In muscle cells, myosin II is involved in the sarcomere structure and muscle contraction. In non-muscle cells, myosin II is often associated to actin filament bundles. Myosin II has a major role in cell motility by generating forces in bundles and actin network.

2.4 The cell membrane

The plasma membrane is a lipid membrane, present in every cell type, which separates the interior components from the outside environment. It acts as a barrier, and as a scaffold various membrane proteins, transmembrane channels and signal receptors.

The cell membrane is made of a lipid bilayer, predominantly of phospholipid molecules which are amphipathic, with a hydrophilic head and a hydrophobic tail. The head of the phospholipid from each layer are faced outward into the aqueous intracellular or extracellular space, while the hydrophobic tails are oriented towards the interior of the membrane. The phospholipid composition enables the membrane to be partially permeable, which allows a diffusion of certain substances through it. For example, it enables the passive diffusion of hydrophobic molecules and prevents polar solutes to pass. Many molecules cross the cell membrane by diffusion and osmosis.

Phospholipids are the most abundant in the membrane, but there is also cholesterol and proteins embedded in the bilayer. Cholesterol helps to stabilize and maintain the fluidity of the cell membrane. The proteins present inside the bilayer can be peripheral or integral. Peripheral proteins are stuck on the inside or outside of the membrane and serve usually as receptors. Integral proteins transverse the membrane and have a function of pump or channel to allow diverse molecules to enter or leave the cell.

Cell membrane interacts with the cytoskeleton, especially the actin cytoskeleton. At the inner face of the plasma membrane, at the cell periphery, actin forms a layer called “cortex”. This cortex is attached to the cell membrane, playing a central role in cell shape control.

2.5 The crawling motion

The crawling motion is a particular type of cell motility, defined generally as the ability of animal cells to move in a tissue or over a substrate using their entire body rather than specific organelles. This mechanism is essential for life, by being involved in process such as embryogenesis, wound healing or immune responses. Crawling motion can be also responsible for many diseases, like cancer metastasis by the migration of malignant transformed cells. A lot of studies are focused on crawling motion because of its very wide involvement in the organism and of its general complexity.

The mechanism of crawling motion is dependent of the actin-myosin cytoskeletal system and can be divided into several steps: protrusion by extension of the front (fig 2.7.b), formation and stabilization of new adhesions (fig 2.7.c), and forward translocation of the cell body by contractile forces with a retraction of the back (fig 2.7.d) and detachment of adhesions at the cell rear (fig 2.7.e). These main steps are coordinated between each other and altogether, form a cycle that represents the elementary repeat crucial for cell motion.

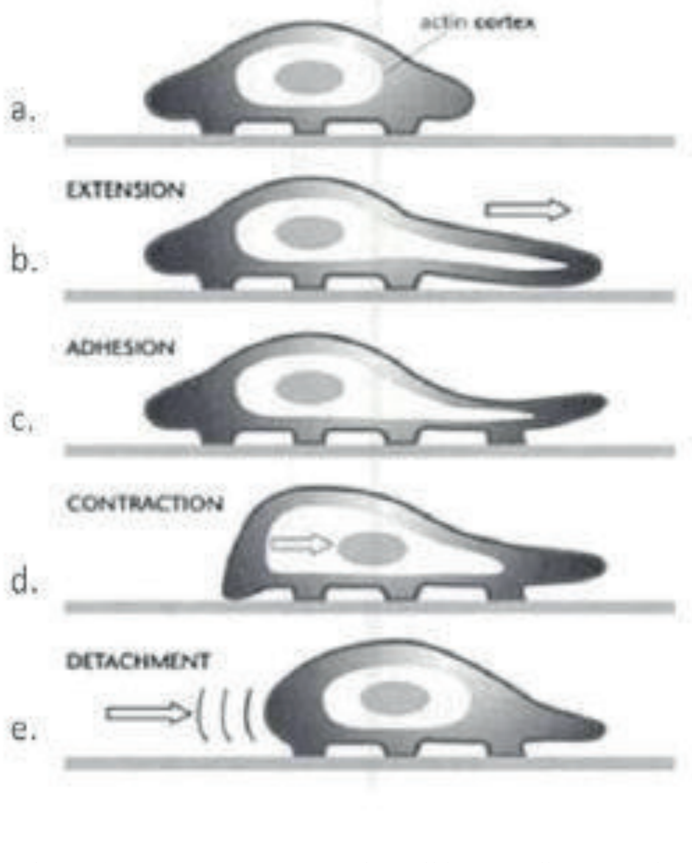

Figure 2.7: Schematic of crawling motion steps. (a) The cell is spreading over the substrate. (b) In order to migrate, the cell protrudes at the front, (c) creates new adhesion and (d) contracts in order to move and retract the cell rear. (e) Finally, the cell detaches at the back and the cycle repeats itself.

2.5.1 Fish keratocyte as a model for crawling motion

Fish epidermal keratocytes represent a favorable model system to study crawling motion. They constitute the most external protective layer of the skin and form a continuous epithelial sheet covering the animal body, which acts as a barrier against environmental damage.

These cells are a convenient model system due to their persistent migration and shape and their simple cytoskeletal organization. In culture, keratocytes form a colony of cells tightly bound to each other, with the cells at the periphery exhibiting large dynamic lamellipodium as they guide the cell monolayer to expand. Cell-cell contacts could be dissociated with proteinase or by chelating bivalent cations and the cells can be separated from each other to obtain individual cells.

Individual migrating cells have a characteristic canoe-like shape with a flat, large (~10 µm large per ~40 µm long) and thin (~0.1-0.3 µm) lamellipodium at the front. Lamellipodium is filled with a dense actin network. At the back, the cell body containing the nucleus, most of the organelles, and microtubules is much thicker (~3-5 µm thick). It was shown by Verkhovsky et al. that neither cell body nor microtubules are involved in the crawling motion. In fact, fragments of keratocytes lacking the nucleus (Verkhovsky et al., 1999) or cells with depolymerized microtubules (Euteneuer and Schliwa, 1984) can migrate in the same way than as a normal cell. As cytoplasmic fragments are able to migrate by themselves, it suggests that the lamellipodium is the essential machinery for crawling motion.

Keratocytes move rapidly (~20 µm/min) in a persistent direction perpendicular to their long axis without any external cue to guide them. They are well coordinated, with the protrusion at the leading edge tightly coupled with retraction of the trailing edge, maintaining a constant shape, area and speed (Keren et al., 2008). The Graded Radial Extension (GRE) is a model which kinematically explains the conservation of the shape for polarized cell motion (Lee et al., 1993). The GRE model proposed that cell extension along the leading edge locally occurs in a direction perpendicular to the cell edge, with an extension rate (distance extended per unit of time) graded from maximal in the middle of the leading edge to minimal at the sides. This explain how cell maintains its overall shape and curvature of the leading edge during migration.

The lamellipodium contains actin network undergoing treadmilling, with assembly at the leading edge and disassembly of filaments at the rear. As the filaments are growing, they push continuously the membrane forward and the protrusion keeps moving. At the same time, in keratocytes, like in most crawling cells, a retrograde flow of actin filaments is observed. After the polymerization of actin near the leading edge, the F-actin network is moving backward (retrograde flow). This mechanism is driven by the forces produced in the lamellipodium by the actin polymerization in one hand and by the myosin II activity in the back of the cell (Ponti et al., 2004). Moreover, as actin filaments are linked to the focal adhesions, the retrograde flow slows down at the adhesive regions (Gardel et al., 2008). Thus, protrusion velocity is equal to the rate of actin polymerization minus the rate of retrograde flow and, in consequence, an inverse relationship is observed between protrusion and actin flow (Vallotton et al., 2005). The maintenance of the cell shape and velocity depends on the regulation of both actin polymerization and retrograde flow (Grimm et al., 2003) (Keren et al., 2008) (Barnhart et al., 2011).

2.5.2 Polarized organization of the cytoskeleton during motion in keratocytes

During crawling motion, the cytoskeleton of fish keratocyte is organized in a polarized manner. The density of the actin cytoskeleton decreases from the cell front to the back. At the leading edge, the protrusion is powered by a dense actin meshwork in the lamellipodium, becoming less dense until it organized in transversal (with respect to the cell motion) bundles at the boundary between the lamellipodium and the cell body (fig 2.8.A). Myosin II co-localized with actin in the boundary bundle (fig 2.8.C) but its concentration is low at the very front of the cell. Myosin II is also present at the back of the cell (fig 2.8.B). So in order to migrate, actin and myosin II are organized in a polarized manner with a reverse gradient of the two within the cell and a co-localization at the boundary (fig 2.8.C inset).

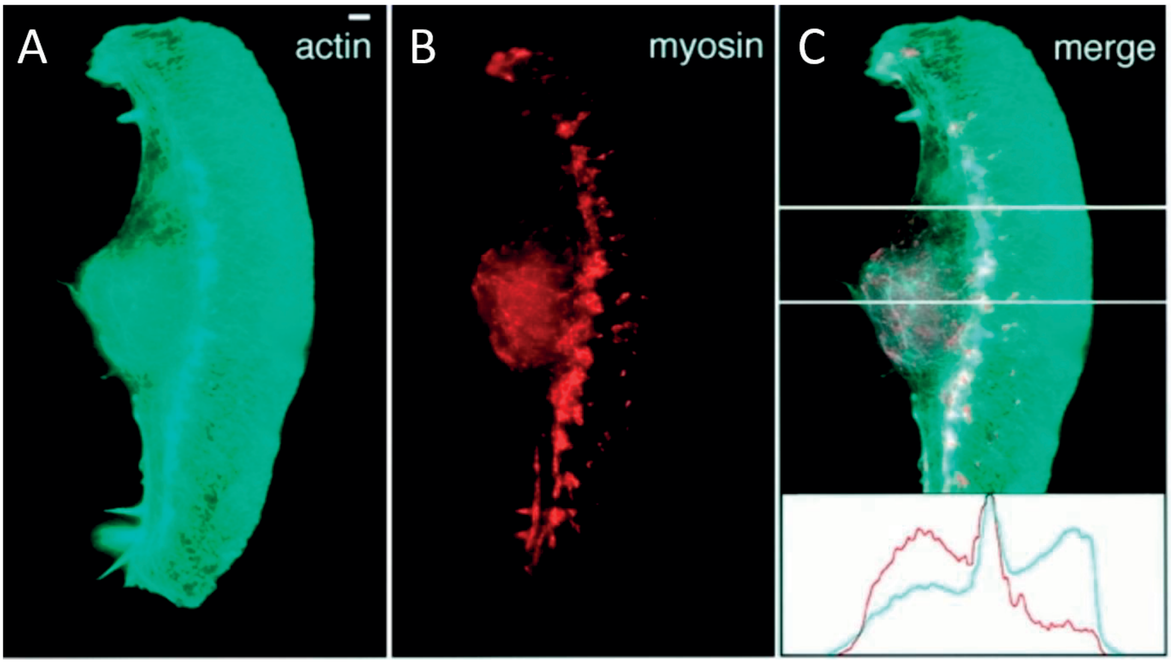

Fig 2.8: *Actin and myosin II localization in polarized fish keratocytes.* TRITC-phalloidin and indirect immunofluorescence staining show the distribution of respectively actin (A) and myosin II (B) in migrating keratocytes. The merge image (C) show a co-localization in the boundary bundle and a reverse gradients of actin and myosin II in the lamellipodium, as illustrated by the intensity profiles in the inset. Scale bar: 2 µm. (Svitkina et al., 1997)

2.6 Cell protrusion

Protrusion is the formation of membrane extensions, which are of different natures regarding cell types. They act like a sensor of the environment by continuously elongating and retracting, creating new adhesions with the substrate. They are useful to sense the neighboring domains before orienting the translocation of the entire cell in a new place. This is the case for the filopodia, a needle like structure formed by parallel actin filaments and highly dynamic (Raftopoulou and Hall, 2004). Lamellipodium is a more stable protrusion, thin, broad, sheet-like structure created at the front of the cell by cross-linked actin filaments. It is approximately 200 nm thick and several micrometers in width. This are the main protrusive structures in the cell which can generate forces by the dynamic polymerization of actin cytoskeleton which pushes the membrane forward (Carlier et al., 2003). The lamellipodium extends and attaches to the substrate by creating adhesions. If it does not attach, protrusion tends to move backward in response to the tension generated in the cell. This switch between protrusion and retraction is called membrane ruffling (Ridley, 1994). This dynamic of the lamellipodium is probably the most important protrusive process involved in crawling motion and its mechanism can be explained using the dendritic nucleation model.

2.6.1 The dendritic nucleation

The dendritic nucleation (Pollard, 2003) is a model that describes the molecular mechanisms controlling actin filament dynamic. It is used to understand the actin network growth at the front of the lamellipodium (fig 2.9), in order to explain the protrusion mechanism in crawling motion. This model is generally accepted, although not all details are known.

To maintain the treadmilling rate constant, the actin network is continuously reorganizing by means of the creation of new barded ends to allow the addition of actin monomers leading to the filaments elongation (Zigmond, 1996). The new actin filaments (daughter filaments) are nucleated at the side of pre-existing filaments (mother filaments) leading to the formation of a branching network (Mullins et al., 1998).

The process starts by the activation of receptors at the plasma membrane by external cues (fig 2.9.1). This activates inside the cell signaling pathways (fig 2.9.2) such as Rho GTPases family or PIP2. They activate in turn the nucleation-promoting factors WASp, N-WASp, Scar and WAVE (fig 2.9.3). This lead to the activation of the Arp2/3 complexes (fig 2.9.4). As mentioned previously, the Arp2/3 binds to the barbed end or to the side of the mother filament, initiating the growth of daughter filaments with a free barbed end (fig 2.9.5) pushing forward the membrane at the leading edge (fig 2.9.6). This complex is also responsible of the dendritic pattern of the actin network, by creating an angle of 70° at the Yjunction (Svitkina and Borisy, 1999) between mother and daughter filaments. The new filaments are rapidly growing toward the cell membrane, due to the presence of a profilin-bound actin pool in the cytoplasm.

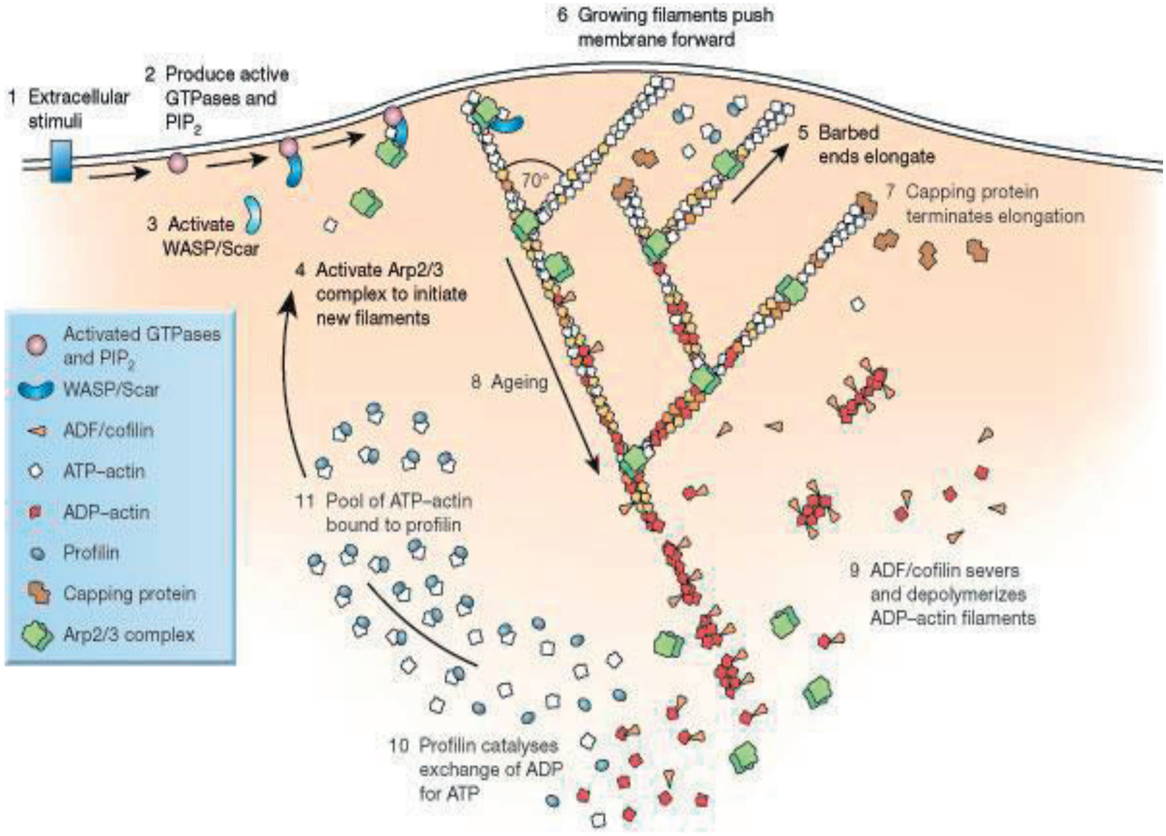
6 Growing filaments push membrane forward
1 Extracellular stimuli
2 Produce active GTPases and PIP2
5 Barbed ends elongate
70°
7 Capping protein terminates elongation
3 Activate WASP/Scar
4 Activate Arp2/3 complex to initiate new filaments
Activated GTPases and PIP2
WASP/Scar
ADF/cofilin
ATP–actin
ADP–actin
Profilin
Capping protein
Arp2/3 complex
8 Ageing
11 Pool of ATP–actin bound to profilin
9 ADF/cofilin severs and depolymerizes ADP–actin filaments
10 Profilin catalyses exchange of ADP for ATP

Figure 2.9: Dendritic nucleation model of lamellipodium protrusion. (1) External cues activate cell membrane receptors (2) which activate in turn signaling pathways such as the GTPases. (3) These then activate Wiskott-Aldrich syndrome protein (WASp) family, (4) which activate the Arp2/3 complex. (5) Active Arp2/3 binds on the sides of existing actin filaments to initiate a branch that grows rapidly in the direction of the barded end. (6) The newly formed actin filaments grow and push the membrane forward. (7) To terminate the elongation, capping proteins bind to the growing ends. (8) The ADP-filament parts present in the older regions of the filament (9) are then served and depolymerized by the actin-depolymerizing factor (ADF)/cofilin. (10) Profilin binds to the ADP-actin subunits to catalyze exchange of ADP for ATP. (11) This forms a new pool of ATP-actin binds to profilin and available for assembly. (Pollard, 2003)

The presence of capping proteins stops the elongation process (fig 2.9.7) by binding on the barbed end of the growing filaments. Then, the oldest filaments containing ADP-actin (fig 2.9.8) are depolymerized with the help of ADF/cofilin proteins (fig 2.9.9). Profilin, which competes with ADF/cofilin for binding ADP-actin, promotes dissociation of ADP and binding of ATP to this dissociated subunits (fig 2.9.10).

Thus, profilin maintains a pool of actin monomers (fig 2.9.11) ready to re-enter into the cycle of the growth of actin filaments. With the help of the hydrolysis of ATP-bound actin, the energy is converted into mechanical force through the constant polymerization/depolymerization of actin filaments. When assembly and disassembly of actin filaments are balanced the crawling motion can happen in a continuous way leading to a directional cell migration.

2.6.2 Protrusive forces

To create and extend lamellipodium, the cell needs to produce forces to push the membrane forward, in a regular and coordinated way. Actin assembly is able itself to push the cell membrane. This protrusive force development has been explained with different models such as the ratchet model or the swelling of actin gel (Marcy et al., 2004) (Dayel et al., 2009).

2.6.2.1 Brownian ratchet model

The Brownian ratchet model was proposed originally by Peskin et al. to explain how a growing polymer (in our case the actin filament) can produce an axial force (Peskin et al., 1993). In this model, the actin polymerization at the leading edge can happen thanks to membrane oscillation due to Brownian motion. Actin filament is considered as a stiff polymer pushing the load (i.e. the cell membrane) that is moving because of thermal vibrations (fig 2.10.a1). The gap created between the growing filament tip and the membrane is sufficient to allow a new monomer to bind to the filament (fig 2.10.a2) and this addition pushes the membrane forward (fig 2.10.a3). By consequence, the polymerization rate is directly proportional to the diffusion coefficient of the load, which is responsible of the formation of the gap and inversely proportional to the size of the monomer to incorporate.

However, this model has a limitation due to the assumption that filament is a rigid structure. However, filaments can bend (fig 2.10.b2). To take this into account, Mogilner and Oster suggested to introduce the notion of flexibility in the original model and propose the *elastic Brownian ratchet* model (Mogilner and Oster, 1996). In this configuration, both actin filament and membrane load are subject to thermal fluctuation: the filament bends and the membrane fluctuates simultaneously, creating a spatial gap for actin monomer addition. Then, the relaxation of the elongated filament pushes the membrane forward (fig 2.10.b3).

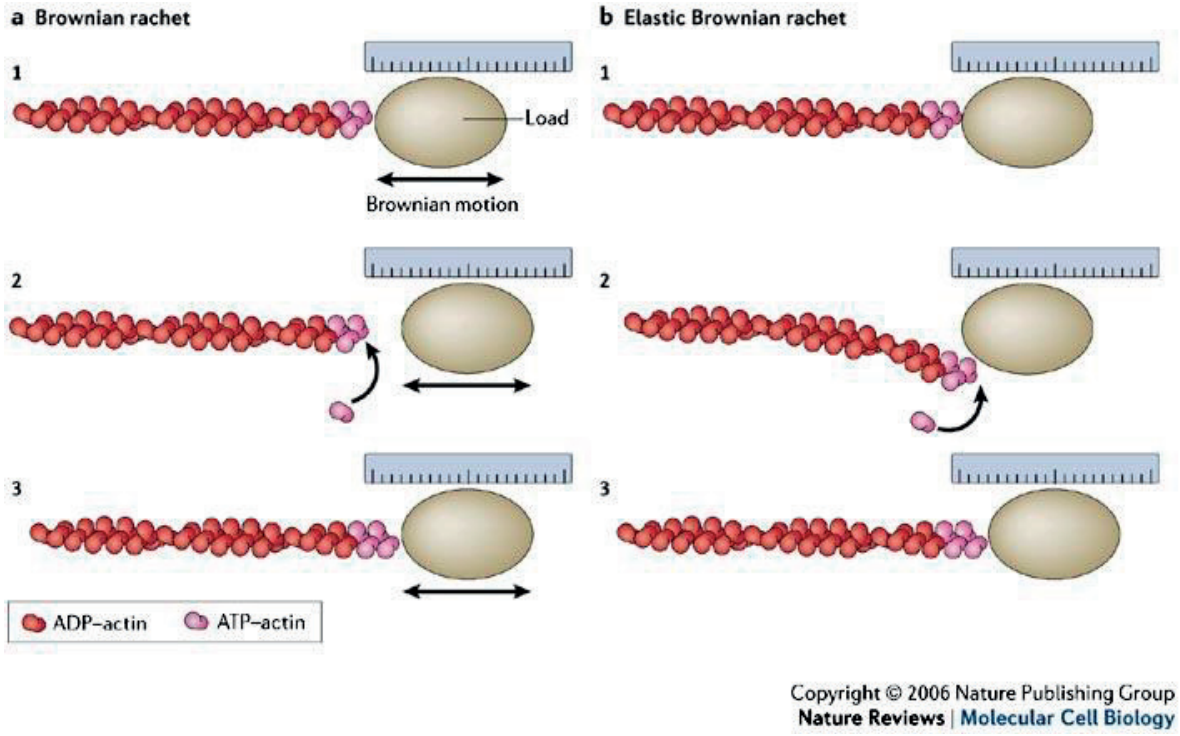
a Brownian rachet
1
Load
Brownian motion
2
3
ADP–actin
ATP–actin
b Elastic Brownian rachet
1
2
3
Copyright © 2006 Nature Publishing Group
Nature Reviews | Molecular Cell Biology

Figure 2.10: The Brownian ratchet models. (a) Brownian ratchet: the load (1) undergoes Brownian motion due to thermal fluctuation. This phenomenon creates a gap between the filament (red) and the load (2), which is in our case the plasma membrane. The space allows an actin monomer (pink) to bind at the tip of the filament. This addition elongates the filament (3) which pushes the load forward. (b) Elastic Brownian ratchet: this modified model include the mention of elasticity. In this case, the filament is flexible (2) and can bend to provide the space for monomer addition. The elastic energy then pushes the load forward after filament elongation. (Kaksonen et al., 2006)

2.7 Cell retraction

We have seen how actin polymerization generates protrusion forces at the cell front. At the same time, the back of the cell has to retract to complete cell motion. Retraction could be driven by different mechanisms including the contraction of actomyosin network, actin depolymerization and membrane tension (Cramer, 2013). In the model system of fish epidermal keratocytes, *dynamic network contraction* model developed by Svitkina and co-workers explains how myosin is thought to pull actin filaments and generate forward motion of the cell body (Svitkina et al., 1997).

2.7.1 Dynamic network contraction

The model is based on the continuous assembly and contraction of the actin-myosin network. In the lamellipodium, clusters of interconnected myosin II bipolar minifilaments are formed spontaneously and bind to actin filaments (fig 2.11.a). At the leading edge, the actin network is dense and rigid so the myosin cannot move along the filaments. As described previously, the actin concentration decreased towards the cell body and myosin concentration increases. In this sparse actin network, myosin II can translocate the filaments (fig 2.11.b) which lead to the formation of transverse bundles (fig 2.11.c). Actomyosin bundles move forward with respect to the lamellipodium and so the cell body, which is linked to the contracting network in the transition zone, is also moving relatively to the lamellipodium. The pulling action on the cell body is produced by the continuous compression of the network which, due to its orientation, leads to the generation of forces along the anterior-posterior axis.

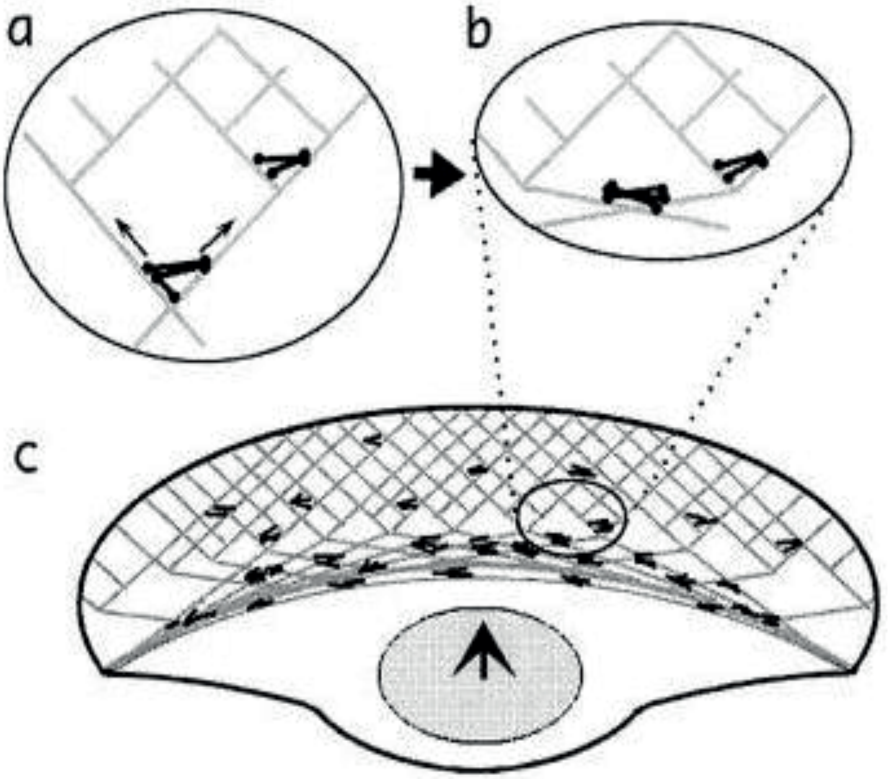

Figure 2.11: The dynamic network contraction model. In the lamellipodium (a), myosin filaments (black) interact with the actin network (gray lines). Close to the front, the myosin clusters are small in a dense network and so they cannot move. Moreover, in the transition zone the network is sparse and bigger clusters of myosin can interact and move forward (b) approaching the barbed ends of the actin filaments. This process results in the formation of actomyosin bundles in the transition zone (c) parallel to the leading edge, and leads in the forward translocation of the cell body. (Svitkina et al., 1997)

2.8 Cell adhesion

Cell adhesion is the physical interaction of a cell with a neighboring cell (cell-to-cell) or with the extracellular matrix (cell-to-matrix). With the help of specific multiprotein complexes, the cell can create adhesions to support tissue integrity, provide stability and rigidity, stabilize cell position and regulate motility (Lock et al., 2008). They play a central role in the cellular communication through the generation and transduction of mechanical signals. Cell adhesions are functional extensions of the cytoskeleton, so it is a highly dynamic structure. They are mediated by transmembrane cell-adhesion molecules (CAMs).

Cell adhesion is a crucial event in crawling motion, which connects the actomyosin network to the extracellular matrix (ECM) to enable the generation of traction forces promoting cell movement. Adhesion size, composition and morphology vary, but they all contain integrins. Integrins are transmembrane receptors composed of α and β-subunit (Humphries, 2000), each penetrating the plasma membrane and possessing small cytoplasmic domains. Integrins allow the cell connect the proteins of extracellular matrix (ECM) such as fibronectin (fig 2.12.A), to the actin cytoskeleton inside the cell. They play a crucial role in signal transduction, which allows the cell to sense the surrounding environment in order to change shape and migrate.

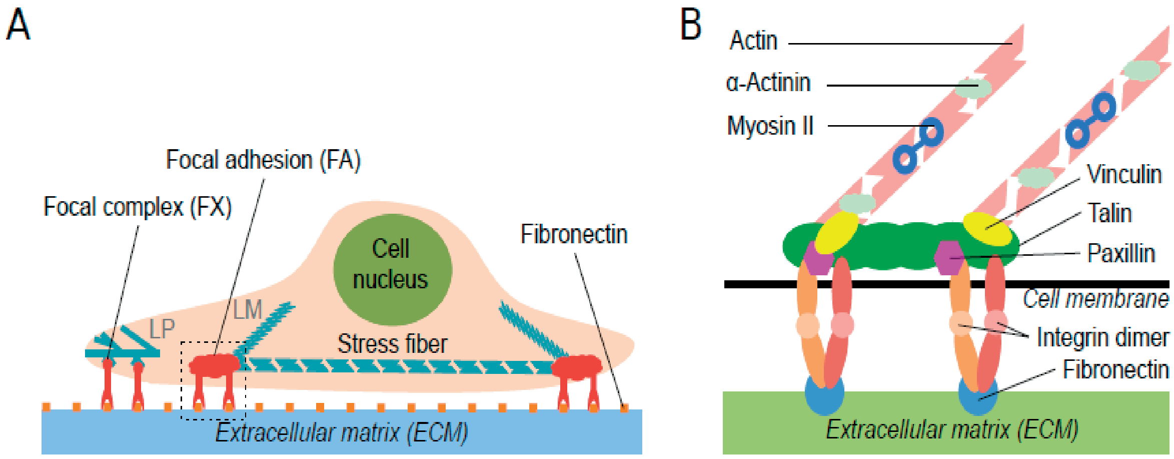

Figure 2.12: Schematic of focal adhesions organization. (A) The cell adheres to the extracellular matrix (ECM) by means of adhesions. Fibronectin, a ligand presents on the ECM, allows the cell to adhere through nascent adhesions. In the lamellipodium (LP) the adhesions are in the focal complexes stage, where they can then mature in the lamella (LM) into focal adhesions. This happens in response to traction forces applied on the adhesions which are connected to stress fibers. The ventral stress fibers connect one focal adhesion to another and the dorsal stress fibers link the focal adhesions to the actin network. (B) Focal adhesions are composed of transmembrane integrins which bind to the fibronectin on the ECM. Integrins are connected inside the cell to actin stress fibers through talin. There is also proteins, such as vinculin or paxilin, which enhance the basic mechanical link of integrin with actin filaments. (Hoffmann and Schwarz, 2013)

During migration, there are mainly two classes of adhesions depending of their functions and position in the cell: focal complexes and focal adhesions. Focal complexes are adhesions in the early stage of maturation. Mechanically, they differ from focal adhesions by the lower force magnitude that they can support before detaching. There are dot-like nascent adhesions and small punctate adhesions, larger than nascent one, present at the boundary of the lamellum and lamellipodium (Giannone et al., 2007). In addition to integrins, focal complexes contain adapter proteins such as vinculin or paxilin (fig 2.12.b). If the focal complexes does not maturate, they are disassembled as the lamellipodium withdraws. However, they become focal adhesions by maturating into larger and stable structures (Zaidel-Bar et al., 2004). Then, focal adhesions remain stationary with respect to the ECM and the cell can generate forces in order to migrate. When the lamellipodium has move enough and the adhesions position is close to the trailing edge, focal adhesions are dissolved. The maturation of focal adhesions is controlled by the Rho-GTPase family. The focal complexes are initiated by clustering of integrin molecules in a process depending on Rac GTPase. Then, the control of the growth and stabilization of the focal adhesion is based on the Rho GTPase which activate myosin promoting force-dependent adhesion maturation.

2.9 Force generation during cell migration

During crawling motion, cells generate forces in order to migrate. As described previously, they generate internal forces, which can be divided into two types: the protrusive forces needed to push the membrane at the leading edge in order to extend the lamellipodium and the contractile forces which allow the retraction of the back of the cell. Stress produced by the cell is transmitted to the substrate through adhesions: these forces are called traction forces and are essential to move over the substrate.

2.9.1 Traction forces

The cell has to adhere to the substrate in order to apply forces against the external matrix that pull the cell body forward. These forces are generated by both actin retrograde flow against the membrane and actomyosin contraction.

In migrating keratocytes, it has been shown (Oliver et al., 1999) that traction forces are mainly localized at the sides of the cell, perpendicularly to the direction of motion. At the leading and trailing edge, traction forces are small. This indicates that the side of the cell are strongly attached to the substrate. At the cell sides, force transmission results from the friction between a slipping actin network and the substrate. In contrast, the stress at the front is transmitted partially independently of actin velocity, indicating a sort of gripping of the actin network to the substrate (Fournier et al., 2010).

2.9.2 Cell traction forces measurement methods

Cell traction forces are defined as tangential tensions exerted by the cells to the underlying substrate. This force transmission is essential for cell shape maintenance, mechanical signal generation and in particular for cell motility. In crawling cells, the magnitude and distribution of traction forces is important for the velocity, directionality and efficiency of the migration. For these reasons, the quantification of the traction stress is crucial in the study of cell motion. To measure the traction forces that the cell applies on the substrate, different techniques can be used, as described in the next sections.

2.9.2.1 Cell-populated collagen gel

In this method, cells are embedded into a collagen gel disk, usually bovine collagen type I. The traction stress developed by the embedded cells induces the deformation of the collagen gel. The decrease in the diameter of the gel disk is then used to determine cell traction forces (Moon and Tranquillo, 1993). This method allows the measurement of traction forces generated by a population of cells. It is a qualitative tool for cell traction force assay but it does not allow the measurement of the traction forces of individual cells.

2.9.2.2 Thin silicon membrane

This method is based on the use of thin silicon membrane to measure cell traction forces. It comes from the observation of Harris and co-workers (Harris et al., 1981) who showed for the first time that fibroblasts generate forces, by discovering that cells create wrinkles on thin silicon membrane.

Burton and Taylor (Burton and Taylor, 1997) developed this technique to apply it to the single cell traction forces quantification (fig 2.13). With the use of a flexible microneedle, the wrinkles caused by the cell are reversed to estimate the force generated. The deformation of the needle needed to recover the wrinkles is measured, and as the flexibility of the microneedle is known, the traction force of the cell can be calculated.

Nevertheless, the wrinkling present a non-linear problem and there is no computational methods to accurately predict the wrinkles caused by a complex, non-isotropic cell traction force field. This implies that absolute values of local forces cannot be measured and it only reflects overall cell stress.

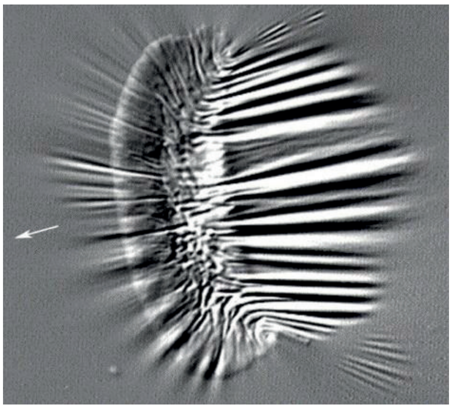

Figure 2.13: *Traction forces of fish keratocyte on a thin silicon membrane*. The keratocyte can attach and migrate on the silicon membrane. As it applies forces, the rubber substrate wrinkles. White arrow indicates direction of migration. (Beningo and Wang, 2002)

2.9.2.3 Force sensor array

Using microfabrication lithography, an array of microspot force sensors can be fabricated. These structures are cantilever beams which bend under traction forces applied by the cell (fig 2.14). Knowing the flexibility of the microstructures, the traction forces are calculated based on the beam deflection-force relationship (du Roure et al., 2005).

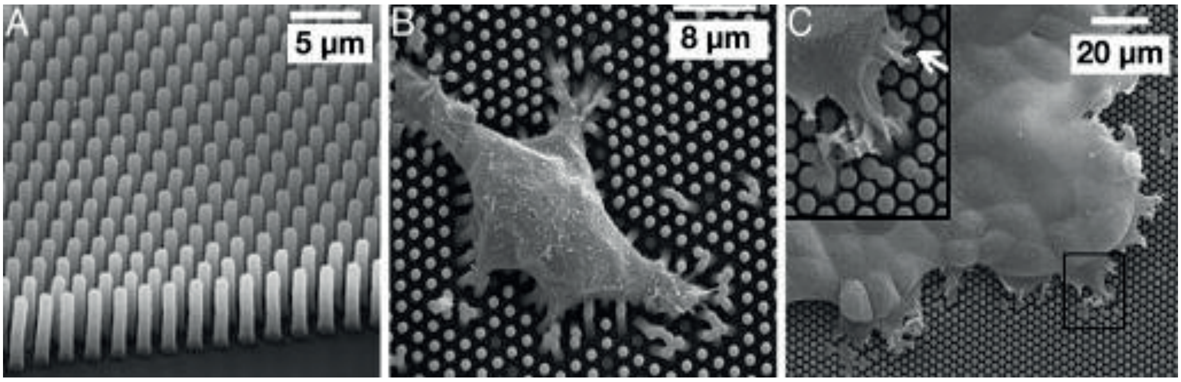

Figure 2.14: *Force sensor array method.* These images are obtained by scanning electron microscopy (A) Silicon (PDMS) molding of microspots closely spaced. (B) Individual cell on force sensor array (1 µm diameter and 2 µm distance center-to-center). (C) A cell monolayer on cantilever beams (2 µm diameter and 3 µm distance center-to-center). (C *inset*) Magnified view of the black square area: cells are spreading and make adhesions only on the top of pillars. (du Roure et al., 2005)

This technique allows to measure independently local force, as each microspot works as an individual force-sensor unit. However, when using the highly flexible beams to enable the detection of small forces, in order to measure the highest forces applied by the cell, the cantilever beams have to be spaced enough, which reduces the spatial resolution.

2.9.2.4 Traction force microscopy

This experimental method uses a continuous gel substrate to register the deformation that the adhesive cell induces. The gel is usually polyacrylamide that is coated with extracellular proteins such as fibronectin, allowing the cell to attach and spread on the surface, or gelatin substrate. Fluorescent microbeads are put inside the polymerized gel to enable the tracking of the gel deformation under traction stress. The spatial resolution is given by the concentration and dimensions of the fluorescent beads and the deformation resolution can be modulated by changing the gel stiffness, as polyacrylamide or gelatin are highly compliant substrate. For these reasons, traction force microscopy (TFM) allows the highest spatial resolution to measure deformation. This method allows the local measurement of tractions stress exerted by a single motile cells.

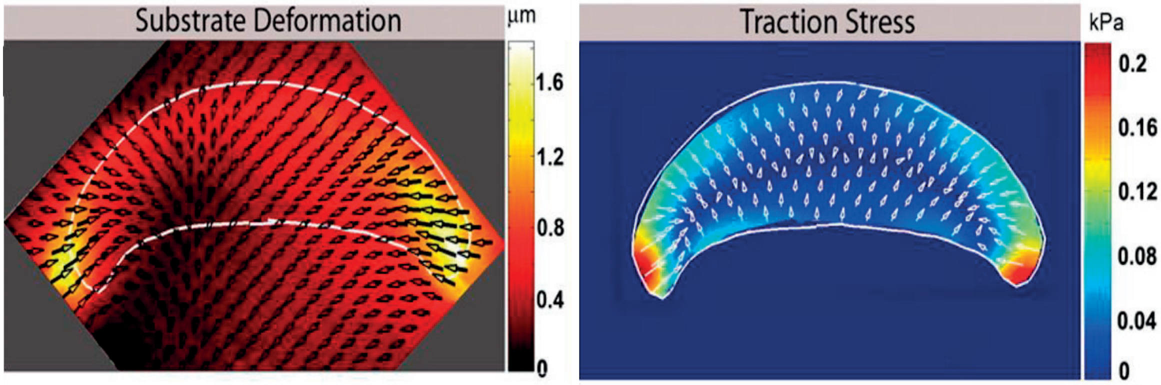

Figure 2.15: Force transmission in keratocyte migrating cell. The substrate deformation map (left) of a deformable gel is used to calculate the traction stress map (right) of a migrating fish keratocyte. Arrows indicate the direction and relative magnitude of deformation field and traction stress. (Fournier et al., 2010)

In order to get the forces applied by the cell on the deformable gel, the displacement of the fluorescent beads is analyzed. For that, the substrate is divided on small regions and the correlation between the undeformed and the deformed state of the gel gives the local displacement of beads (Dembo and Wang, 1999). From this displacement field, it is possible to obtain a traction stress map with the knowledge of the stress-strain behavior obtained with the gel rigidity.

This method provides the most reliable and comprehensive information on cell traction force. This is a common approach to study traction stress of crawling cell and it enables the study of forces during fish keratocyte motion (fig 2.15).

2.10 Membrane tension

Cell motility is powered by the dynamics of the cytoskeleton, which is in close proximity to the plasma membrane. Membrane generates a tension on the surface which is related to the force that is needed to deform it. In motile cells, membrane tension applies a force (fig 2.16.A) that resists actin polymerization (Keren et al., 2008). Membrane tension is in most cases constant along the surface, and a local perturbation is quickly compensated by membrane flow to maintain an isotropic membrane tension (Kozlov and Mogilner, 2007). Exception are rapidly moving cells, such as keratocytes, where continuous membrane flow is associated with a gradient of membrane tension (Lieber et al., 2015).

Temporary variation of membrane tension happens in several processes. Events such as blebbing, endo- and exo-cytosis or cell swelling and shrinking involve local or global membrane surface deformation. Endocytosis is generally promoted by a decrease of membrane tension (fig 2.16.B), and inversely exocytosis is promoted by an increase of the tension (Boulant et al., 2011). Cell shrinking or swelling changes the membrane tension, which induces the creation or flattening of membrane invaginations to regulate the global tension (fig 2.16.C).

To estimate and manipulate cell surface tension, there exist many techniques. The most common methods is the use of optical tweezer: membrane tethers (cytoplasmic extension without continuous cytoskeleton) is pulled out of the cell surface and the force needed to extract them is recorded. This force is directly related to the membrane tension. In motile cells such as fish keratocytes, membrane tension is tightly coupled to the cytoskeletal activities such as protrusion, adhesion and retraction (Lieber et al., 2013). As membrane tension is a load which counteract filaments growth, it controls and regulates actin protrusion in the way that lowering membrane tension is expected to increase protrusion and an increase in the tension would decrease membrane extension or promote retraction.

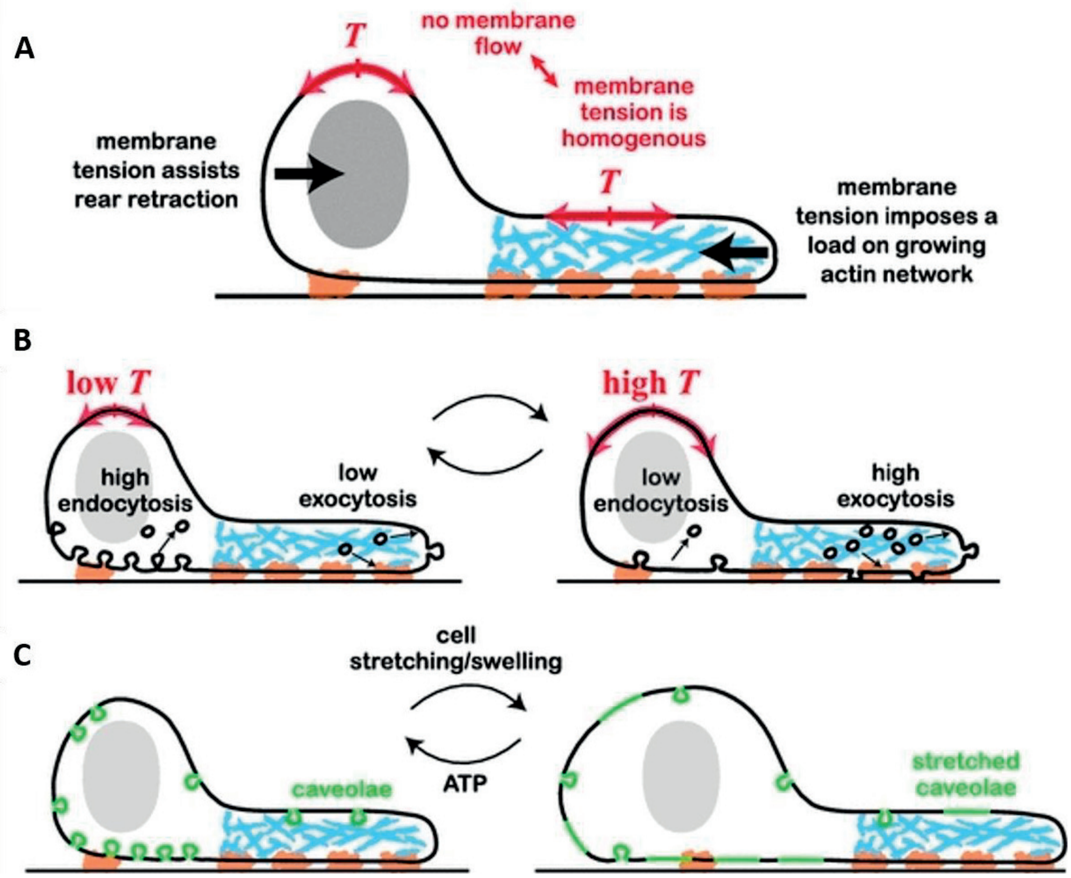
A
T
no membrane flow
membrane tension is homogenous
membrane tension assists rear retraction
T
membrane tension imposes a load on growing actin network
B
low T
high T
high endocytosis
low exocytosis
low endocytosis
high exocytosis
C
cell stretching/swelling
caveolae
ATP
stretched caveolae

Figure 2.16: Membrane tension in crawling cell. (A) Membrane tension exerts forces perpendicular to the cell boundary (black arrows). If there is no membrane flow, the tension T is spatially homogeneous. Actin network growth is opposed to the membrane tension at the leading edge, while for the back of the cell the membrane tension helps for the retraction. (B) Decrease of membrane tension leads to an increase of endocytosis rate. And increase of the tension leads to an increase of exocytosis rate. (C) If the cell is swelling or stretching, it produces a rapid increase on tension, which is buffered by rapid flattening of the caveolae, providing additional surface area. (Keren, 2011)

2.11 Cell polarization

To move directionally, the cells have to polarize, i.e. make a transition from a stationary and approximately round symmetric state to the anisotropic migrating state. Before polarization, the cell edge fluctuates, doing alternatively protrusions and retractions all around the cell periphery. These protrusion-retraction fluctuations are thought to serve an exploratory purpose and were investigated in many studies (Ryan et al., 2012) (Allard and Mogilner, 2013). This activity is believed to be related to eventual polarization, but the exact relationship is not clear (Verkhovsky, 2015). Then to start motion, cells undergo a structural and cytoskeletal rearrangement resulting in a segregation of the activity of the edge in two separated domains: a front edge with protrusive activities and a rear with a prevalence of retraction. This polarized configuration can be maintained more or less persistently in time depending on the crawling cell type. In the case of keratocyte, the level of temporal coordination between the different steps leads to a smooth translocation of the cell, while the movement is more irregular for the fibroblast cell type.

Cell polarization can occurs due to external directional signals that force the cell to polarize. It can be achieved with physical and chemical factors (chemotaxis) in the cell's environment, causing cell polarization and hence, migration in a specific direction. Dictyostelium and neutrophils normally polarize in response to chemoattractant gradient and move afterwards along it. However, as actin cytoskeleton has the intrinsic ability to break symmetry on its own, polarization can also happen spontaneously (Verkhovsky et al., 1999) in the absence of any spatial cues, thus in random direction. To explain spontaneous emergence and subsequent maintenance of the polarized organization of the cytoskeleton and cell edge activity, the mechanism involving feedback at different levels have been suggested. One class of the mechanisms involves feedback between regulatory signaling components through reaction-diffusion mechanisms, while another class comprises different types of mechanical feedback at the level of the cytoskeletal machinery, e.g. feedback between actin flow and contractility or between membrane tension, shape and edge dynamics.

2.11.1 Signaling networks

Positive and negative feedback loops may stochastically activate signaling pathways controlling protrusion and retraction, so that at some point the isotropic state becomes unstable. This intrinsic regulation is enabled through different signaling pathways involving proteins as the small GTPases of the Rho-family. Rho GTPases are small guanosine triphosphatases (GTPases) of the Ras superfamily, which act as molecular switches between an inactive GDP-bound and an active GTP-bound form. Rho GTPases are present in all eukaryotic cell and are important for several process (Etienne-Manneville and Hall, 2002) by interacting with downstream effectors to generate various intracellular responses. In mammals, the Rho family contains 20 members, Rho, Rac and Cdc42 being the most extensively studied (Raftopoulou and Hall, 2004). Rho is involved in the assembly of contractile actin-myosin II bundles, also called stress fibers and in the formation of focal adhesions. Rac participates in the formation of lamellipodia at the cell periphery to promote membrane fluctuation. And Cdc42 promotes the formation of filopodia protrusions. Members of Rho GTPases family act like key molecular regulators of the organization of actin cytoskeleton and by consequence, of the mechanism of cell polarization and subsequent migration. Due to their cycle between active and inactive form, GTPases can be involved in reaction-diffusion mechanism which can amplify and sustain cell polarization. Recent model based on Rho GTPases and their interaction with phosphatidyl inositol signaling system (Marée et al., 2006) explained how the cell polarity can emerge in fish epidermal keratocytes and how they maintain their polarized shape. However, in this model a strong externally imposed gradient is necessary for initiation of polarity, which subsequently can be maintained independently of the gradient. Unlike chemotactic cells like neutrophils and Dictyostelium, so far there is no experimental evidence that small GTPases are indeed involved in spontaneously polarizing keratocytes.

2.11.2 Actin flow

While in chemotactic cells, the polarization is initiated at the front (Servant et al., 2000), spontaneous polarization could be due to the events at the back of the cell. For epidermal fish keratocytes, a study showed that polarization is driven by contraction and initiated at the prospective cell rear and the perinuclear region (Yam et al., 2007). Initially, the cell is stationary displaying small oscillation at the edge, but largely an isotropic shape (fig 2.17.a). The authors reported an increase in the actin filaments flow speed associated with the prospective trailing edge (fig 2.17.b) inducing a retraction of the back of the cell, without significant changes in the leading edge. After this retraction step, the back is completely collapsed and the front starts to protrude showing a net polymerization of actin filaments (fig 2.17.d). The same mechanism was observed in fibroblast (Cramer, 2010), where cell migration starts with retraction at the back of the cell, creating the cell rear first, followed by development of the lamellipodium at the front (Mseka and Cramer, 2011).

How does the actin flow promote polarization? Early work (Verkhovsky et al., 1999) suggested that the flow and the cell motion itself could be a part of the feedback loop maintaining and reinforcing cell polarity. This idea was tested and reinforced in a recent study (Maiuri et al.) that reports a universal coupling between speed and directional persistence in many types of migrating cells, resulting from a positive feedback loop between actin flows and cell polarity. This feedback likely works by concentrating myosin II through the flow to the back of the cell where it promotes contraction and favors continuing movement in the same direction. Another recent study (Barnhart et al., 2015) implicated two feedback loops involving actin flow in polarization of fish keratocytes. One is a negative feedback between actin flow and adhesion, where fast flow weakens adhesion which further reinforces the flow. This relationship cooperated with positive feedback between actin flow and myosin contractility, where flow concentrated myosin II while myosin contractility reinforces flow.

General weakness of the models of this type is that the cell has to be already moving, or actin flow should be already strongly asymmetric for the feedback mechanism to start working. Consequently, these models cannot fully explain the initiation of polarization and cannot relate it to the previous oscillatory dynamics in the isotropic state, in particular, in (Barnhart et al., 2015) model a very strongly spatially and temporally correlated perturbation was necessary to induce polarization.

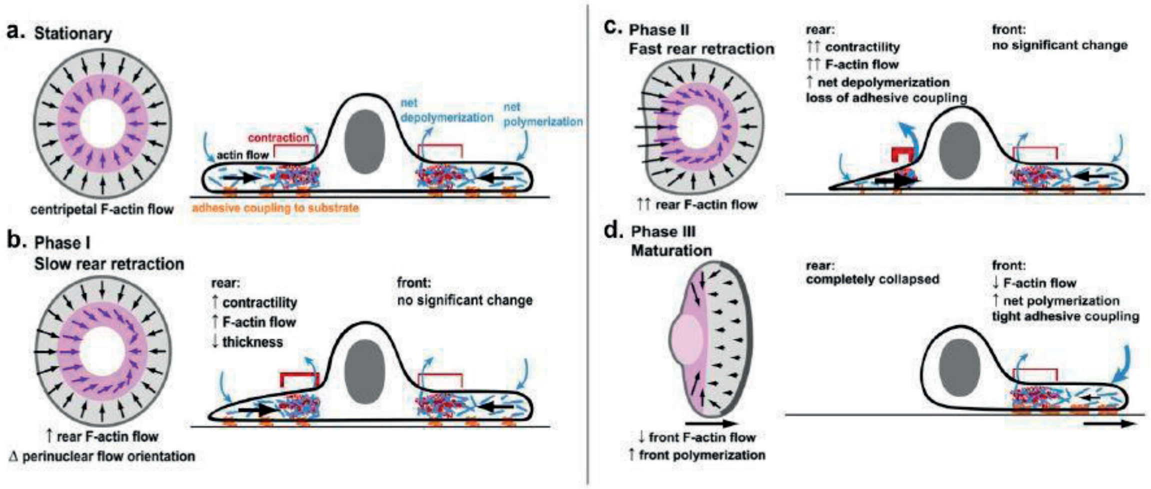
a. Stationary
centripetal F-actin flow
contraction
actin flow
net depolymerization
net polymerization
adhesive coupling to substrate
b. Phase I
Slow rear retraction
rear:
↑ contractility
↑ F-actin flow
↓ thickness
front:
no significant change
↑ rear F-actin flow
Δ perinuclear flow orientation
c. Phase II
Fast rear retraction
rear:
↑↑ contractility
↑↑ F-actin flow
↑ net depolymerization
loss of adhesive coupling
front:
no significant change
↑↑ rear F-actin flow
d. Phase III
Maturation
rear:
completely collapsed
front:
↓ F-actin flow
↑ net polymerization
tight adhesive coupling
↓ front F-actin flow
↑ front polymerization

Figure 2.17: Model for symmetry breaking and motility initiation in keratocytes. (a) Arrows represent the F-actin network flow in the peripheral (gray) and perinuclear (purple) regions. The cell cross-section of stationary shows that the flow is centripetal, driven by a net actin polymerization at the periphery and by myosin contraction and met actin depolymerization in the perinuclear region. (b) Perinuclear contractility causes an increase in the F-actin network flow speed at the prospective cell rear and partial polarization of the perinuclear F-actin network flow in the direction of cell movement. The rear edge retracts slightly and decreases in thickness. (c) Increase in F-actin network flow speed at the prospective cell rear, caused by an increase in perinuclear contractility, leads to a huge retraction and a loss of adhesion at the back of the cell. (d) Finally, perinuclear actin bands are transformed into an actin axle. F-actin flow speed at the cell front decreases relative to the substratum, whereas the adhesive coupling to the substrate and net F-actin polymerization increases. This leads to protrusion of the front edge, and the entire cell moves rapidly and persistently (Yam et al., 2007).

2.11.3 Membrane tension and cell shape

A recent study on neutrophil migration (Houk et al.) suggests that once the leading edge is established, protrusive activity in the other part of the cell is suppressed due to membrane tension. This indicates that membrane tension can play a role in the establishment of cell polarity, even if it is not clear why in this case tension does not suppress also protrusion at the leading edge. Moreover, since in rapid migrating cells there is a gradient of membrane tension with the highest tension at the front (Lieber et al., 2015) this tension is more likely to suppress protrusion at the front rather than in other parts of the cell. A mechanism of how membrane tension could act locally was suggested by our recent study (Gabella et al.) which considers the cell edge as a triple interface between the cell membrane, substrate and extracellular medium. Modifying the local tridimensional shape of the cell edge changes the component of membrane tension acting in the substrate plane and consequently influences the load on actin polymerization and thus the protrusion rate. Retraction and rounding the cell would decrease the load and promote protrusion, while spreading and flattening the cell would have the opposite effect. This hypothesis suggests a feedback between tridimensional cell shape and edge dynamics which could participate in the oscillatory protrusion-retraction behavior as well as cell polarization.

3) Materials and Methods

All the abbreviations for the chemical products are explained at the end of Materials and Methods (3.11 Glossary).

3.1 Cell culture

Fish epidermal keratocytes were obtained from Black Tetra fishes, by extracting fish scales with tweezers, placing them on a dry glass coverslips or directly onto the polyacrylamide gel, and allowing to adhere for 30 to 60 seconds to prevent floating. DMEM culture medium (DMEM, HEPES modification, high glucose; Sigma-Aldrich, St. Louis, MO, USA) supplemented with 20% of FBS, fungizone (Ampotericin B 250 µg/ml, Gibco), gentamicin, penicillin (100 units/ml, Life Technologies Corp.) and streptomycin (100 ug/ml, Life Technologies Corp.) was then added and the keratocytes were allowed to migrate overnight at 30°C to form colonies onto the substrate. To obtain free locomoting keratocytes, cell colonies were treated with EDTA (85% PBS and 2.5 mM EDTA, pH 7.4) (Yam et al., 2007) for few minutes and part of the cells were removed by pipetting in order to have individual cells not in contact with each other. In the case of Trypsin individualization, colonies on glass coverslip were treated with Trypsin (0.25 Trypsin-EDTA, Sigma-Aldrich) for few minutes, detached by pipetting, transferred onto the gel surface and let adhere for 1-2 minutes before adding culture medium. Work with fishes was performed according to the protocol approved in animal work license number 2505.

3.2 Microscopy

3.2.1 Phase-contrast and fluorescence microscopy

Phase-contrast and fluorescence microscopy were performed on an inverted microscope (Eclipse T*i*, Nikon) with either Nikon Plan Apc 60x, NA 1.4 Oil or Nikon Plan Fluor 100x, NA 1.3 Oil objectives. The images were acquired using a digital camera (C11440, Hamamatsu) operated with Visiview software (Visitron System). Fluorescence images were obtained using PhotoFluor II (89-North) illuminator with a 200 W metal halide lamp.

For traction force microscopy experiment, consecutive images of the cell using phase contrast and the beads using fluorescence were acquired at an interval of 10 s. The last image was taken when the cell was out of the field in order to have the undeformed state of the gel. For fluorescence bead acquisition, a Nikon Perfect Focus System was used in order to stabilize focus drift.

3.2.2 Scanning electron microscopy

Scanning electron microscopy (SEM) was used at the Center of Micronanotechnology at EPFL. SEM Zeiss Leo 1550 was used with a GEMINI column's electron source, which is a Schottky Field Emission type made of tungsten and Zirconium (ZrO_2). The sample image of topographic substrate (section 3.9) was acquired using the SE2 detector installed out of the column axis for a better topography visualization and a low acceleration of 1kV due to the insulating sample.

3.3 Cell treatment

3.3.1 Cytoskeleton inhibitors

- *Blebbistatin*: it is a cell-permeable inhibitor of the activity of the non-muscle myosin II. It is likely that blebbistatin binds the head domain, which opens and closes during myosin II cycle (described in chap.2.3.2). It is thought to stabilize the complex of myosin with ADP and phosphate, inhibiting the phosphate release that precedes the force generation. In our experiments, we used the active enantiomer (-)-Blebbistatin (Sigma-Aldrich): stock solution was dissolved in DMSO at 5 mg/mL and conserved at -20°C. For the experiments, stock solution was diluted in culture medium to a concentration of 100 μM.

- *Cytochalasin D*: it is a mycotoxin which is used as a cell-permeable inhibitor of actin polymerization. Cytochalasin D is believed to bind to the barbed end of microfilaments, as a capping protein, which prevents the addition of actin monomers and thus blocks actin polymerization. Stock solution of cytochalasin D (from *Zygosporium mansonii*, ≥ 98%, Sigma-Aldrich) was dissolved in DMSO at 1 mM and conserved at -20°C. For the experiments, stock solution was diluted in culture medium at a low concentration of 0.2 μM. This concentration reduces actin polymerization but does not disrupt actin network in the cell.

- *Nocodazole*: it is an antimitotic agent that disrupts microtubules by binding to the β-tubulin. Stock solution of nocodazole (Sigma-Aldrich) was dissolved in DMSO at 25 mM and conserved at -20°C. For the experiments, stock solution was diluted in culture medium at a concentration of 10 μM.

3.3.2 Hypo-osmotic treatment

Hypo-osmotic treatment was performed replacing the culture medium by the hypotonic solution: a dilution of 50% of regular culture medium with 50% water.

3.4 Immunostaining

Cell fixation of keratocytes was performed by replacing the culture medium by the fixative solution. The protocol differs depending on the specific staining.

Myosin staining: cells were fixed using 1% glutaraldehyde (G5882, Sigma-Aldrich) in regular medium for 5 min, following by an incubation for 10 min with 1% Triton (X-100, Sigma-Aldrich) in PBS buffer to permeabilize the cells. The excess of glutaraldehyde was inactivated by placing twice for 5 min the cells in a solution of 0.5% sodium borohydride (Fluka) in PBS. To reduce the non-specific staining the cells were then treated with 2% of BSA in PBS for 5 min. Cells were then incubated 45 min with the primary antibody anti-myosin light chain (ab2480, 1/400, abcam) diluted in a solution of PBS supplemented with 2% of BSA. Subsequently, cells were washed 3 times 5 min with PBS and incubated 45 min with the secondary antibody conjugated with Alexa-568 (A-11011, 1/200, Molecular Probes) for myosin staining and with Phalloïdin-Alexa-488 (A-12379, 1/100, Molecular Probes) to stain the actin filaments, in PBS-BSA. Samples were washed 3 times 5 min with PBS and fixed on 2 μL drops of PVA (Sigma-Aldrich) on a slide.

Vinculin staining: cells were fixed using 4% paraformaldehyde (paraformaldehyde, 16% w/v aq. soln., methanol free, Alfa Aesar) with 0.32 M sucrose in PBS for 15 min (Barnhart et al., 2011), following by an incubation for 10 min with 0.5% Triton in PBS buffer (Phosphate Buffered Saline) to permeabilize the cells. To reduce the non-specific staining the cells were then blocked using a solution of PBS-BT (3% BSA, 0.1% Triton-X100, and 0.02% sodium azide in PBS) for 5 min. Cells were then incubated 45 min with the primary antibody anti-vinculin (ab11194, 1/400, abcam) diluted in a solution of PBS-BT. Subsequently, cells were washed 3 times 5 min with PBS and incubated 45 min with the secondary antibody conjugated with Alexa-568 for vinculin staining (A-11004, 1/250, Molecular Probes), and with Phalloïdin-Alexa-488 (A-12379, 1/100, Molecular Probes) to stain the actin filaments, in PBS-BT. Samples were washed 3 times 5 min with PBS and fixed on 2 μL drops of PVA on a slide.

3.5 Polyacrylamide gel fabrication

Analysis of traction forces generated by keratocytes requires the use of flexible substrate, usually around 3 kPa for fast migrating cells (Lee, 2007). We decided to start with a rigidity of about 1.67 kPa (± 0.14, standard deviation). Then, we decided to work with rigid gels and we tested cell behavior on polyacrylamide gels with a rigidity of 4.47 kPa (± 1.19), 8.73 kPa (± 0.79), 16.70 kPa, 19.66 kPa (± 1.19) and 40.40 kPa (± 2.39). We selected 16.7 kPa gel for the experiments (see Results).

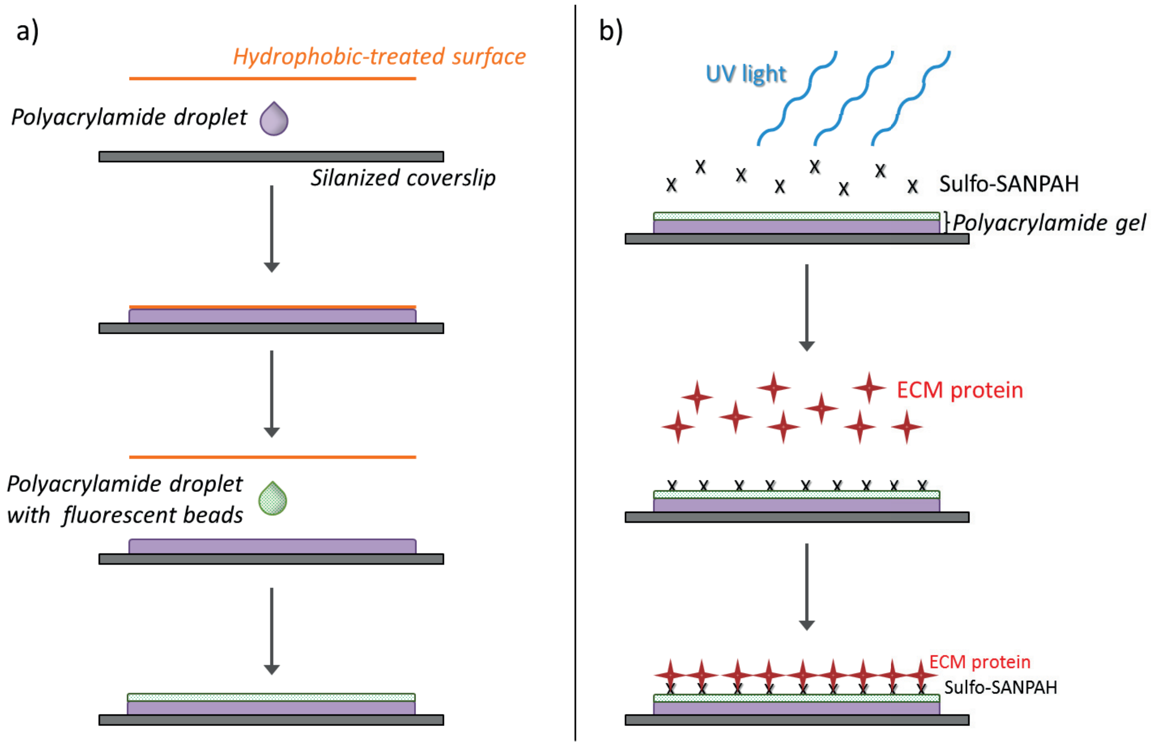
a)
Hydrophobic-treated surface
Polyacrylamide droplet
Silanized coverslip
Polyacrylamide droplet with fluorescent beads
b)
UV light
Sulfo-SANPAH
Polyacrylamide gel
ECM protein
ECM protein
Sulfo-SANPAH

Figure 3.1: *Preparation of polyacrylamide gel.* a) A drop of polyacrylamide is put on a silanized coverslip and let polymerize between it and a hydrophobic-treated surface. After polymerization, the hydrophobic surface is removed and the same step is repeated on the gel layer with a drop of polyacrylamide containing fluorescent beads. b) To coat the polyacrylamide gel with extracellular matrix protein, a cross-linker (Sulfo-SANPAH) is put on the gel and activated by UV light. Then, protein is incubated on the cross-linked gel.

The protocol of polyacrylamide gel preparation was adapted from Tse and Engler (Tse and Engler, 2001) and the gels were prepared according to the table of rigidities found in their paper and the rigidity was verified using atomic-force microscopy (AFM). To obtain gels allowing an observation of the cell with an inverted microscope and the detection of the fluorescence beads without bright background, the gel was done with two layers. For that, a support glass coverslip was treated 5 min with 0.1 N NaOH. Then, the coverslip was funzionalized with silane (APTMS, 97%, Sigma-Aldrich) for 3 min, thoroughly rinsed with water and placed at 37°C for 10 min. Coverslip were then treated with 0.5 %v glutaraldehyde

(G5882, Sigma-Aldrich) for 20 min and thoroughly rinsed. This functionalized coverslips can be kept for several days inside a vacuum desiccator.

To obtain the polyacrylamide gel, a mixture of acrylamide (A1089, AppliChem) and bis-acrylamide (66669, Fluka) in determined proportion depending on desired gel rigidity, was polymerized by adding TEMED (A1148, AppliChem) and 10% ammonium persulfate (Sigma-Aldrich). Other two coverslips were hydrophobically-treated with 10% Surfacil diluted in chloroform inside vacuum desiccator for 10 min.

The gel was polymerized between the functionalized coverslip and a hydrophobic-treated coverslip (the diameter of the coverslip will define the area of the gel) for 10 min. Hydrophobic coverslip was removed and the same procedure was done with polyacrylamide containing fluorescent beads. Then, cross-linker Sulfo-SANPAH (~1mg/mL, Thermo Scientific) diluted in water was put onto the gel and placed under an ultraviolet lamp for 10 min and rinsed. Fibronectin (Hu Plasma Fibronectin, 10 µg/mL, Merck Millipore) was incubated overnight at 4°C and the gel could be kept for a few hours in PBS until the experiment.

3.6 Traction force microscopy

Traction force maps were obtained from fluorescence images of the beads using algorithms taken from Tseng et al. (Tseng et al., 2011) working with ImageJ software. Particle Image Velocimetry (PIV) is a procedure based on template matching algorithms which divides the image into small regions (interrogative window, IW) and analyzes how each window is displaced compared to a reference image using cross-correlation. This process was repeated 3 times reducing the size of the IW at each step. The previous displacement vector is used as guidance. The final displacement vectors for all sub-images gives the global displacement field at each time-point. For the traction force microscopy images, the smallest window was 32px x 32px (2 x 2 μm^2). PIV was done independently for each frame, comparing it to a reference image of the unstrained gel taken after cells have been detached or left the field of view. Then Fourier Transform Traction Cytometry (FTTC) was used to calculate the traction force from the bead displacements.

3.6.1 Analysis of force map

In order to locally study the forces, the contour of the cell was drawn by hand using ImageJ software. Then the analysis was done using Matlab software. To define a band around the cell contour, the initial contour was resample with a defined number of points (usually 200 points) and was enlarged by offset of around 3.25 μm outside and shrunk by the same offset inside the cell. The resulting band encompassing the cell edge was divided into regions (usually 20 regions) containing equal number of contour points and traction forces were quantified in these windows.

In case of force-time map (chapter 2 section 5.2.2), the initial contour was resampled with 600 points, enlarged and shrunk with the same offset and divided into 60 regions. The mean force was calculated for each region and map of mean forces was linearized and juxtaposed for each contours (time interval of 10 seconds).

3.7 Computational model of cell edge dynamic

3.7.1 Mapping protrusion-retraction switches

Cell outlines were extracted from the phase-contrast image sequences as described (Ambühl et al., 2012) or drawn manually using ImageJ. From segmented cell contours, protruding $\mathcal{P}(n)$ (retracting $\mathcal{R}(n)$) regions were defined as intersections of the parts of the image outside $\bar{\Omega}(n-1)$ (inside $\Omega(n-1)$) the cell contour in frame $n-1$ with the regions inside $\Omega(n)$ (outside $\bar{\Omega}(n)$) the contour in frame n.

$$\mathcal{P}(n) = \bar{\Omega}(n-1) \cap \Omega(n)$$
$$\mathcal{R}(n) = \Omega(n-1) \cap \bar{\Omega}(n)$$

Consequently, switches from protrusion $PR(n)$ (retraction $RP(n)$) to retraction (protrusion) were determined as intersections of protruding (retracting) regions between frames n and n - 1 with the retracting (protruding) regions between frames n and n + 1 (fig 3.2).

$$PR(n) = \mathcal{P}(n) \cap \mathcal{R}(n+1)$$
$$RP(n) = \mathcal{R}(n) \cap \mathcal{P}(n+1)$$

Each pixel located in $PR(n)$ and $RP(n)$ defines a switching site in a substrate-fixed coordinate system. For migrating cells, switching sites defined for each three consecutive frames were subsequently aligned with the cell position throughout the image sequence.

The frame rate was chosen to keep edge displacement between frames significantly smaller than the cell size to resolve small regions of protrusion and retraction, but at the same time large enough to reliably detect them with the segmentation algorithm. This algorithm detected the small features of the cell edge with high accuracy, except small edge irregularities (for example, small and thin retraction fibers) which were regularized by the torsion stiffness of the active contour model. We tested how frame rate influenced switch distance distribution and the number of switches detected per time unit. We observed similar distributions in an interval of frame rates between 2 and 10 s/frame for migrating cells and between 6 and 14 s/frame for polarizing cells. There was no significant difference in number of switches between polarizing and migrating cells, except at a low frame rate, which produces an artificially high switch frequency in moving cells due to a large edge displacement. Thus, switch frequency and switch probability distribution were largely independent of frame interval. Most of the analysis was performed with the frame interval of 2 s for migrating cells (where edge displacement was faster allowing for accurate segmentation with a shorter time interval) and of 10 s for polarizing cells.

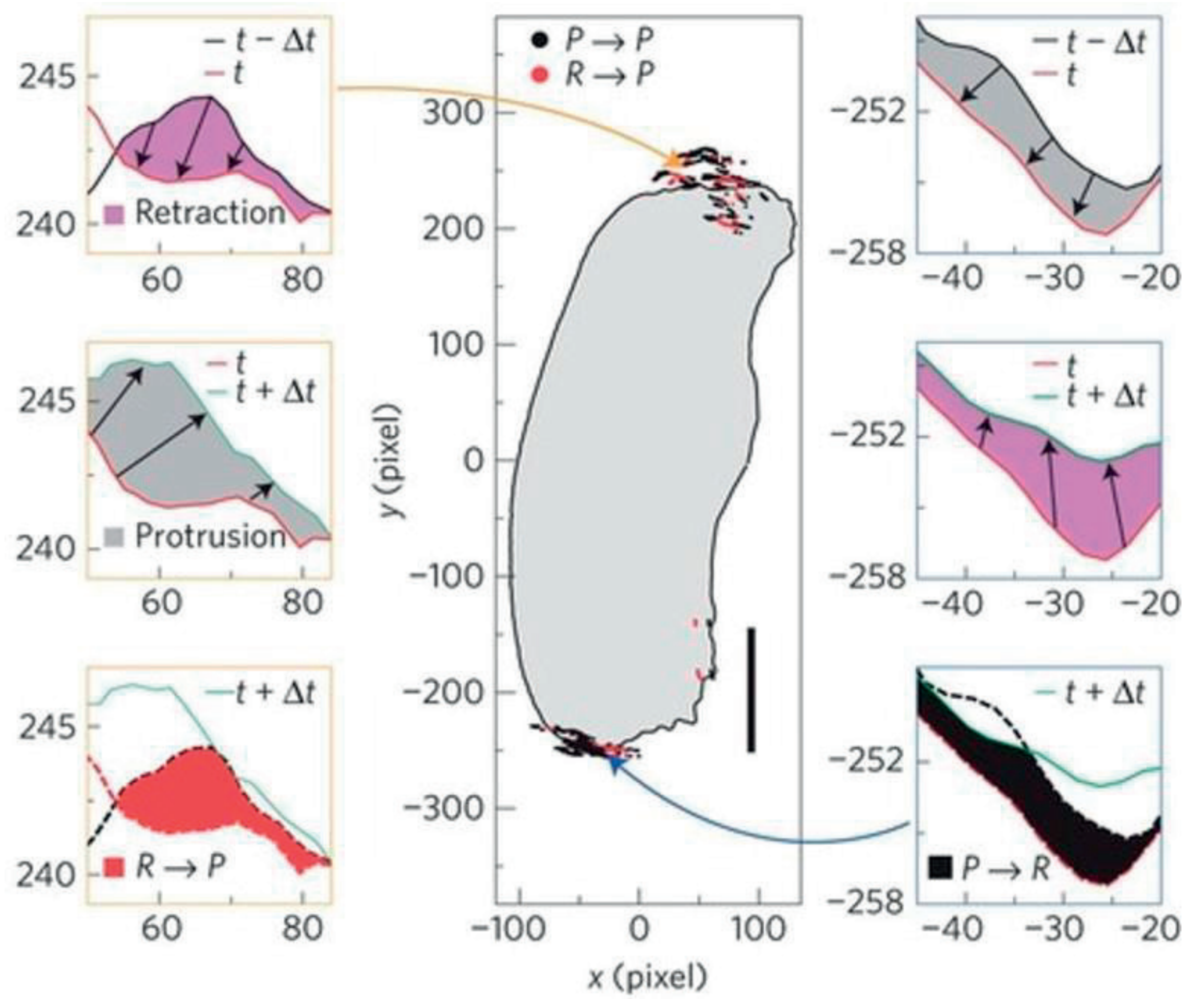

Figure 3.2: Minimal model for spontaneous cell polarization and edge activity. Localization of protrusion-retraction (black) and retraction-protrusion (red) switches during 82s of migration plotted in the co-moving frame (central panel). Detection of switching regions as intersections of protrusion (gray) and retraction (pink) in three consecutive contours (left and right panels).

3.7.2 Model parameters

To represent a smooth cell contour, simulations must be run with a sufficient number of points. We have used 4,096 points to describe the cell edge. $r_{\max}$ is the most probable distance from the cell center for switches from protrusion to retraction; it defines the maximal cell extension ($2r_{\max}$).

The other parameter values were defined in units of $r_{\max}$ (the velocities of protrusion and retraction were chosen to be small with respect to $r_{\max}$ to ensure a smooth evolution of the cell edge). From typical cell sizes and velocities, the real time equivalent of the simulation time step could be estimated. The simulation protrusion velocity was $r_{\max} \times 10^{-4}$, taking $r_{\max} = 20\ \mu\text{m}$ gives a protrusion velocity of 2 nm/time step. Comparing it to a typical experimental cell velocity of 250 nm s^{-1}, we obtain time step equivalent of 8 ms.

3.7.3 Cell center, loop elimination and contour re-sampling

In both experiments and simulations, we calculate at each time step the coordinates (x_c, y_c) of the cell center as the centroid of a non-intersecting polygon:

$$x_c = \frac{1}{6\mathcal{A}} \sum_{0}^{n-1} (x_i + x_{i+1})(x_i y_{i+1} - x_{i+1} y_i)$$
$$y_c = \frac{1}{6\mathcal{A}} \sum_{0}^{n-1} (y_i + y_{i+1})(x_i y_{i+1} - x_{i+1} y_i)$$

where (x_i, y_i) are the coordinates of the cell edge points defining the vertices of the polygon, and $\mathcal{A}$ is the signed area of the polygon.

$$\mathcal{A} = \frac{1}{2} \sum_{0}^{n-1} (x_i y_{i+1} - x_{i+1} y_i)$$

Because the previous equations are valid only for non-intersecting polygons, in the simulations we use at each time step a sweep-line algorithm (Wein, 2015) to check if loops have formed. In every detected loop, the inner points are deleted and these points are re-inserted in the sparsest region of the contour. These re-inserted points are in protrusion (resp. in retraction) states if the two surrounding neighbors are in protrusion (resp. retraction) states; otherwise their states are chosen randomly.

To ensure a homogeneous distribution of points along the evolving cell edge, the simulated contour is re-sampled (re-meshed) at each time step according to the following procedure: When the maximal distance between two adjacent points is larger than twice the minimal distance, we add a new point in the middle of the largest segment and replace the two points bordering the smallest segment by a single point in their middle. The state of the new points is defined as in the loop elimination procedure.

3.8 Actin microinjection

3.8.1 Microinjection

Microinjection of phalloidin was done using glass capillaries (Borosilicate glass capillary, thin wall: 1 mm outer diameter x 0.78 mm inner diameter, GC100T-10, Clark Capillaries) pulled into micropipettes with the pipette puller (Flaming/Brown Micropipette Puller, Model P-97). The parameters of the puller were selected in order to produce a micropipette with a small diameter of the tip and a very short thin extremity: PRESSURE = 500 (used to cool the filament and glass during the pull cycle), HEAT = 270 (controls the level of electrical current supplied to the filament), PULL = 200 (force of the hard pull), VELOCITY = 150 (velocity of the glass carriage system) and TIME = 200 (length of time the cooling air is active).

The micropipette was filled with phalloidin solution (see next part 3.8.2) and connected to a pump (Transjector 5246, Eppendorf) to apply a constant pressure (around 0.5 PSI) and fixed to a micromanipulator, at approximately 45 degree angle. To inject, the tip of the micropipette was gently and quickly put in the cell near the cell body few times. Then, image sequences of fluorescence were acquired (interval of 5 s between frames) with x100 magnification, to visualize actin dynamic.

3.8.2 Phalloidin solution

Phalloidin conjugated with Alexa-568 (A-11011, Molecular Probes) was used for microinjection to label actin filaments. Stock solution of phalloidin was prepared using methanol (300 U dissolved in 1.5 mL methanol) then 5 μL of the stock solution were let evaporate for about 90 min under the hood. After evaporation, resulting pellet of phalloidin was dissolved in 1.5 μL DMSO. Then, 6 μL of PIPES buffer (10 mM, pH=7.2, Sigma-Aldrich) were added and the solution was centrifuged to remove possible aggregates. The solution cannot be prepared in advance and has to be kept during all the steps on ice to avoid phalloidin degradation.

3.9 Topographic substrate

3.9.1 Fabrication of features

The designs were created using AutoCAD software and fabricated by standard photolithography process in a cleanroom at the Center of Micronanotechnology at EPFL. We used round features with a diameter of 50 µm spaced by 50 µm (fig 3.3.A). The structures were produced using a positive photoresist AZ ECI 3027 (standard protocol, AZ Electronic Materials) in order to have 5 µm height structures.

The structures were then reflowed in a hotplate at 120°C for 5 min to soften and round up the structure according to the reflow process of photoresist for MicroChemicals (http://www.microchemicals.com/technical_information/reflow_photoresist.pdf). The reflow process does not modify the diameter but increases height of the feature to about 7-8 µm (fig 3.3.B).

Finally the designs were replicated using polydimethylsiloxane (PDMS, Sylgard 184, Dow Corning Corp., USA). Briefly, a thin layer of spin-coated PDMS was polymerized between the silicon master and glass coverslip, the adhesion between glass and PDMS being ensured by treating the glass surface with NaOH alkaline solution (0.1 M in water, Sigma Aldrich). This replication scheme allowed obtaining holes directly compatible with high-magnification transmission microscopy. To obtain hills, the designs were replicated from the first PDMS structure to obtain the negative of original holes.

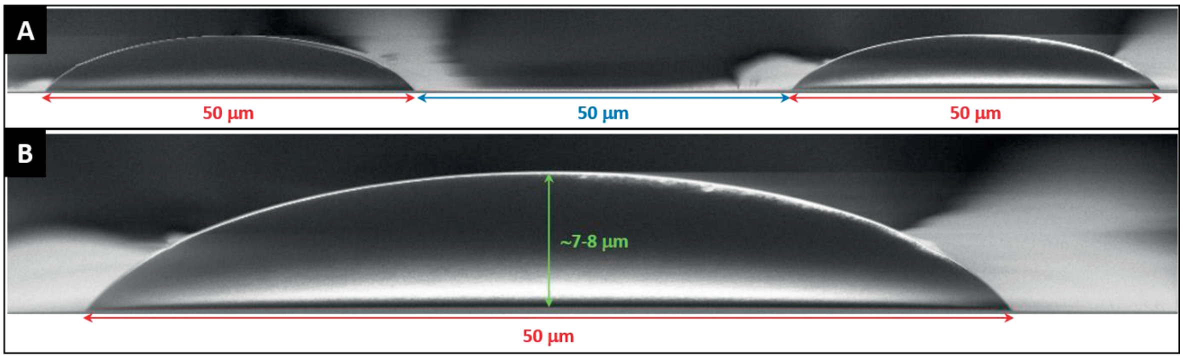

Figure 3.3: Features of topographic substrate. Scanning electron microscopy image of feature cross-section after reflow. (A) The diameter of the features is 50 µm and they are spaced by 50 µm. (B) The height of the structure after reflow is about 7-8 µm.

3.9.2 Switch frequency measurement near the feature

To quantify the influence of the topographic feature on the occurrence of switches, the number of switches per unit length of the cell edge near the feature and in the rest of the cell was measured. For that, a region around the feature (chapter 3, fig 6.6.C) was delimited: the initial contour was resampled with a defined number of points (usually 200 points) and was enlarged by offset of around 2.7 µm outside and shrunk by the same offset inside the feature. Then, the number of switches and the perimeter of the cell edge inside and outside the resulting ring region was calculated and the frequency of switches was defined as the ratio between switches and perimeter for each case.

3.10 Fluorescence displacement method

To evaluate the shape of vertical profile of the leading edge, a thin PDMS chamber (approximatively 30 μm height) [a gift from Prof. Alex Groisman, University of California, San Diego] was placed on top of the coverslip with cells and filled with culture medium containing 25 μM rhodamine D isothiocyanate-dextran ($M_W = 10\ 000$ g.mol^{-1}, Sigma-Aldrich, USA). Vacuum were applied inside the chamber in order to lower the ceiling and thus reduce the chamber height to about 12 μm height. Florescence images of the cell were acquired to produce shadow-like images, and the cell height was estimated from the difference of intensity between the cell and the background.

3.11 Contribution to cited papers

This thesis includes materials from several published papers by our lab. In the Nature Physics paper (Raynaud et al., 2016), I contributed to the experiments and gave the necessary data for the switch analysis during both fluctuation and motion. In the Current Biology paper (Gabella et al., 2014), I made the experiments of traction force and I developed in parallel the substrate topography. For my work thesis, I improved the feature manufacturing and proposed new design. The presented unpublished data are entirely my original work.

3.12 Glossary

APTMS: (3-Aminoropyl)trimethoxysilane

BSA: bovine serum albumin

DMEM: Dulbecco's Modified Eagle Medium

DMSO: dimethyl sulfoxide

EDTA: Ethylenediaminetetraacetic acid

FBS: fetal bovine serum

HEPES: N-(2-hydroxyethyl)-piperazine-N'-(2-ethanesulfonic acid)

NaOH: sodium hydroxide

PBS: phosphate-buffered saline

PDMS: polydimethylsiloxane

PIPES: piperazine-N,N′-bis(2-ethanesulfonic acid)

PVA: polyvinyl alcohol

Sulfo-SANPAH: N-Sulfosuccinimidyl-6-[4'-azido-2'-nitrophenylamino] hexanoate

TEMED: tetramethylethylenediamine

Chapter 1

4) Cell edge dynamics during the process of motility initiation

Fish epidermal keratocytes are simple, fast and persistent cells which constitute an ideal model to study cell motility. They are able to spontaneously break symmetry and initiate motility: the individual cells which are isotropic become polarized by defining a front region undergoing protrusion and a back region exhibiting retraction and acquiring a characteristic canoe-like shape. Many studies were done to understand the sequence of structural events during the cell polarization: Yam et al. (Yam et al., 2007) have shown that the first event of cell polarization is a retraction at the prospective rear due to an increase of actin retrograde flow in this region. Then, the cell front also become reorganized in order to protrude and guide the persistent motion.

However, our observations show that an individual retraction event at the cell edge does not necessarily lead to symmetry breaking and initiation of motility. Rather, the cells often exhibit multiple protrusions and retractions and form small protruding and retracting regions that propagate along the edge and eventually coalesce into a single retracting back and protruding front. This behavior was not analyzed in previous studies. We aimed to investigate these dynamics and find out how it is related to eventual polarization and directional motility.

4.1 Experimental cell edge dynamics

In order to study edge dynamics during polarization, cells plated on glass coverslip were separated from each other using EDTA treatment (details in section 4.3). To observe dynamics of individual cells not in contact with each other, part of the cells was removed by pipetting. Remaining cells re-spread on the surface, polarized and initiated migration.

4.1.1 Cell fluctuation

Cells on glass exhibit an extended period of edge fluctuation before breaking symmetry and initiating motility (fig 4.1.A). This state is characterized by constant change of shape involving protrusion and retraction events all along the cell edge. In some cases, the cells form several protruding segments that propagate along the edge in the same direction giving the impression of cell rotation. These “rotating” states could appear transiently in the midst of apparently disorganized edge fluctuations or persist for several minutes (see the section 4.2.1 below) before the cells eventually initiate directional motion.

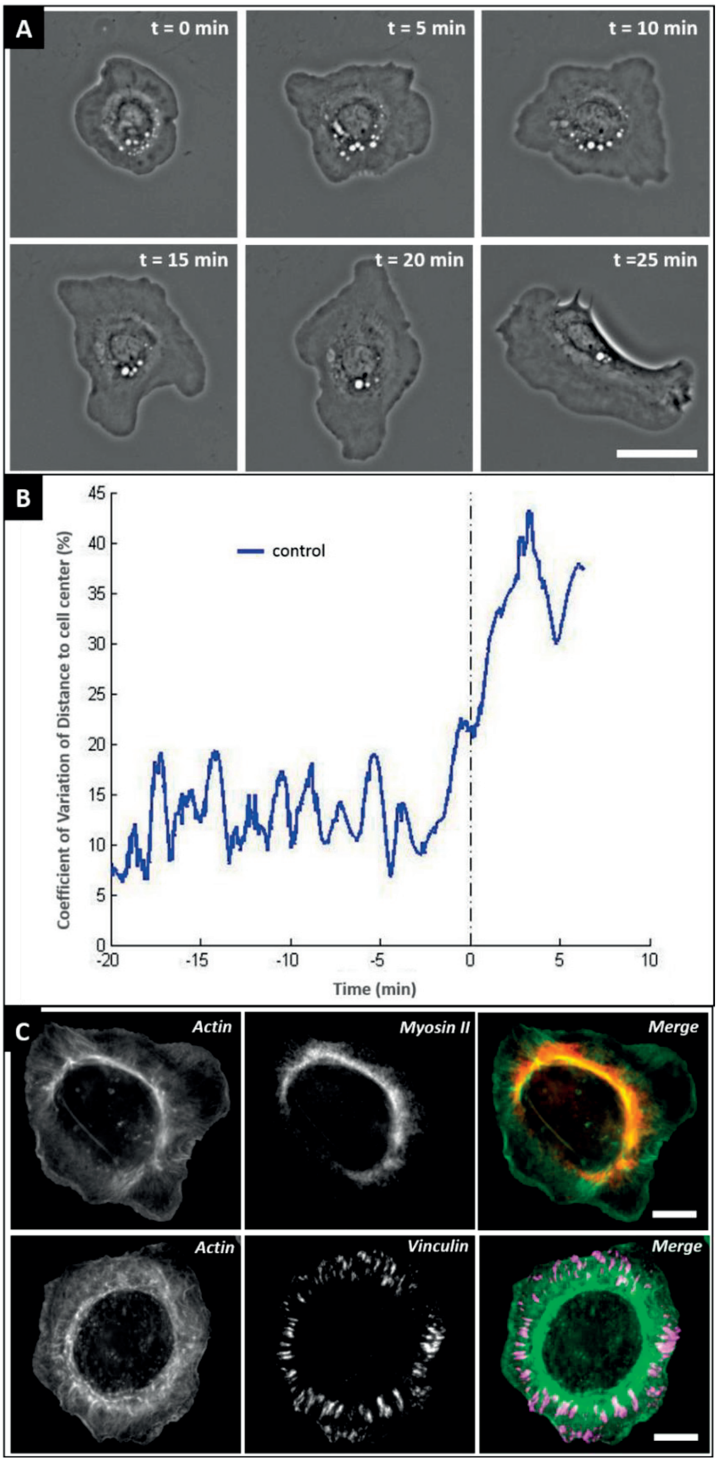
A
t = 0 min
t = 5 min
t = 10 min
t = 15 min
t = 20 min
t =25 min
B
control
Coefficient of Variation of Distance to cell center (%)
0
5
10
15
20
25
30
35
40
45
-20
-15
-10
-5
0
5
10
Time (min)
C
Actin
Myosin II
Merge
Actin
Vinculin
Merge

Figure 4.1: Cell edge dynamics of fish keratocytes. The cells were plated on glass coverslip and individualized by EDTA treatment. (A) Under normal condition, the cell displays large cell edge fluctuation. (B) Coefficient of variation of cell edge distance from the center of the cell. The dashed line represents the transition from isotropic to polarized state. (C) Immunostaining of the cell cytoskeleton. In the merge picture in color: green for actin, red for myosin II and magenta for vinculin in the cell adhesions. Scale bar = 10 µm.

To characterize cell shape dynamics during polarization, we plot the standard deviation of the distance of points along the contour from the geometrical cell center, divided by their mean distance for each frame. This measure, termed coefficient of variation of edge distance displayed large fluctuations before initiation of motion, corresponding to the continuous protrusion/retraction events and shape changes (fig 4.1.B). When the cell became polarized, the coefficient increased reflecting the fact that the cell acquired elongated shape. The coefficient then still fluctuated around a higher value indicating that the shape of polarized cell was not completely stable.

We investigated the organization of the cytoskeleton during cell edge fluctuation. Immunofluorescent staining (fig 4.1.C) revealed actin network at the cell periphery, prominent bundles of actin and myosin II in the perinuclear region and well-developed, elongated focal adhesions. The same cytoskeletal elements are apparent in polarized cells, although their distribution is asymmetric with actin network in the front lamellipodium, acto-myosin bundles at the boundary between the lamellipodium and the cell body and at the back of the cell, and focal adhesion predominantly at the cell sides (Svitkina et al., 1997) (Anderson and Cross). These results suggest that the transition from fluctuating to polarized state does not involve a major change in the overall level of organization of contractile or adhesive structures of the cell, but rather their redistribution.

4.1.2 Myosin II inhibition

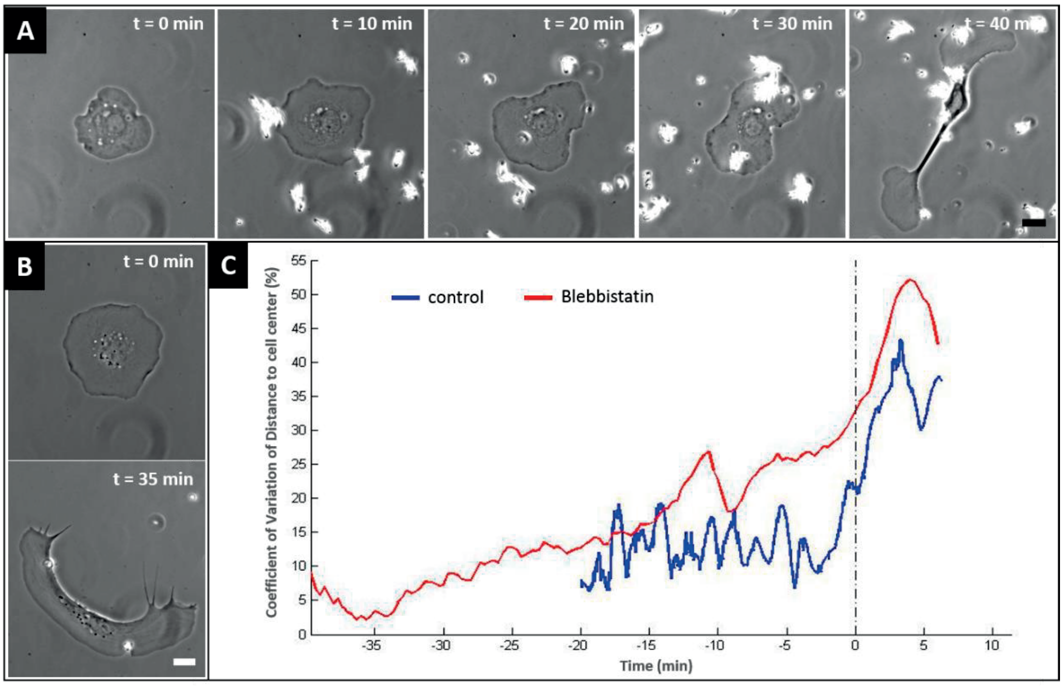

Figure 4.2: Cell edge dynamics of blebbistatin-treated cells. The cells were plated on glass coverslip and individualized by EDTA treatment. (A, B) Cells treated with blebbistatin to inhibit myosin II activity exhibited small fluctuations at the edge. During motion, the cell can splits in several parts or acquired an elongated typical polarized shape. (C) Coefficient of variation of cell edge distance from the center of the cell. The dashed line represents the transition from isotropic to polarized state. Scale bar = 10 μm.

Yam et al. (Yam et al., 2007) and Barnhart et al. (Barnhart et al., 2015) reported that inhibition of myosin-dependent contractility with blebbistatin blocks cell polarization. Consequently, we have investigated how inhibition of myosin influences cell edge fluctuation dynamics and cytoskeletal organization. Blebbistatin-treated cell showed significantly less edge fluctuations than control cells (fig 4.2.C). In contrast to what was report by Yam et al. (Yam et al., 2007) and Barnhart et al. (Barnhart et al., 2015), we observed that the majority of blebbistatin-treated cells eventually developed large contracting and protruding regions and initiated migration, but the onset of migration was delayed, with respect to control cells (fig 4.3.A). In the process of initiating migration and after the onset of motion, blebbistatin-treated cells often exhibited progressively elongating shape or split into several parts (fig 4.2.A, B).

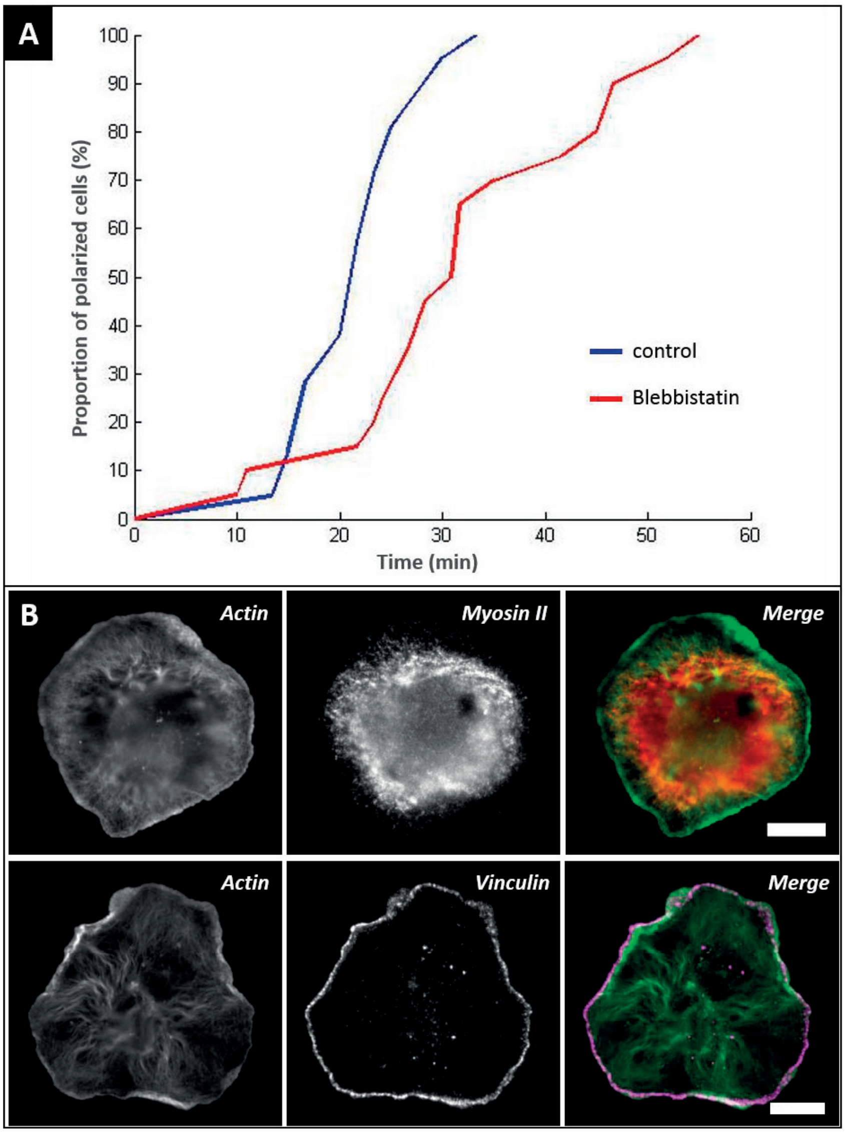

Figure 4.3: Behavior of blebbistatin-treated cells. The cells were plated on glass coverslip and individualized by EDTA treatment. (A) Proportion of cells which become polarized in order to migrate in function of time. Total number of cells for control (n = 21) and for blebblistatin (n = 20). (B) Immunostaining of the cell cytoskeleton. In the merge picture in color: green for actin, red for myosin II and magenta for vinculin in the cell adhesions. Scale bar = 10 μm.

This suggests that myosin-dependent contractility is not essential for the initiation of motility *per se*, but is important for the maintenance of shape and integrity of the cell during motion. Myosin II was still present in the form of distinct spots in the perinuclear region of blebbistatin-treated cells, but these spots were less clustered (fig 4.3.B). Adhesions were also less developed than in the control, looking like small dots localized all around the cell periphery.

4.1.3 Actin polymerization inhibition

Retraction at the prospective back of the cell was previously considered the key event initiating cell polarization (Barnhart et al., 2015) (Yam et al., 2007). To investigate the role of protrusion in polarization, we treated the polarizing cells with cytochalasin D, a mycotoxin that binds to the actin filaments and blocks polymerization. We have chosen a low concentration of cytochalasin D (0.2 µM) that inhibited protrusion, but did not induce cell retraction or complete destruction of actin network (Schaub et al., 2007).

Cytochalasin-treated cells remained round for about 1 hour, displaying small oscillations at the edge but never polarized nor initiated motion (fig 4.4.A). The plot of the coefficient of variation of edge distance was nearly flat, indicating that the cell edge did not fluctuate significantly and the cell shape remained constant and isotropic (fig 4.4.B). The lack of cell edge fluctuation indicated that, interestingly, partial inhibition of actin polymerization with cytochalasin suppressed not only protrusion, but also retraction. Cytochalasin treatment influenced the actin network which was less dense and myosin II clusters were more dispersed inside the cell (fig 4.4.C). Adhesions were organized in a similar way as in control but were less elongated.

In summary, blebbistatin and cytochalasin treatment suppressed or disrupted both the cell edge fluctuation and the eventual polarization suggesting that the two processes are different manifestation of the same cytoskeletal activities.

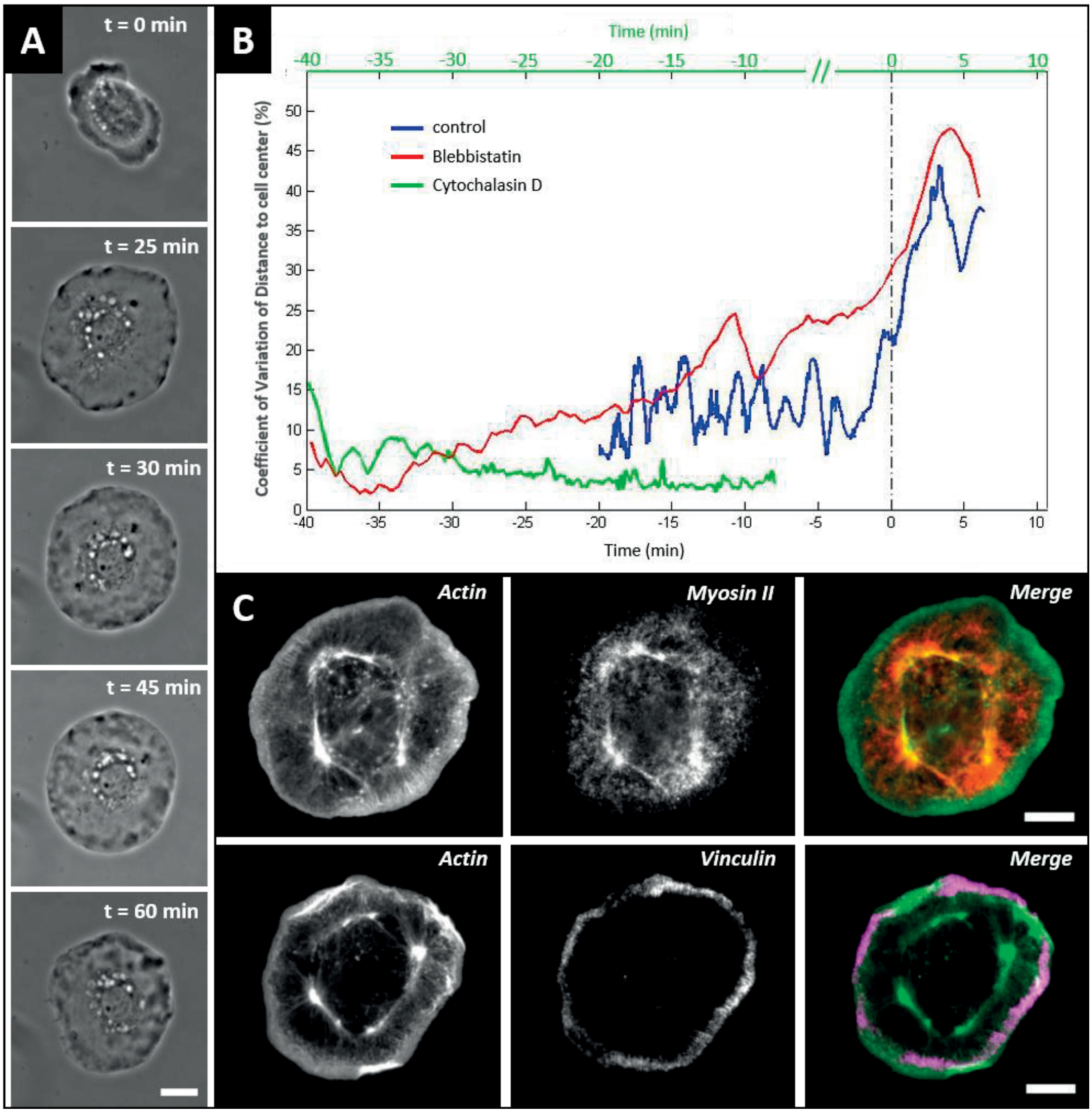

Figure 4.4: Cell edge dynamics of cytochalasin-treated cells. The cells were plated on glass coverslip and individualized by EDTA treatment. (A) Cell treated with cytochalasin to inhibit actin polymerization does not exhibits fluctuations at the edge and stays round without polarization and subsequent motion. (B) Coefficient of variation of cell edge distance from the center of the cell. The dashed line represents the transition from isotropic to polarized state. Blue corresponds to control cell, red to blebbistatin-treated cell and green to cytochalasin-treated cell. (C) Immunostaining of the cell cytoskeleton. In the merge picture in color: green for actin, red for myosin II and magenta for vinculin in the cell adhesions. Scale bar = 10 µm.

4.2 Protrusion-retraction transitions in cell polarization

In the process of cell polarization, multiple fluctuating regions of protrusion and retraction reorganize into a single protruding and a single retracting region by means of local transitions between protrusion and retraction. To understand how this happens and to identify the principles governing edge dynamics during the polarization process, we decided to map positions of the edge where the transitions from protrusion to retraction (PR) and from retraction to protrusion (RP) take place. The algorithm to map PR and RP switches from the sequences of segmented edge contours was developed by Mark Ambühl, a PhD student in our laboratory.

4.2.1 Distribution of protrusion/retraction switches during cell polarization

In the fluctuating cells with apparently disorganized distribution of protruding and retracting regions, the analysis showed a uniform switch distribution along the cell edge (fig 4.5.C) and an almost equal repartition between the two types of transition: 55% of the total number were PR switches and 45% were RP switches. Importantly, plotting the distribution of switch positions in terms of distance from the geometrical cell center demonstrated that PR switches were predominantly at the maximal cell extension (fig 4.5.A) while a peak of RP switches was observed at intermediate distances. We have also separately investigated switch distribution in the cells that exhibited extended periods of rotation of several retracting and protruding regions around the cell periphery. In these cells, the PR switches also happened at the maximal distance, corresponding to the tip of the rotating segments (fig 4.5.B) and the RP switches localized at short distance at the base of rotating segments. The two types of switches were slightly unbalanced with 65% of PR switches.

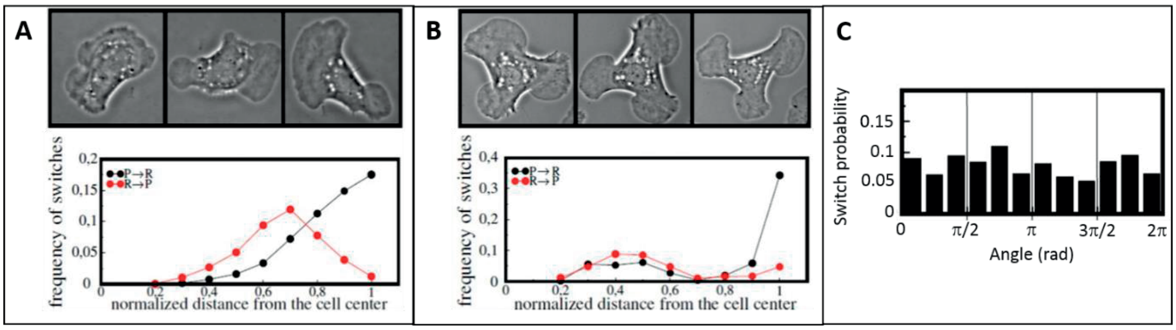

Figure 4.5: *Distribution of switches between protrusion and retraction in fluctuating and rotating cells.* Switch probability for a fluctuating (A) or rotating (B) cell as function of the normalized distance from the cell center. Top panels show phase-contrast image of the cell behavior. (C) Protrusion-retraction switch probability for a fluctuating cell as function of the angular position along the contour. Angle = 0 rad corresponds to the position at the middle of the leading edge. (Raynaud et al., 2016)

During this transition to the single protruding and retracting edge and initiation of directional motion (fig 4.6.A), the same pattern of the switch distribution was observed: PR switches remained near the maximal cell extension (fig 4.6.B), despite the constant change of cell shape.

In polarized migrating cells PR switch distribution also shows a distinct peak near the maximal cell extension. In this case, 70% of the total switches were localized at more than 90% of the maximal extension (fig 4.6.C), which corresponds to the lateral extremities of the cells (fig 4.6.D). These switches were mostly from protrusion to retraction, but we observed also RP events at the same locations (around 15% of the total number of switches). Some switches appeared at the intermediate distances (≤ 5%) which corresponded to the back of the cell and could be attributed to the dynamics of retraction fibers.

These experiments suggest the relation between cell-edge dynamics and distance from the cell center which may be important for cell polarization.

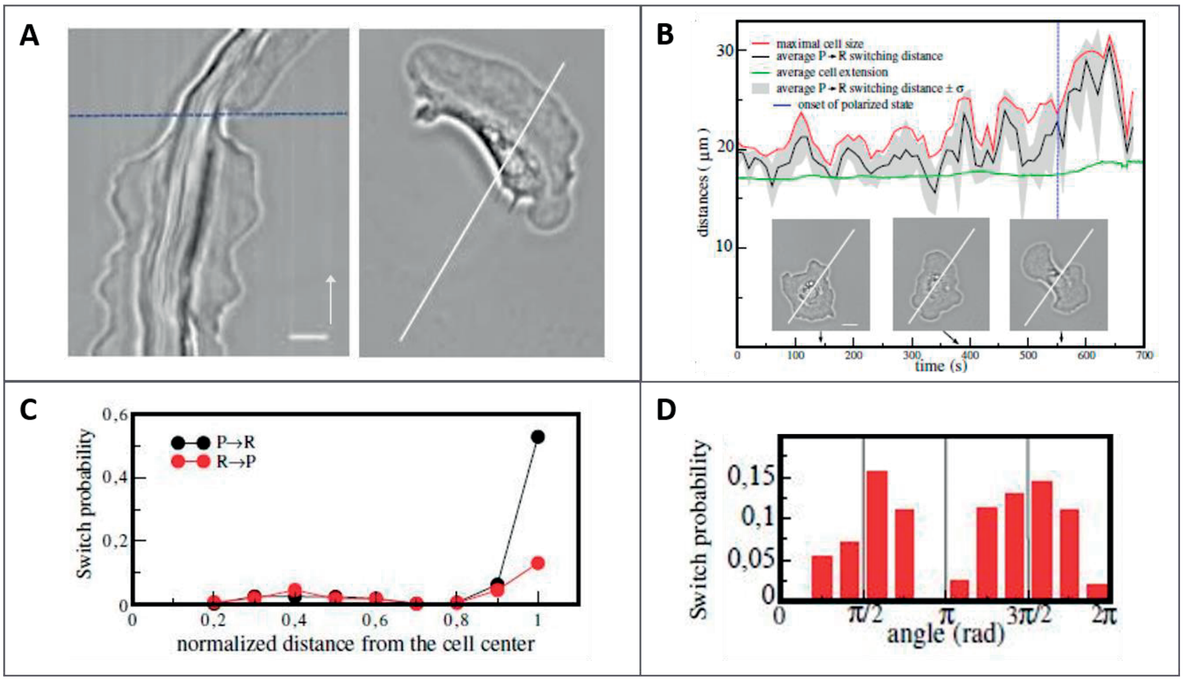

Figure 4.6: Switches distribution in control cell. (A) Kymograph (left panel) of a polarizing cell taken along the white line (right panel). The transition between fluctuating and migrating state (t = 550 seconds) is indicated by the blue dashed line. White arrow represent the time. (B) Time course of maximal (red) and minimal (green) cell extension, and the average PR switching distance (black) during polarization process. Phase-contrast image shows the cell shape at different time during polarization as indicated. (C) Protrusion-retraction switch probability as function of the angle for migrating cell. Angle = 0 rad corresponds to the position at the middle of the leading edge. (D) Switch probability for protrusion to retraction (PR) and for retraction to protrusion (RP) as function of the normalized distance from the cell center. Distances are normalized by the maximum distance from the cell center in order to aggregate data from cells of different size. Contours were extracted with an interval of 2 seconds from five different cells for a total of 236 contours. Scale bars = 10 µm. (Raynaud et al., 2016)

4.2.2 Induced cell shape perturbation

In the cells prior to polarization, PR switches are happening at the maximal cell extension and are distributed isotropically around the cell perimeter. In contrast, in migrating cells switching corresponds at the same time to the maximal cell extension and to the parts of the cell edge displacing orthogonally to the direction of the motion. To find out which factor determines the localization of switches: distance from the cell center or the orientation with respect to the direction of motion, we have manipulated the cell shape to increase or decrease the distance from the edge to the center at different orientations.

In order to increase the distance from the leading edge to the cell center, a micropipette was placed parallel to the glass surface, so that it blocked the nucleus but allowed the front lamellipodium to pass below (fig 4.7.A). Despite the fact that the cell body was blocked, the leading edge maintained its directional motion at constant velocity until the cell extended to a distance similar to its original maximal lateral extension. When this extension was reached, the edge stopped, showed small fluctuation, and eventually switched to retraction resulting in a reversal of cell motion (fig 4.7.B).

The decrease of distance from the edge to the center was performed by cutting one lateral part of the migrating cell (fig 4.7.C) using a glass needle. The cut side displayed persistent protrusion (fig 4.7.C inset) and recovered its original shape and width. The protrusion could also propagate from the site of the cut to the back of the cell, resulting in a turning of the entire cell in the direction of the cut position.

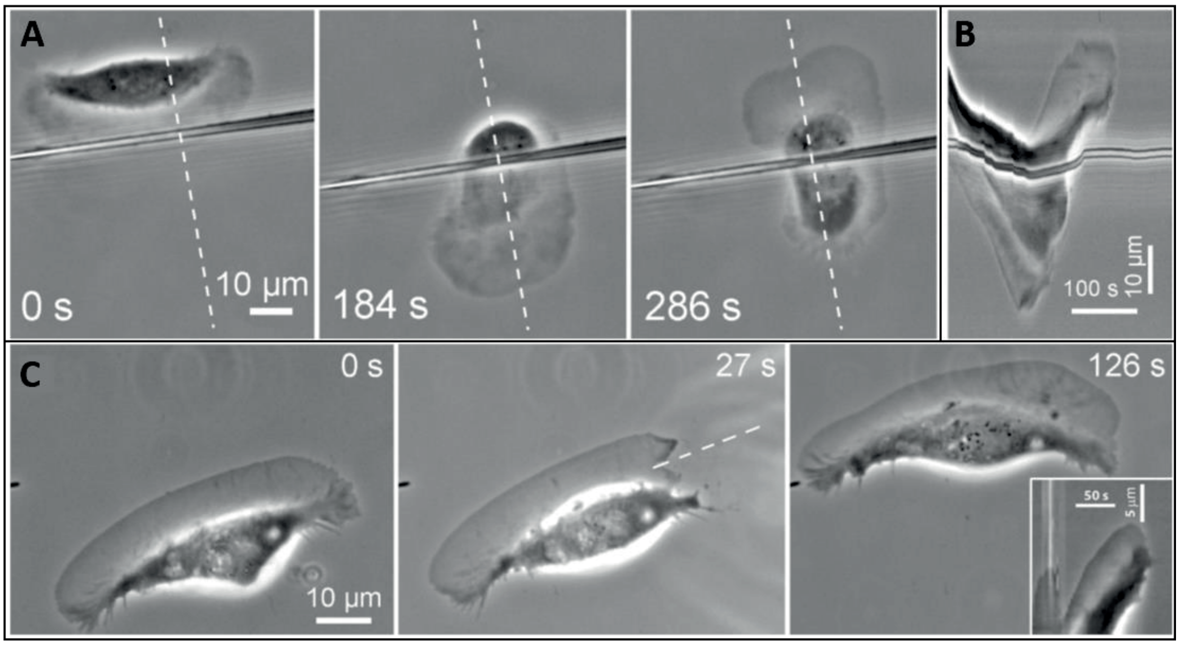

Figure 4.7: Shape-induced perturbation in migrating cells. (A) Phase-contrast image of a migrating cell with its body blocked by a micropipette. Time (seconds) starts after the encounter with the pipette. (B) Kymograph of the cell represent in A taken along the white dashed line, with a frame interval of 2 seconds. (C) Phase-contrast of migrating cell before, 1 second and 100 seconds after the cut of its right lateral part with a glass needle. Inset panel represent the kymograph of the cell taken along the white dashed line, with a frame interval of 3 seconds. (Raynaud et al., 2016)

Both the pipette and the cut experiments demonstrate that the protrusion/retraction switches are regulated by the distance from the cell center and not by the orientation with respect to the motion direction: increasing the edge-to-center distance initiates protrusion-retraction switches at the front, while decreasing this distance suppresses protrusion-retraction switches at the sides. If switches were regulated by the orientation, they should have persisted at the cut side of the cell and did not occur at the cell front.

Switch mapping and cell shape manipulation experiments indicate that the cell edge somehow senses its distance from the cell center and switches from protrusion to retraction at a certain limiting distance. To understand how this limiting distance corresponding to maximal cell extension is controlled we have tested the effects of the manipulation of myosin contractility, microtubule system, and the cell volume on the cell width and on the cell behavior in body-blocking experiments. Microtubule system was tested because microtubules are implicated in cell-size control in several cell types other than keratocytes (Martin, 2009) (Picone et al., 2010).

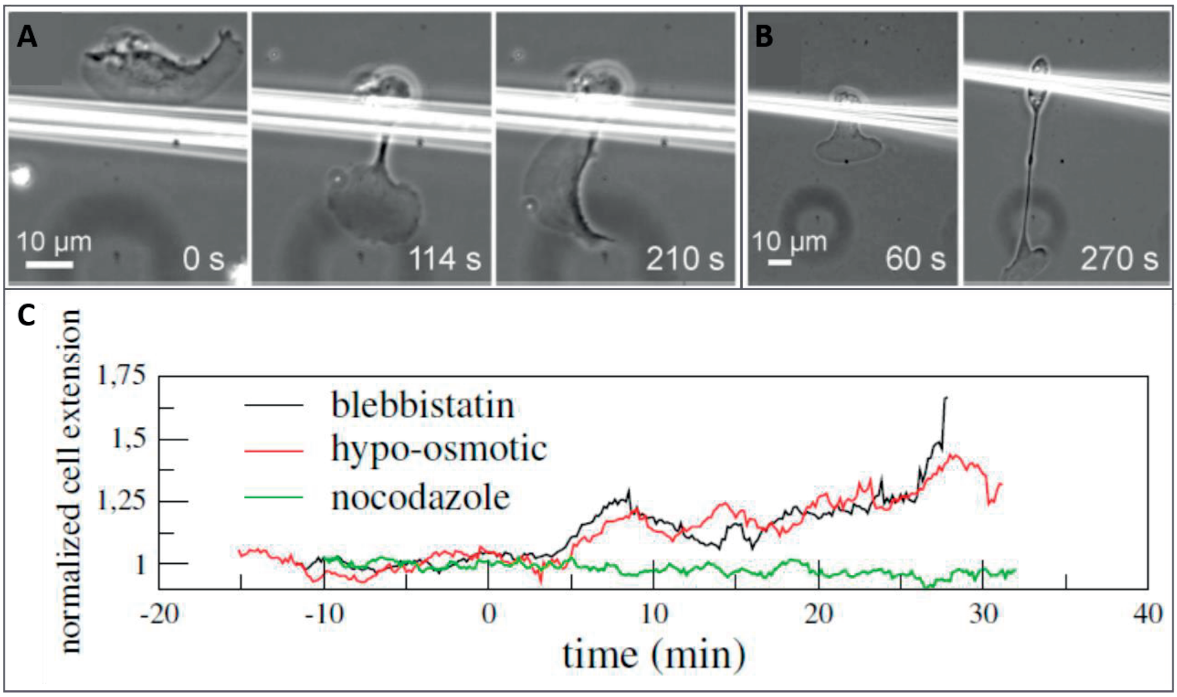

Figure 4.8: Effect on maximal extension in treated cells during body-blocking experiment. (A) Cell after hypo-osmotic shock (t = 0) keeps extending its front protrusion. (B) Blebbistatin-treated cell extends its front and eventually turns parallel to the micropipette. (C) Dynamics of the average cell width after treatment (t = 0) with blebbistatin (black, n = 11), hypo-osmotic shock (green, n = 10) or nocodazole (red, n = 9). The width of each cell is normalized with its average before treatment. (Raynaud et al., 2016)

Treatment with the myosin II inhibitor blebbistatin and hypo-osmotic treatment to increase the cell volume, both lead to an increase in cell width, with an eventual cell fragmentation in the case of blebbistatin. In cell-body blocking experiments, hypo-osmotic treatment lead to a partial suppression of the distance sensing: half of the cells (3 out of 6) kept extending their leading edge until it eventually detached from the cell body (fig 4.8.A). Blebbistatin-treated cells also behaved differently from control cells in body-blocking experiments: they extended forming a narrow stalk instead of a wide cytoplasmic bridge in control case. In 75% of the cases (9 out of 12) the front protrusion did not extend continuously, instead turning to a motion parallel to the micropipette (fig 4.8.B). In contrast, disruption of the microtubule system with nocodazole did not affect the cell width (fig 4.8.C) and did not change their behavior in body-blocking experiments (not shown). These results suggest that distance-sensing involves the mechanism related to the cell contractility and cell volume, but not the microtubule system.

4.2.3 Computational model of cell edge dynamic

The experiments described in the previous chapter indicate that the cells during polarization and in the polarized state universally exhibit switch from protrusion to retraction at a maximal cell extension. To test if this feature is sufficient to explain spontaneous cell polarization and directional motion, Franck Raynaud, a postdoc in our lab, developed a stochastic model based on distance-dependent switch mechanism. In this model, the cell edge is described by a set of points in two possible states: protrusion (P) or retraction (R). The switches from protrusion to retraction (PR) occurs at a high threshold distance from the geometrical cell center, while retraction to protrusion (RP) switches occur at a smaller threshold distance. The state of a point also changes if most of its neighbors within a defined interaction range are in the opposite state, providing coupling that enables local ordering of the edge activity. Simulations of cell behavior with this model demonstrated that this simple rule of distance-limit allows to reproduce the same contour behavior that the cells exhibit in the experiments: starting from a circular outline with a random distribution of protruding and retracting points, the edge displays strong shape fluctuation before initiating persistent migration with a typical and stable keratocyte shape, elongated perpendicular to the direction of motion. In migrating cells, only the lateral extremities reach the critical distance which leads to protrusion to retraction switches stabilizing the width of the cell. The regions of the cell edge at the front and the back of the cell move in concert and maintain their state as long as they do not pass the critical distance threshold. This shows that the distance-limit property of the cell edge is able on its own to produce the cell edge fluctuation, to break symmetry and initiate motility.

The physical mechanism of distance-sensing is unclear, but cell contractility and the cell volume or shape are likely involved.

4.2.4 Actin dynamics during protrusion-retraction fluctuations

Cell edge-velocity in actin-dependent cells is a vectorial sum of actin polymerization velocity and actin flow velocity, so if the edge velocity changes it could be due to a change of either polymerization velocity, flow velocity or both (Barnhart et al., 2011). It was previously suggested that retraction at the prospective rear of polarizing cells is due to the increase of flow velocity, but, to our knowledge, the dynamics of the onset of retraction and the actin flow were not followed simultaneously during these retraction events.

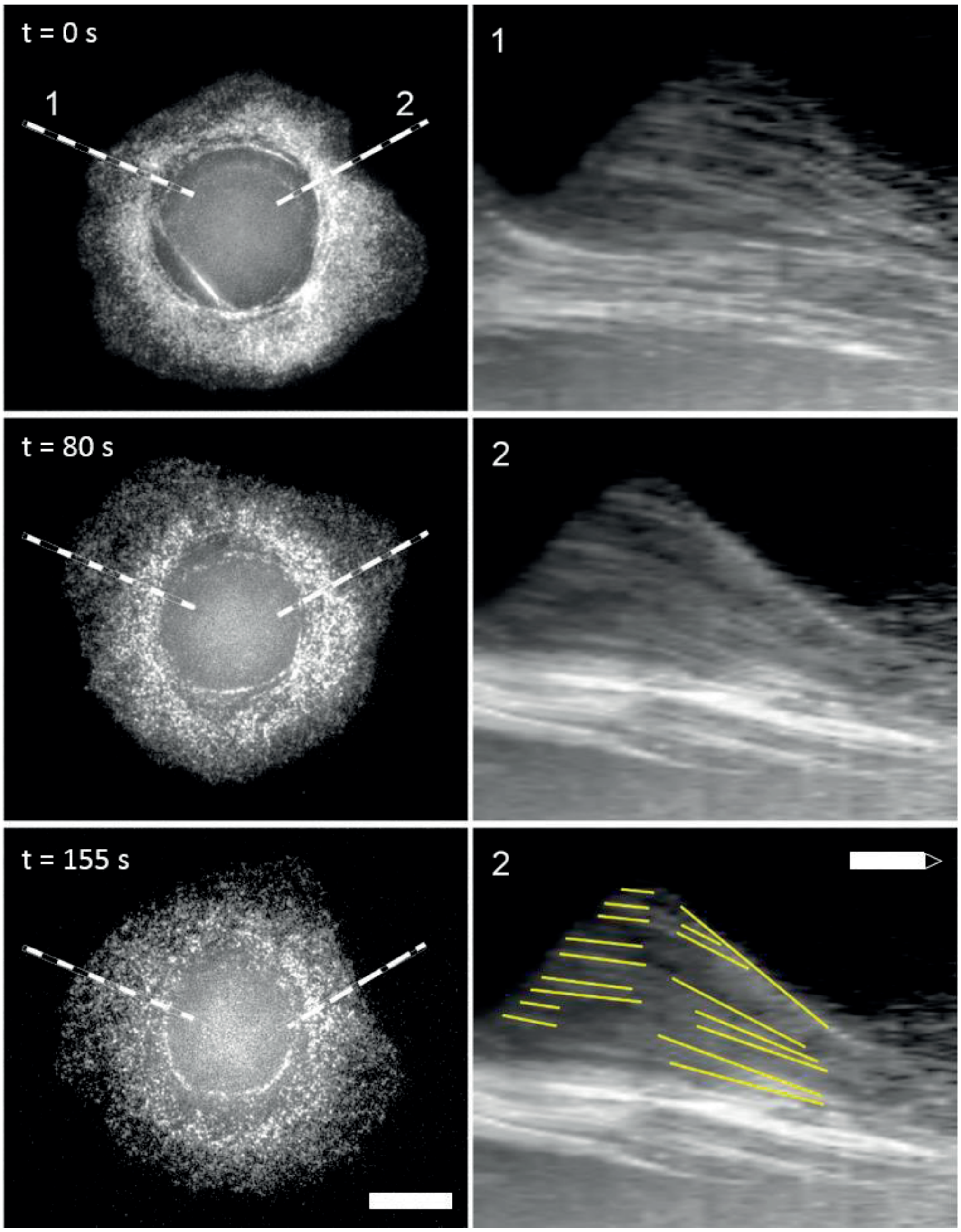

Figure 4.9: Actin flow during protrusion-retraction transition. (Left) Fluorescent images of phalloidin-injected cell during fluctuation. (Right) Kymograph taken along the white lines. The yellow lines represent the actin flow dynamic (for the kymograph taken along the line 2). Interval between frames is 5 seconds. Scale bar = 10 μm; time scale bar in kymograph = 30 seconds.

To understand what changes of actin dynamics are associated with protrusion-retraction transitions, we injected the fluctuating cells with fluorescent phalloidin and recorded time-lapse sequences of protrusion-retraction events. Kymographs of the time-lapse images (fig 4.9) demonstrated that actin retrograde flow velocity was constant during the protrusion phase but increased at the moment of initiation of retraction. At the same time, new actin features ceased to appear at the retracting edge, suggesting that actin polymerization was abruptly arrested. Increase in retrograde flow velocity happened simultaneously at the cell edge and in the actin network at a distance from the edge. During retraction phase, actin network contracted telescopically, i.e. the structures closer to the edge exhibited higher flow velocity than those deeper in the cytoplasm leading to progressive condensation of actin structures towards the perinuclear zone, but during protrusion the structures at different distances from the edge moved parallel to each other at the same velocity (fig 4.9). These observations allow excluding one hypothetical mechanism of protrusion-retraction switch, namely, that retrograde flow velocity increases with the distance and gradually overcomes polymerization velocity leading to retraction. Rather, our observations suggested a sudden detachment of the portion of the cell edge from the substrate leading to its telescopic collapse. Such detachment could be due either to the weakening of cell substrate adhesions or to increase of the traction force causing adhesion rupture.

4.3 Cell edge dynamics on flexible gel substrate

Cell contractility may be involved in distance-sensing by generating traction forces between the cell and the substrate. One could expect that if the traction stress reaches a certain limit, cell edge detaches from the substrate and consequently switches from protrusion to retraction. To elucidate how contractility is involved in the distance-dependent mechanism, we analyzed the link between critical distance and traction stresses generating by the actomyosin network. To measure traction forces, the cells have to be plated on flexible substrate such as polyacrylamide gel (PAA gel). Before investigating the cell traction stress, we tested if the cells show the same polarization behavior on flexible gel as on rigid glass substrate. Several previous studies have shown the influence of the rigidity in the cell behavior. For example, Lo et al (Lo et al., 2000) introduced the term “durotaxis” relating the preference of a cell for stiff substrate: cells migrate up the gradient of substrate rigidity. The influence of substrate rigidity on cellular regulation has been shown by Park et al. (Park et al., 2011), who demonstrated that the substrate stiffness controls stem cell differentiation. To find the optimal conditions to study traction stresses during cell-edge fluctuation and polarization, we tested different cell detachment procedures and different substrate rigidities.

4.3.1 Cell detachment methods

The cells were plated on the polyacrylamide (PAA) gel coated with fibronectin to enable the cell to attach. We initially used gel with a stiffness of 1.5 kPa, a soft gel that was previously reported to provide large bead displacement to measure relatively weak traction forces of keratocytes (Fournier et al., 2010). To be individualized, the cells were separated from the monolayer using EDTA treatment as for the previous experiments on glass. Ethylenediaminetetraacetic acid (EDTA) acts as a chelating agent and has the ability to sequester metal ions such as calcium (Ca^{2+}) or magnesium (Mg^{2+}) which support cell adhesion. For example cadherins, transmembrane proteins involved in cell to cell adhesion, are dependent on calcium (Kim et al., 2011). Integrins which are transmembrane receptors playing a central role in cell to extracellular matrix adhesions, bind bivalent cations, and magnesium alone is capable to activate them (Zhang and Chen, 2012). In the absence of free calcium and magnesium, the cell adhesions are disrupted and cells separate from each other and detach from the substrate. Then, the addition of fresh medium to the individualized cells provides new cations to restore cell adhesiveness.

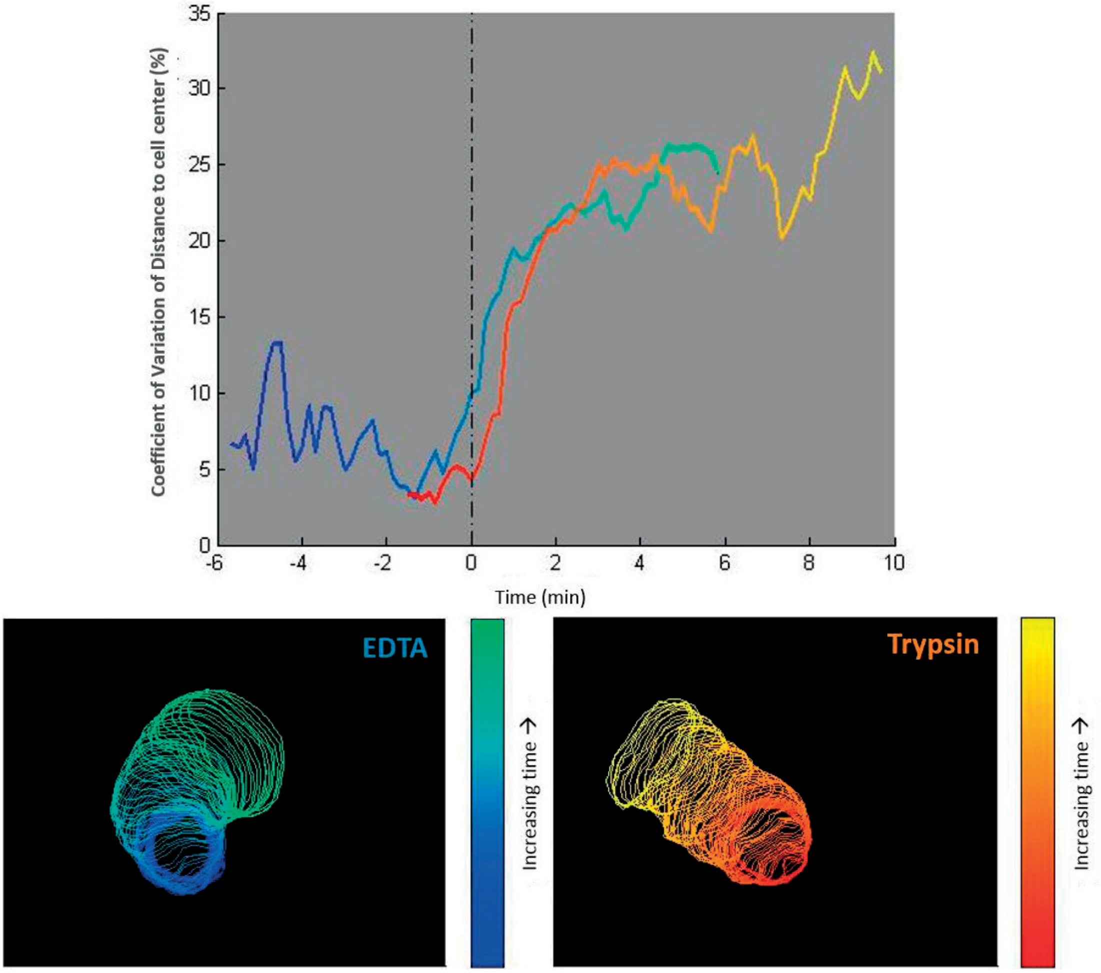

Figure 4.10: Cell behavior on soft gel for cells individualized with EDTA or Trypsin. (A) Coefficient of variation of cell edge distance from the center of the cell. The dashed line represents the moment of round-to-polarized transition. (B) Evolution of cell contour in function of time (colorbar). Interval of 10 seconds between each contours.

We observed that on soft gel, the cells individualized with the same technique as in experiments on glass, polarized rapidly and did not exhibit large edge fluctuation (fig 4.10 *blue*). The cells were also less well spread than on glass (approx. spread area e.g. 700 vs 1500 μm^2 (fig 4.10, *dotted lines*)), which made quantification of the edge dynamics more difficult. We tested another technique to individualize the cells. Trypsin is a common proteolytic enzyme used to dissociate the cells by disrupting cell-to-cell and cell-to-matrix adhesions. It is a serine protease which cleaves peptide chains mainly at the C-terminal side of Lysine and Arginine amino acids. With its proteolytic activity, trypsin digests the adhesion proteins that link the cell to the extracellular matrix resulting in detachment of the cell from the substrate. As proteolytic activity of trypsin could affect the fibronectin coating of the gel surface, the cells were plated on glass and treated with Trypsin to detach them and transfer onto the gel. The individual cells were able to attach to the fibronectin-coated gel after their transfer but they did not spread better than EDTA-treated cell, did not show significant edge fluctuations, and the polarization was even faster than after the EDTA treatment (fig 4.10 *red*). Small cell area, small extend of edge fluctuation and fast polarization on the soft gel made it difficult to study the relation between traction forces and the protrusion-retraction switches. Next, we tested higher gel rigidity. We decided to use EDTA to individualize the cells in all experiments as it is used in the glass experiments and it produces more extended edge fluctuation on gel compared to trypsin (fig 4.10).

4.3.2 Polyacrylamide gel rigidity

Several values of gel stiffness were analyzed (1.67 kPa; 4.47 kPa; 8.73 kPa; 16.70 kPa; 19.66 kPa; 40.40 kPa) and the best results were obtained with gel rigidity of 16.7 kPa. At this stiffness, it is still possible to analyze traction forces and the cell displays large area and large edge fluctuation as on glass coverslip. As shown in the figure 4.11, the cell on rigid gel individualized with EDTA are exhibiting high edge dynamics: the coefficient of variation of the distance from the cell center is fluctuating until the polarization step, where the coefficient increases and continues to fluctuate reflecting the changes in cell shape and motion direction. In contrast, the cell on soft gel (1.5 kPa) dissociated in the same way with EDTA, shows smaller fluctuations and polarizes faster. Thus, the use of EDTA and gel with a stiffness of 16.7 kPa will allow the measurement of traction forces in relation to protrusion-retraction switches during all the process of the cell motion, from fluctuating state to migration.

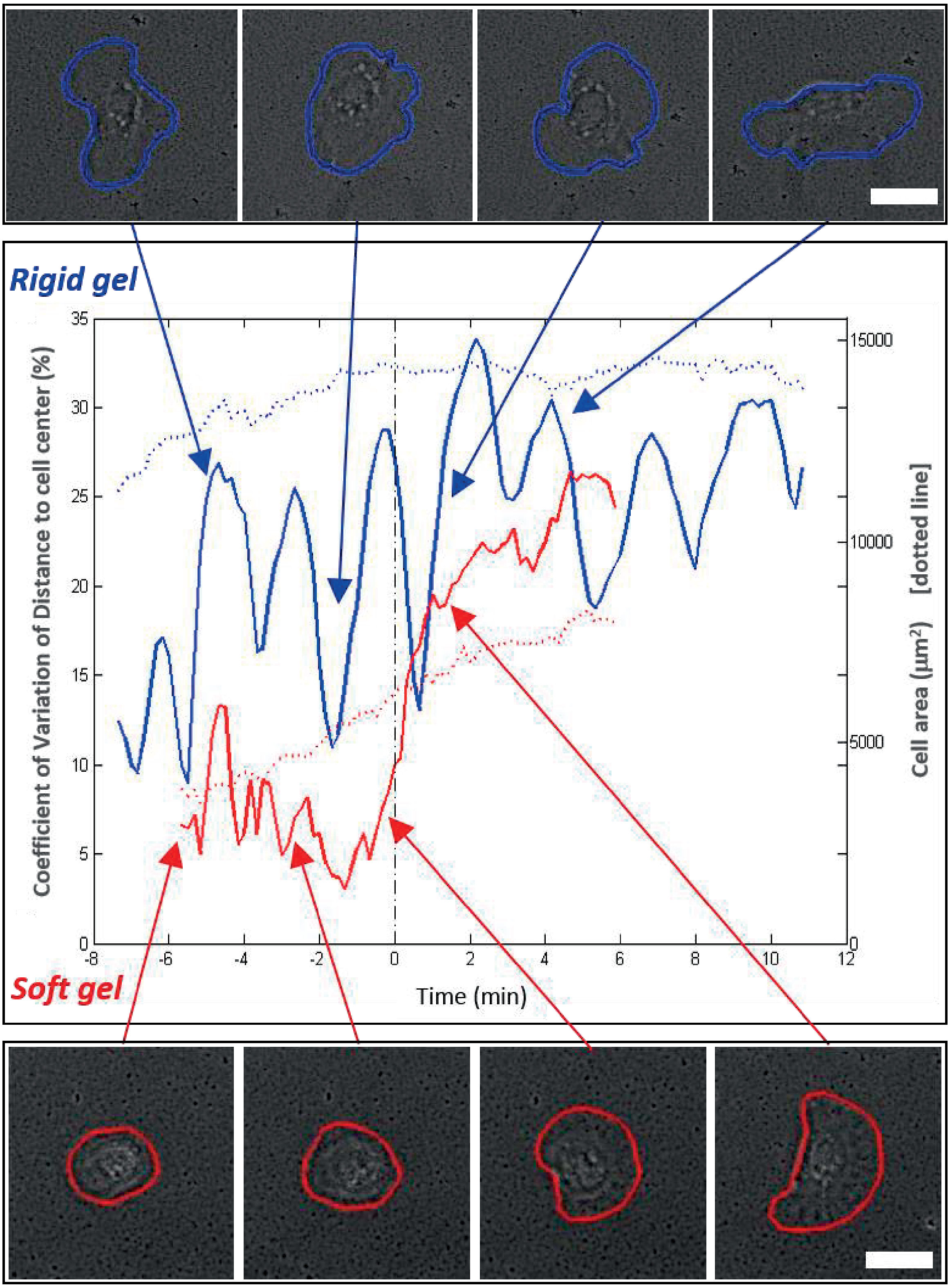

Figure 4.11: Edge dynamic of individual cell on polyacrylamide gel. Coefficient of variation of cell edge distance from the center of the cell and cell area (*dotted line*). The vertical dashed line represents the moment of round-to-polarized transition. Experiments were done on soft (1.5 kPa) or rigid (16.7 kPa) gel using EDTA for cell individualization. In the curves and the cell contour in phase contrast images, red refers to the soft gel and blue to the rigid gel. Scale bar = 10 µm.

4.4 Conclusion

Cell edge fluctuation is an important process that leads to cell polarization and subsequent migration. Our results indicate that distance-dependent switches from protrusion to retraction are critical for transition from isotropic fluctuations to a polarized state and that distance-sensing mechanism is dependent on actomyosin contractility and on the cell volume, but not on the microtubule system. Observation of actin dynamics showed that actin flow velocity was constant during the protrusion phase of the protrusion-retraction cycle, but increased at the moment of the switch to retraction, consistent with the detachment of the cell edge by the traction forces. To elucidate how contractility is involved in the distance-dependent mechanism, we have to analyze the link between critical distance and traction stresses generating by the actomyosin network. We have selected the conditions for this analysis to obtain large edge fluctuation and sufficient gel deformation for the force measurement. This analysis is described in the next chapter (chapter 2). In the last chapter, we aim to understand the role of tridimensional cell shape in the distance sensing, by analyzing the effect of the contact angle of the edge with the substrate (chapter 3).

Chapter 2

5) Relation between traction forces and protrusion-retraction switches

Cell applies traction force on the substrate through actomysion network and adhesions. Our hypothesis is that the stresses generated by the cell cytoskeleton scale with the size of the actomyosin network; therefore, forces increase with the distance from the cell center and at a critical distance induce the detachment of the network from the substrate leading to a retraction of the cell edge. To test this hypothesis, we measure the traction forces applied by the cell on the substrate during cell fluctuation and polarization in relation to the edge dynamics and protrusion-retraction switches.

5.1 Traction forces microscopy

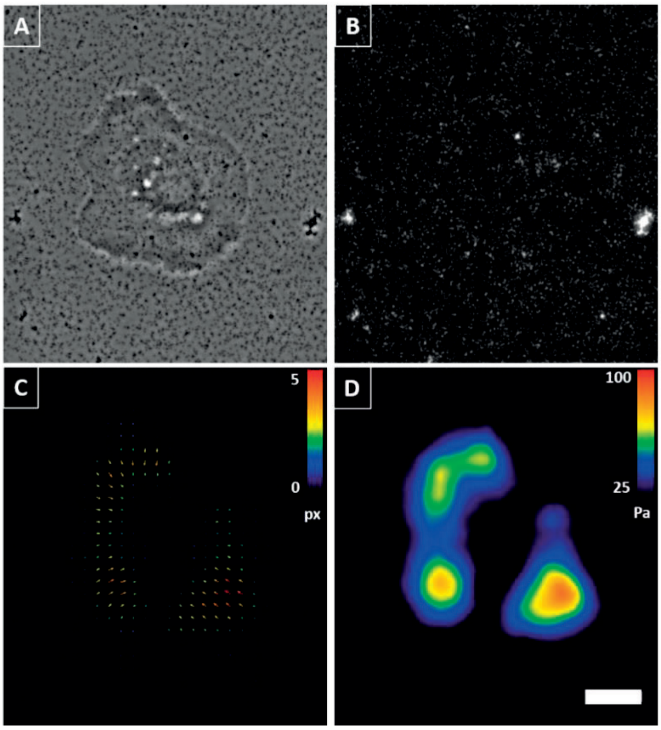

Figure 5.1: Mapping of forces of the cell on polyacrylamide gel. A) Phase contrast image of the cell on polyacrylamide gel. B) Image of fluorescent beads embedded inside the gel. C) Movement of the beads due to deformation of the gel under traction forces exerted by the cell is measured using Particle Image Velocimetry (PIV). Arrows indicate bead displacement. D) Based on the known substrate rigidity, the displacement of the beads is converted into a map of forces. Scale bar = 10 µm; 1 px = 0.0645 µm.

Measuring forces generated by the cell requires a flexible substrate, with embedded fluorescent beads to be able to visualize the substrate deformation. We used polyacrylamide gel of adjustable rigidity coated with fibronectin, a protein of the extracellular matrix allowing cell adhesion. We acquired sequences of phase contrast and fluorescence images of the cell (fig 5.1.A) on the gel with fluorescent beads (fig 5.1.B). Using Particle Image Velocimetry (PIV), the movement of the beads was tracked and converted into displacement (fig 5.1.C). The displacement of the beads was then analyzed and converted into map of forces (fig 5.1.D) using a Traction Force Microscopy (TFM) algorithm (Tseng et al., 2011). To analyze the forces at specific positions along the cell edge, we defined a band around the cell contour (offset ~3.25 µm inside and outside), subdivided this band into 20 segments based on curvilinear distance along the cell contour and measured forces in individual segments (fig 5.2).

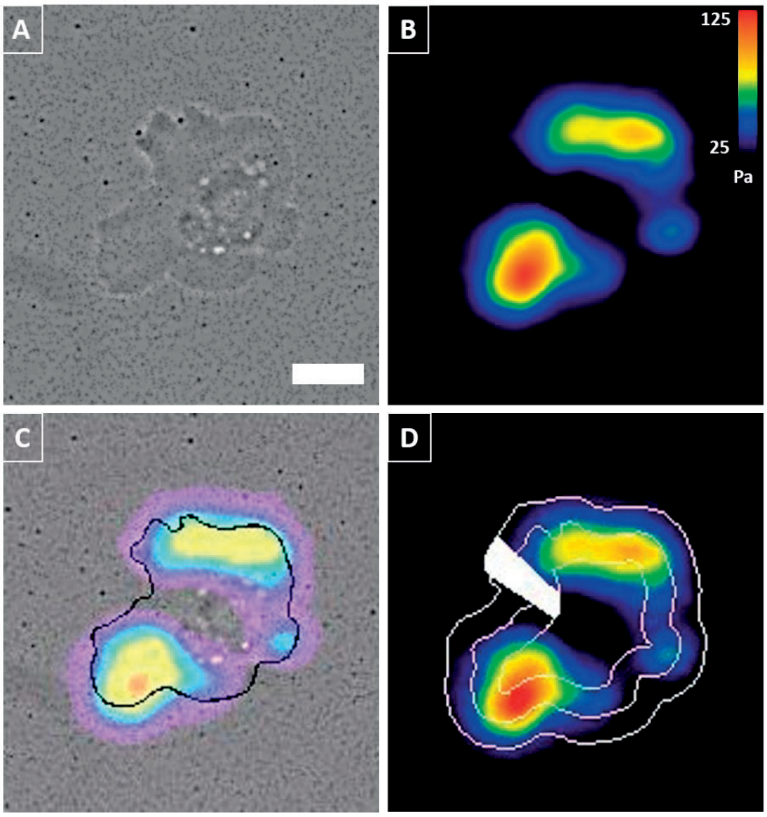

Figure 5.2: Analysis of traction forces. (A) Phase contrast picture and (B) force map of a cell on polyacrylamide gel. (C) Overlap of phase contract image, force map and the cell contour (black line). (D) Force map with the band around the cell contour and an individual segment (white) where the forces are measured. Scale bar = 10 µm.

5.2 Traction forces during cell polarization on soft gel

Substrate rigidity influences cell behavior (e.g. durotaxis) and cellular regulation. It has been shown that fibroblasts migrate preferentially towards and exert stronger traction forces on stiff substrate (Lo et al., 2000). As described in the previous chapter, we observed that on soft gel the cells spread less, showed less edge fluctuation and polarized faster than on rigid gel (chapter 1 fig.4.11) or glass substrate suggesting that breaking of symmetry and motility initiation can happen through different pathways depending on conditions. In this section, we describe different types of polarization behavior and analyze the traction force dynamics on soft gel.

5.2.1 Two distinct pathways to initiate motility

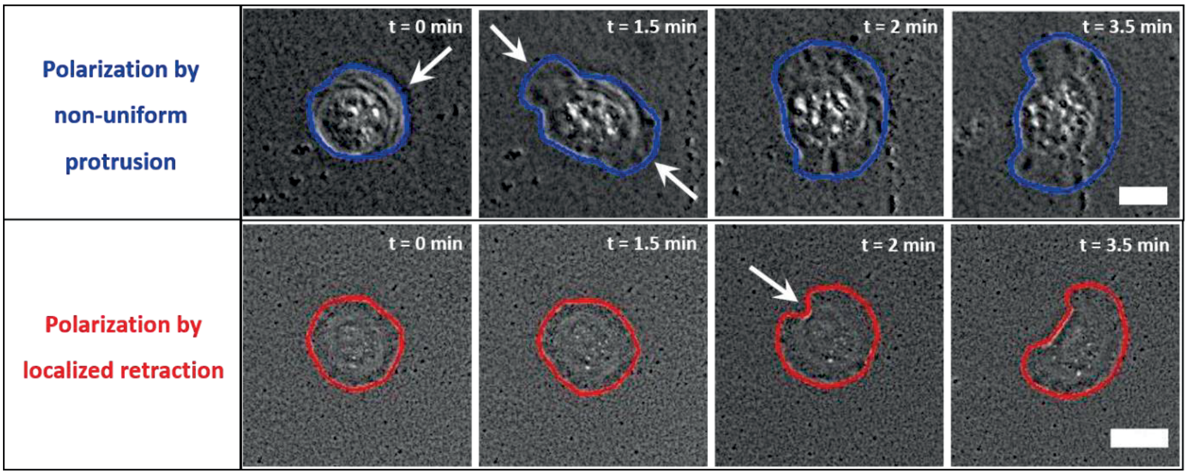

Figure 5.3: Cell polarization on soft gel. Cell polarization on soft polyacrylamide gel (1.5 kPa) for cells transferred from glass using Trypsin. Cell contours are plotted over phase contrast image for polarization by non-uniform protrusion (*blue*) and polarization by localized retraction (*red*). White arrows show the development of non-uniform protrusions in one case and the localized retraction in the other case. Scale bar = 10 µm.

On soft gel, we identify two types of cell polarization behavior. In one type of behavior (fig 5.3 *blue*), the cells initiate motility very soon after the initial attachment and concomitantly with spreading over the soft gel. In this case, the cells do not spread uniformly around the edge and usually start to move in the direction of the biggest protruding region. In the other type of behavior (fig 5.3 *red*), cells first spread nearly isotropically into circular shape and exhibit small cell edge oscillations and one or several local retraction events. Eventually, they move in the direction opposite to the local retraction but it is not necessarily the first retraction event that initiate the directional motion. Thus only a small part of the cells broke symmetry via a single event of retraction at the prospective rear as described in the previous studies on cell polarization in keratocytes (Yam et al., 2007).

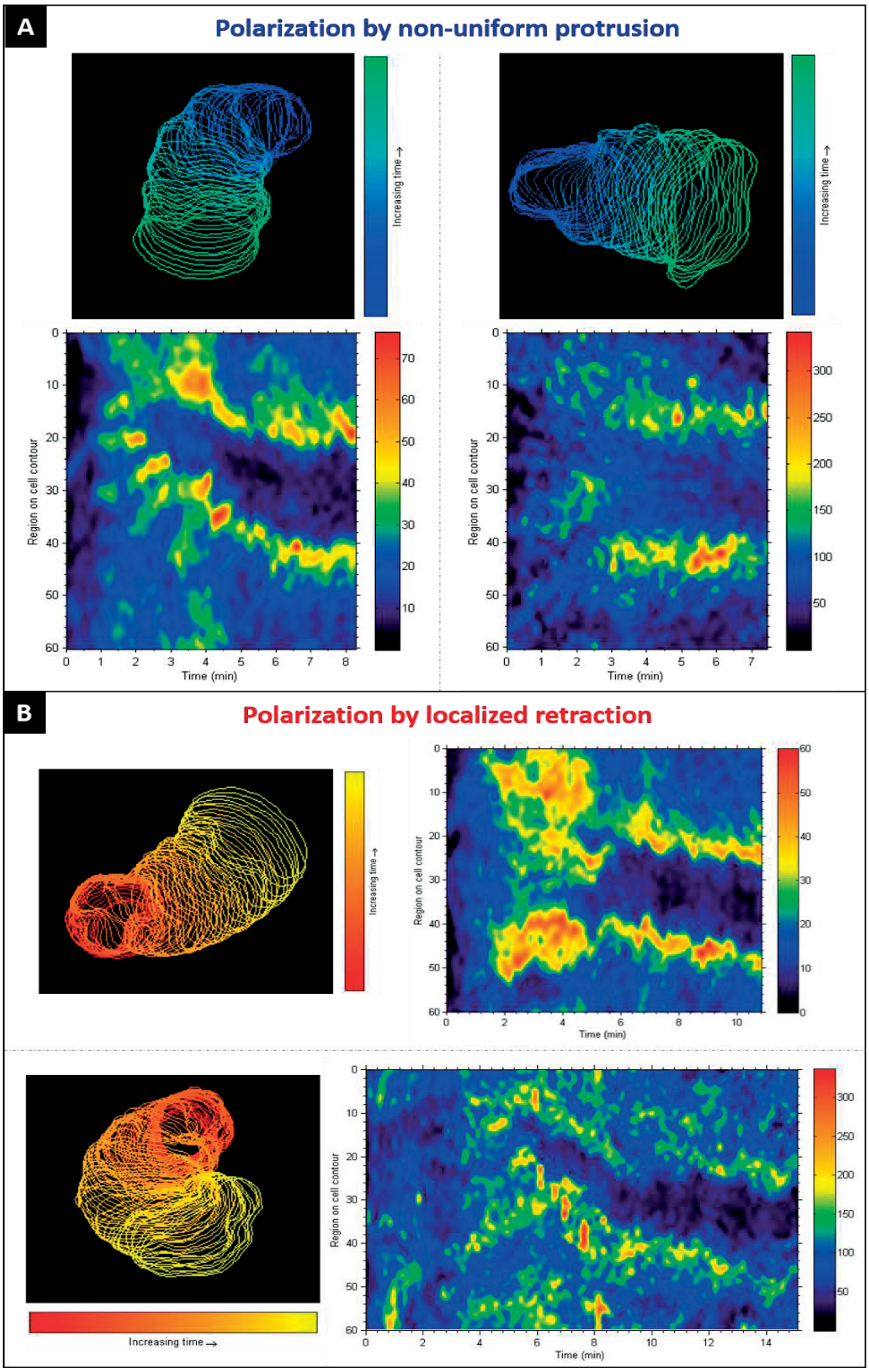

Figure 5.4: Traction force evolution during polarization on the soft gel. (A) Polarization by non-uniform protrusion versus (B) polarization by localized retraction. Edge contours and force evolution maps are shown for two representative cells in each case. Force maps are created by linearizing the bands along the cell contours from the force images and juxtaposing them versus time. Average force data in each band are sampled from 60 small regions encompassing the entire cell contour. Unit for force maps is Pascal (Pa). Interval of 10 seconds between each contours.

5.2.2 Distribution of traction forces on soft gel

To visualize traction force dynamics, force-time maps were created by linearizing the bands along the cell contours from the force images and juxtaposing them versus time (see Materials and Methods, section 3.6.1). Bands were aligned in a way that 0 coordinate always corresponded to the same angular position with respect to the cell center.

These force evolution maps (fig 5.4) show that migrating cells, for both types of polarization, typically exhibit the absence of forces at the leading and trailing edges and the localization of highest forces at the sides. Prior to polarization, the cells show either a disorganized force pattern, or a pattern with forces locally elevated at the prospective rear. This is not consistent with the recent study (Barnhart et al., 2015), which attributed the break of symmetry to a local loss of adhesion at the prospective rear resulting in a decrease in traction forces. Instead our force maps suggest that traction forces increase before polarization and then are released when the rear of the cell detaches and starts to move.

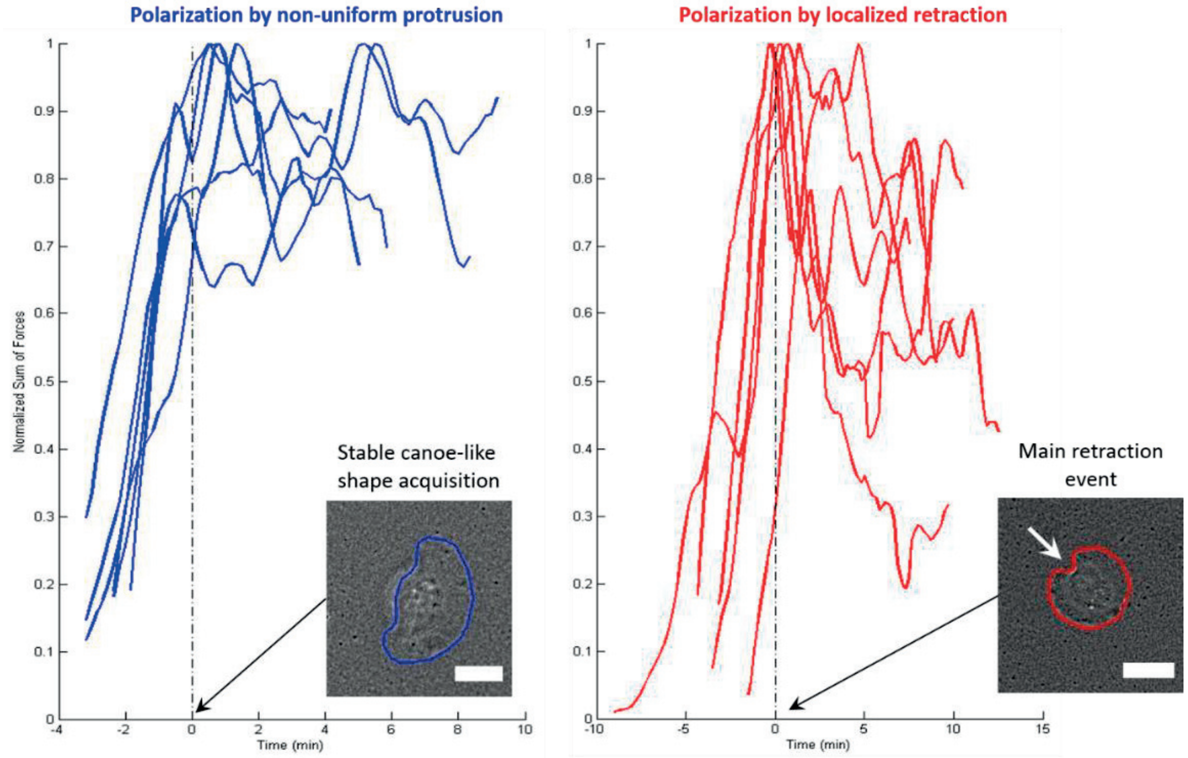

Figure 5.5: Total traction force evolution on soft gel. Normalized total force evolution for cell polarizing by non-uniform protrusion (left, *blue*) or by localized retraction (right, *red*). The curves are aligned with the time when the cell acquired a stable canoe-like shape for polarization by non-uniform protrusion and by the time of main retraction event for the polarization by retraction. For both cases, number of cells n = 6.

Plotting the evolution of total traction force per cell (fig 5.5) provides further support to the idea that polarization is preceded by the increase of traction force. In the case of polarization by non-uniform protrusion, we observed that forces increased until the cell acquired the stable canoe-like shape and then remained nearly constant. In the case of localized retraction, the forces increased until the main retraction event and then decreased before stabilizing during migration.

5.2.3 Force-distance relationship on soft gel

In the previous chapter, we have demonstrated that protrusion-retraction switches happen preferentially at the maximal distance from the cell center and this feature is critical for spontaneous polarization mechanism. If these switches are induced by increase of the traction force, we should expect that traction force increases with the distance from the cell center. On the soft gel, the cells did not exhibit large protrusion-retraction fluctuations. Therefore, it was difficult to correlate traction forces with individual protrusion-retraction switches. Nevertheless, plotting average forces in the small regions around the cell contour versus distance of the corresponding region from the cell center, showed a correlation between the force and the distance (fig 5.6). It is not surprising to see this correlation for migrating cells, because it was previously shown (Lee et al., 1994) (Fournier et al., 2010) that highest force are localized at the lateral wings of the cell, which are also the sites that are the most distant from the center.

However, we have also observed force-distance correlation (higher forces were observed at longer distances from the center, Pearson correlation coefficient R = 0.40) for the cells polarizing by localized retraction before they acquire elongated canoe-like shape (fig 5.6.B), although the window of distances was narrow as the cell maintained a global circular shape. Interestingly, local forces reached approximately the same maximal levels in the same cell before and after acquisition of an elongated shape although the maximal distances from the center were higher in elongated migrating cells. In contrast, in the cells polarizing by non-uniform protrusion, the local forces prior to polarization were smaller and the force-distance correlation (Pearson correlation coefficient R = 0.67) less pronounced than when the cell developed stable canoe-like shape (fig 5.6.A). The absence of high traction forces before polarization in the cells polarizing by this pathway is consistent with the fact that they do not exhibit significant retraction.

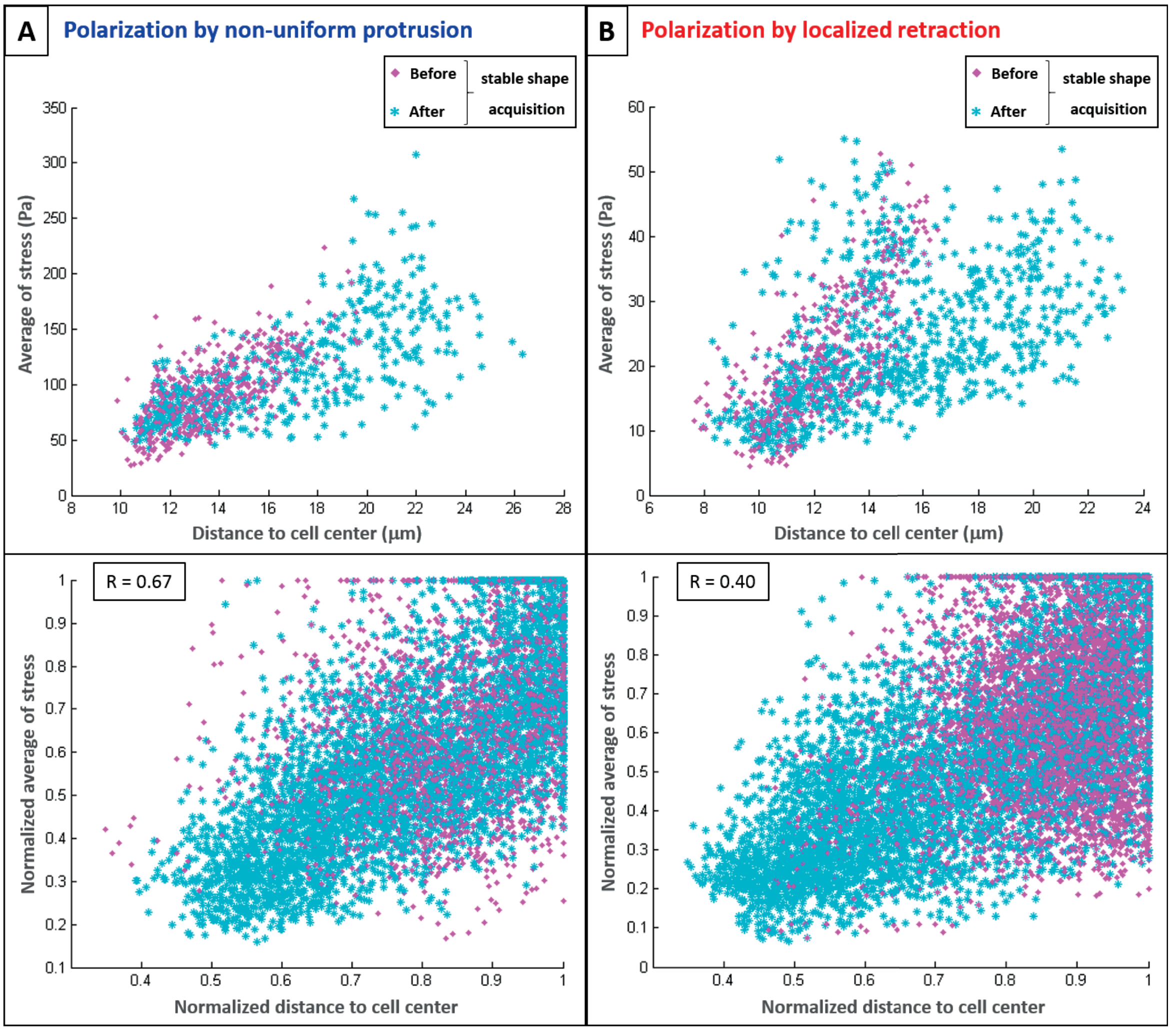

Figure 5.6: Force-distance relationship during polarization on soft gel. (A) Polarization by non-uniform protrusion versus (B) polarization by localized retraction. Average of force on each region along the contour are plotted in function of their distance from the cell center, before (*magenta*) and after (*cyan*) stable shape acquisition. For each case, the top panel shows one example cell and the bottom panel shows several cells together (n = 6). R corresponds to the Pearson coefficient correlation.

To conclude, we find that on soft gel, cells can polarize through two different sequences of events, each with its characteristic pattern of forces evolution. Observed differences are probably due to the timing of the symmetry breaking. For polarization by non-uniform protrusion the cell starts to move early and tension is released before the cell develops maximal traction, so the force magnitude monotonically approaches the level characteristic of migrating cell. For polarization by localized retraction, the cell first develops strong forces in the "frustrated" state where the tractions from opposite sides show a tug-of-war-like dynamics. Later, part of these forces are released due to detachment and retraction at the prospective rear, resulting in a decrease in the overall traction.

5.3 Traction forces and switches during cell polarization on rigid gel

On rigid gel, cells exhibit large protrusion-retraction fluctuations before breaking their symmetry and initiating motility. During fluctuation, the cells form several extended segments that protrude and retract and in some cases move around the cell perimeter. Traction forces were localized mostly at the termini of these segments (fig 5.7). Force evolution maps showed several clusters of high force moving around the cell edge until they consolidated and stabilized in two regions corresponding to the lateral extremities of the polarized migrating cell (fig 5.7).

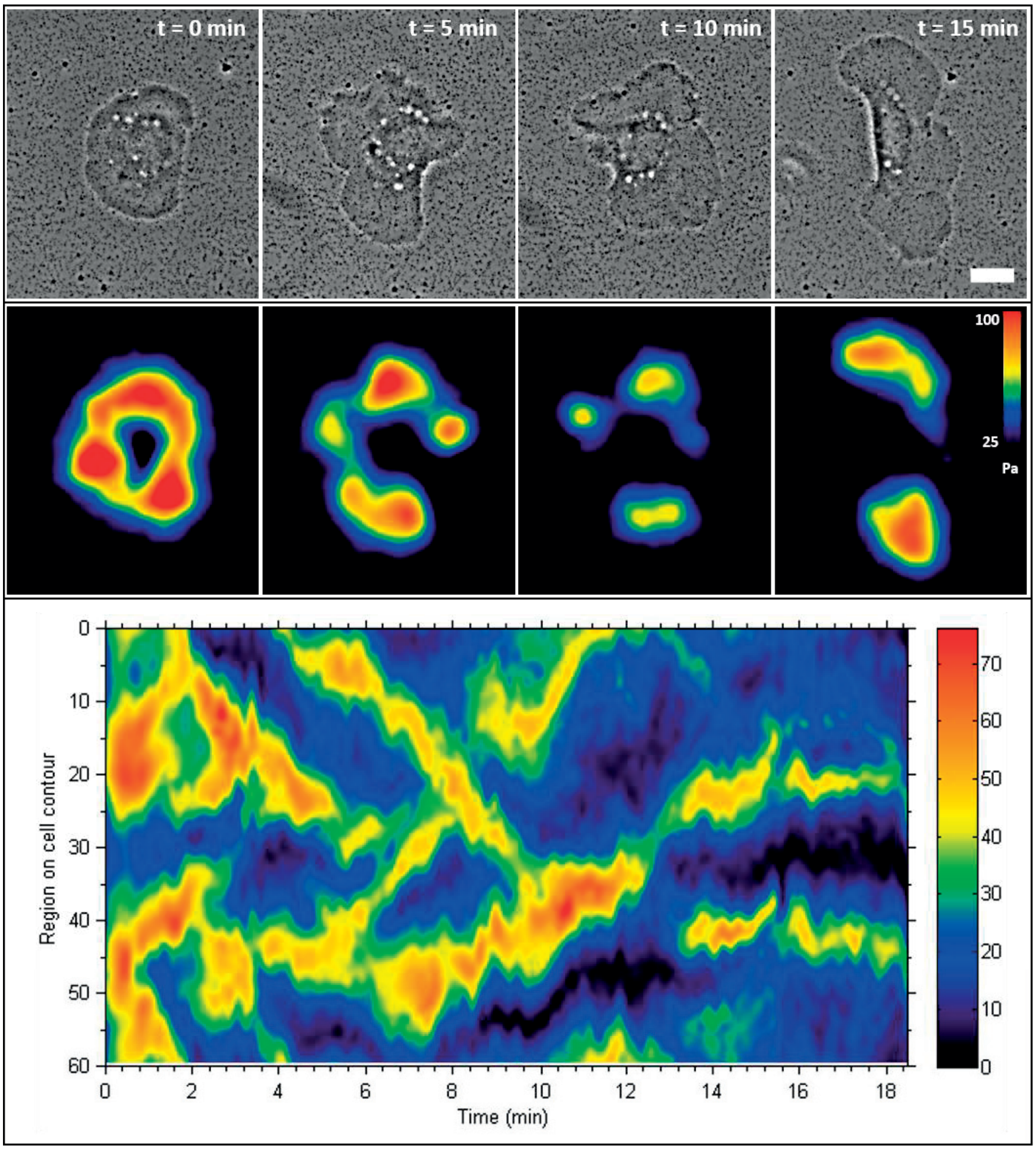

Figure 5.7: Timelapse of forces map of fluctuating cell. Phase contrast picture and related forces of cell on 16.7 kPa polyacrylamide gel. Force maps are created by linearizing the bands along the cell contours from the force images and juxtaposing them versus time. Average force data in each band are sampled from 60 small regions encompassing the entire cell contour. Unit for force maps is Pascal (Pa). Scale bar = 10 μm.

It was already demonstrated in previous studies on keratocytes (Lee et al., 1994) (Fournier et al., 2010), that migrating cell exhibits low forces at the front and back, and high forces at the lateral extremities of the cell (fig 5.7). Thus, during both cell fluctuation and migration, the forces seem to be maximal at the cell extremities corresponding to the maximal distance of the edge from the cell center. As we have shown previously (chapter 1) switches from protrusion to retraction also occur at the cell extremities. Large edge fluctuations observed in polarizing cells on rigid gel give an opportunity to investigate the relationships between forces, switches, and the distance from the cell center.

5.3.1 Force-distance relationship

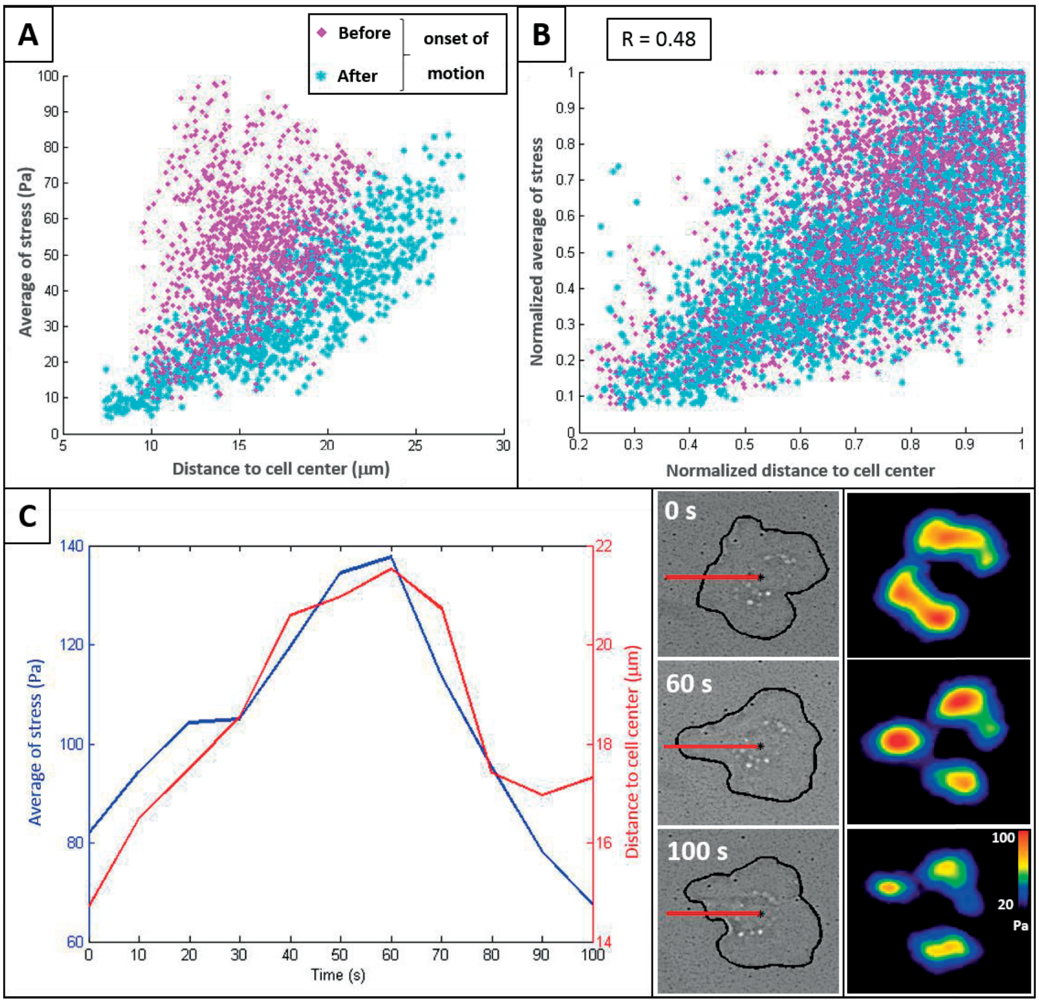

Figure 5.8: Cell traction forces correlate with the distance of the protruding edge from the cell center. (A) Average of force on each region along the contour are plotted in function of their distance from the cell center, before (*magenta*) and after (*cyan*) onset of motion for (A) one example cell and for (B) several cells together (n = 3). R corresponds to the Pearson coefficient correlation. (C) Average of forces and distance of the edge from the cell center for an individual protrusion to retraction event, represented in the inset pictures. A region is defined to measure the forces by taking the intersection between the fixed red line and the contour as the middle.

Similar to what was observed on soft gel, the scatter plot of local forces versus distance from the cell center showed positive force-distance correlation (Pearson correlation coefficient R = 0.48) during both fluctuation and migration (fig 4.8.A-B). Our analysis revealed that there exists not only a general force-distance correlation but also maximal forces corresponded to the maximal distances during individual protrusion-retraction events. Plotting the average force in a small region at the tip of the protruding cell segment and the distance between the edge and center at this location over time showed that the force and the distance increased and decreased synchronously and reached the maximum at nearly the same moment (fig 5.8.C), suggesting that protrusion-retraction switch happened at the maximal force.

5.3.2 Induced cell shape perturbation

In chapter 1, we have shown that protrusion-retraction switches can be induced at the front of a migrating cell by artificially increasing the distance of the edge from the cell center. This was done by blocking the cell nucleus with a pipette. We have tested if these induced switches are also correlated with local increase of forces. The pipette was placed in front of cell migrating on rigid gel, so that the nucleus was blocked but the leading edge passed between the pipette and the gel, while taking a special care not to deform the gel with the pipette.

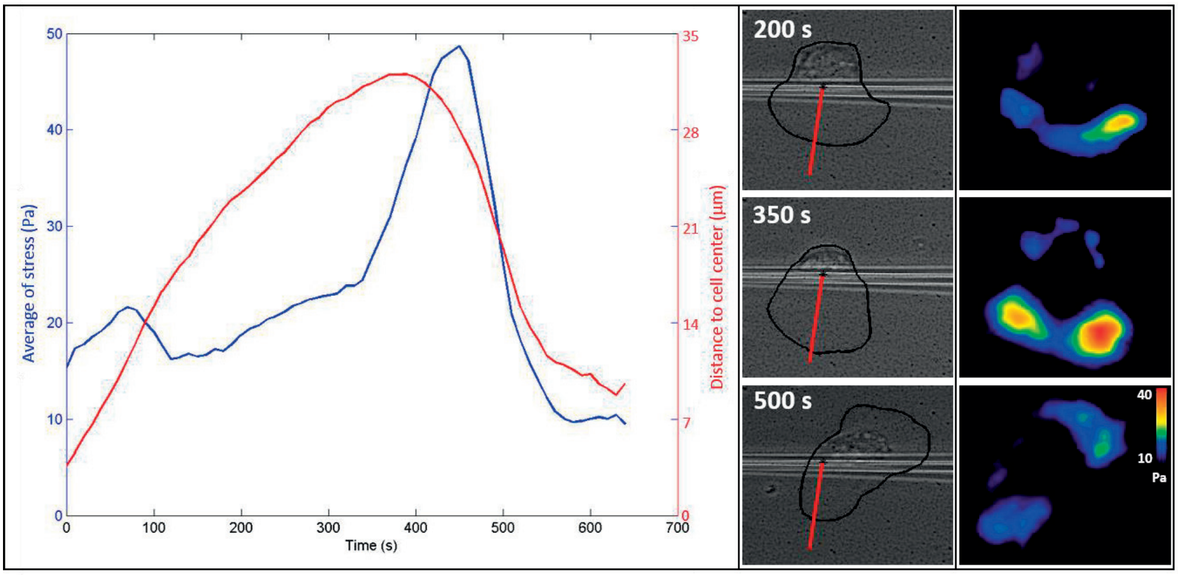

Figure 5.9: Cell traction forces correlate with their distance from the blocking pipette. Average of forces and distance of the edge from the pipette for the protruding region, represented in the inset pictures. The region is defined by taking the intersection between the fixed red line and the contour.

For this experiment, the study of the force-distance relationship was done by considering the distance between a defined point on the pipette position where the cell body is blocked and the extremity of the protruding edge (fig 5.9). We observed a correlation between the distance from the edge to the pipette and traction forces, as was observed before for naturally occurring protrusion-retraction events. However in the pipette experiment, the forces continued to increase for a short time after initiation of retraction. This increase of force is not contradictory to the possibility that a switch to retraction was induced by a critical force: if the tension was not immediately released by retraction, the forces could still accumulate above a critical level. Thus, the extension of the cell induced by experimental manipulation was associated with the increase of a traction force in a manner similar to the extension occurring naturally during cell fluctuation. These results are consistent with the possibility that switch from protrusion to retraction is induced by the increase of force.

5.3.3 Correlative mapping of switches and traction forces

Next we investigated relative distribution of switches from protrusion to retraction and traction forces. We used the algorithm described in Chapter 1 to map switch distribution and we overlaid resulting switch images over thresholded force images (fig 5.10.A-B). We observed that switches localized mainly at the edge positions close to the regions of maximal forces (fig 5.10.A). During edge fluctuation, regions of maximal forces moved along the edge and switch locations were observed to follow in most cases the dynamics of forces (fig 5.10.B-C).

However, switch positions did not coincide completely with the local force maxima. Such coincidence in fact should not be expected because switches are localized at the cell edge, but the force regions are mostly found inside the cell contour, consistent with the fact that the cell applies forces through focal adhesions that are located at some distance from the cell edge (see fig 4.1.C in Chapter 1). Plotting the normalized probability to find the force over a given threshold in function of normalized distance from the cell center (fig. 5.11) showed that probability maximum shifted towards the maximal distance with increasing threshold. At the same time, the maximum of the switch probability localized at the maximal center-to-edge distance. The distance between the maxima of the switch probability and force probability (Fig. 5.11 *inset*) thus decreased with increasing force threshold (to approximately 10-15% of the maximal cell radius). This result indicates that maximal forces are mainly localized close to the cell edge with distance between the forces and the switches probably reflecting the distance between the focal adhesions and the cell edge. This is consistent with the idea that forces over a certain threshold induce detachment of focal adhesions in the vicinity of the cell edge and switch from protrusion to retraction at the edge.

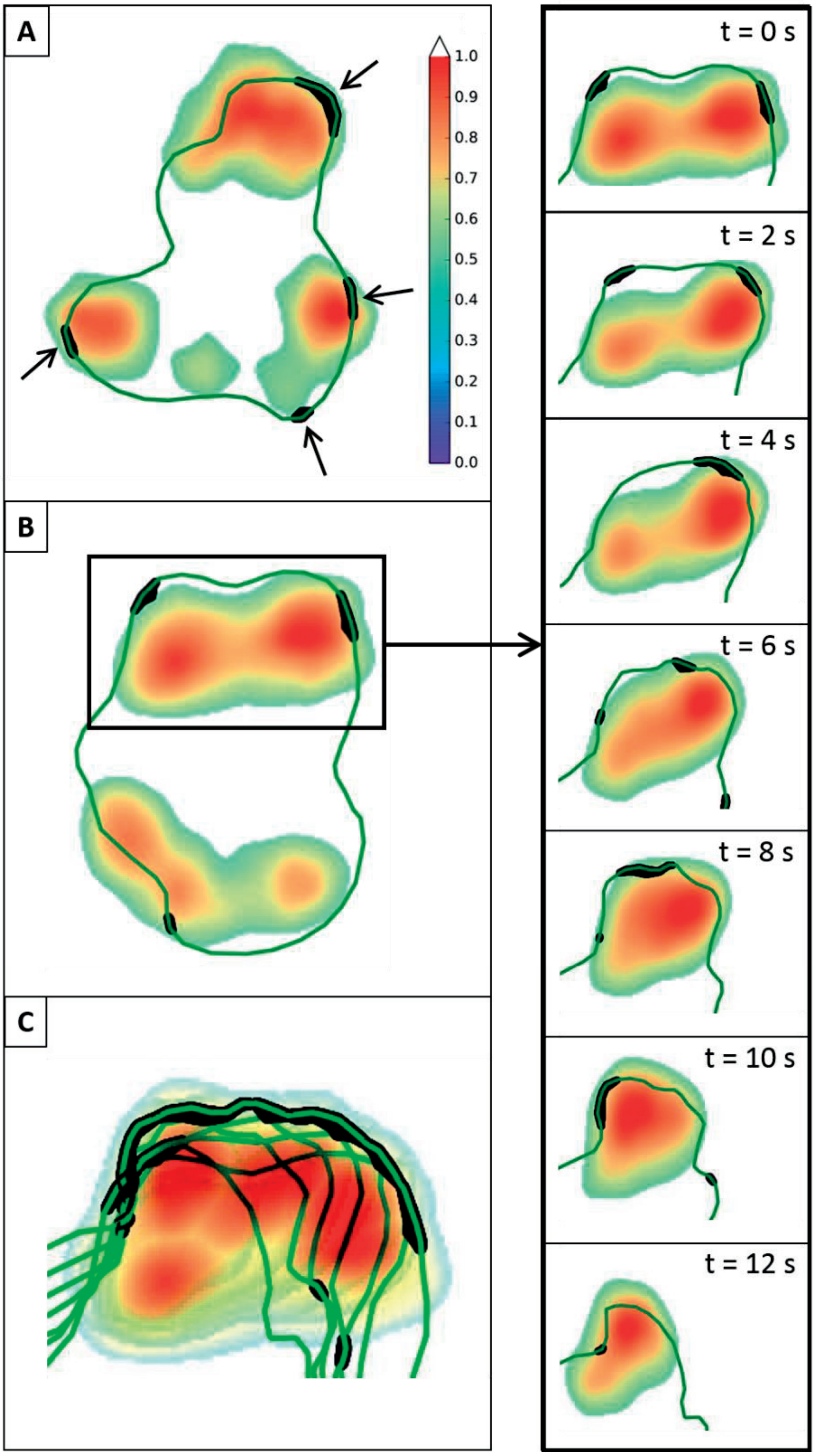

Figure 5.10: Switches correlation with maximal traction forces. A) Overlap of switches, cell contour and force image. Arrow shows the position of switches from protrusion to retraction. B) Another example of switch/force overlay. The right panel represents a time sequence of the switch and force dynamics in the region boxed in (B). C) Overlap of switches, contours and forces in all frames of the same sequence.

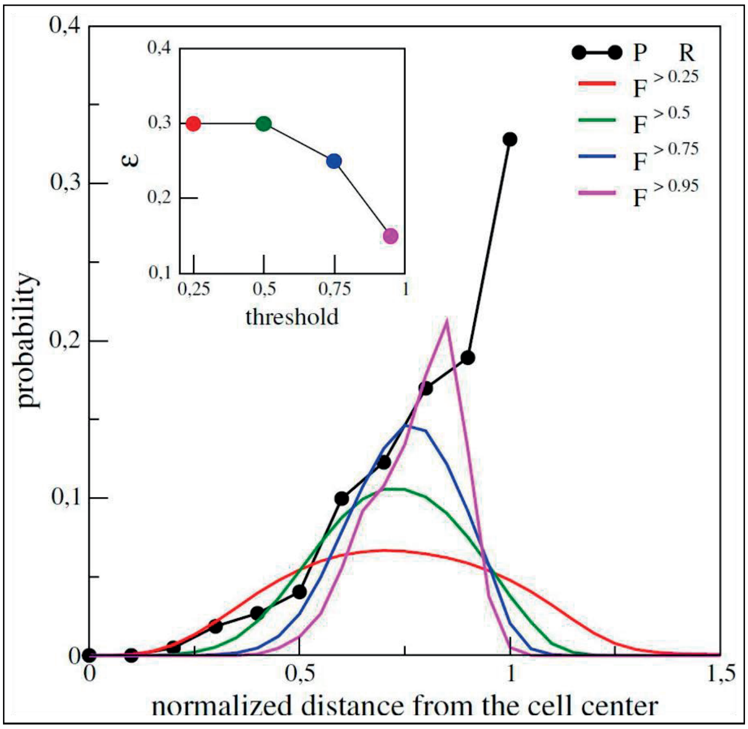

Figure 5.11: Switch correlation with maximal traction forces. Normalized probability to find threshold forces in function of normalized distance from the cell center. The inset shows the distance (ε) between the maxima of switch probability and force probability.

5.4 Cell contractility inhibition on rigid gel

5.4.1 Distribution of traction forces in contractility-inhibited cells

To evaluate the effect of myosin contractility on the distribution of traction forces, we treated the cells with Blebbistatin, an inhibitor of actin-myosin II interaction. As expected, Blebbistatin treatment resulted in a significant decrease of stress (fig 5.12.A-B).

In contrast to control cells, plotting the local forces in function of the distance from the cell center did not reveal a significant force distance correlation. Before motion, the cells maintained nearly round shape making the distance distribution very narrow, and displayed variable but generally weak forces. During motion, the cells expanded and often split into fragments resulting in wide distribution of center-to-edge distances, but the forces were low for all distances. Assuming that cell edge fluctuations and the development of a stable canoe shape after polarization are the result of distance-dependent protrusion-retraction switches mediated by traction force, the absence of fluctuation and the failure to maintain a stable shape after the onset of motion in blebbistatin-treated cells are consistent with the low level of traction forces and the lack of force-distance correlation (Pearson coefficient correlation R = -0.16).

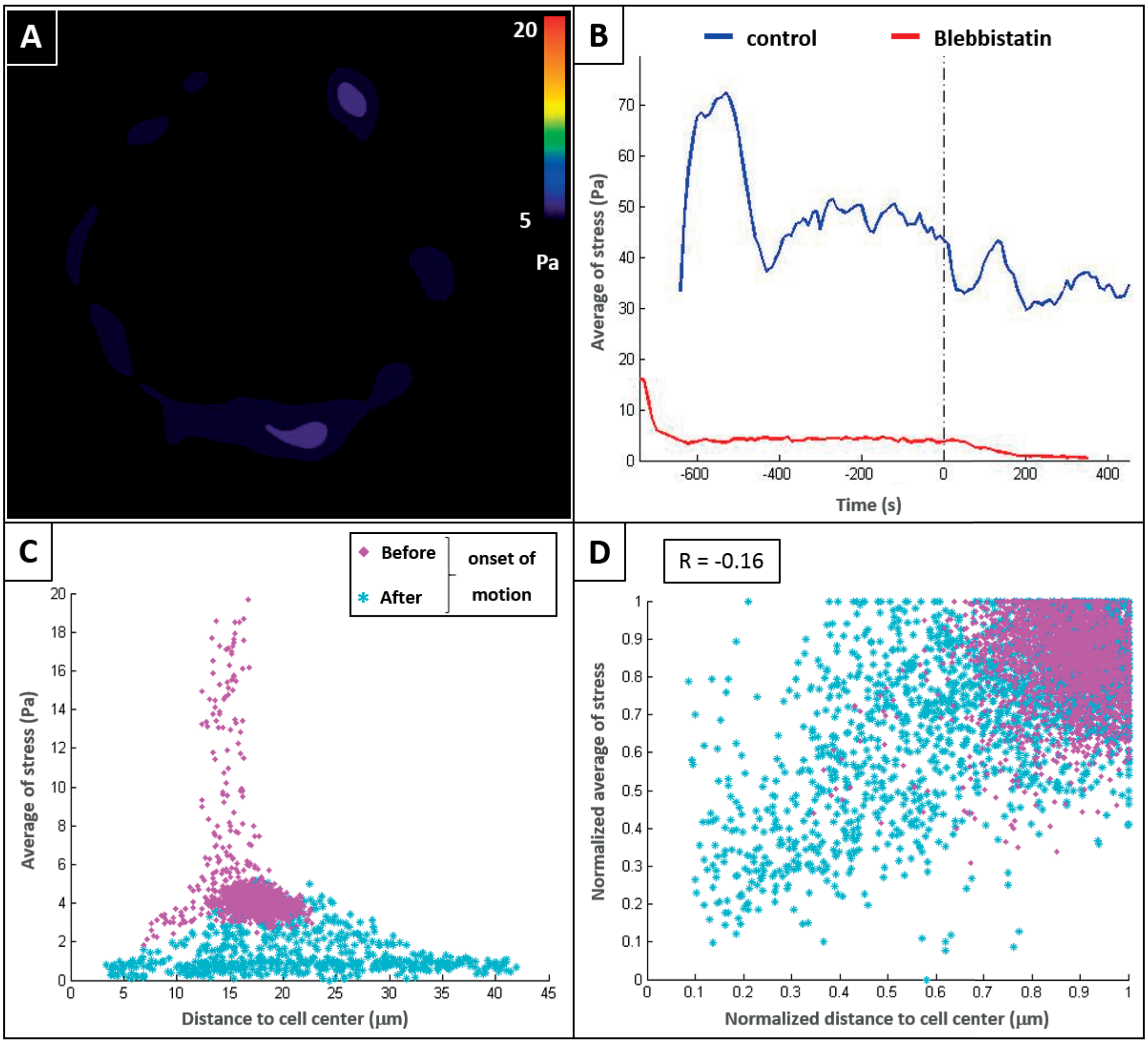

Figure 5.12: Cell traction forces in contractility-inhibited cells. (A) Traction force image of blebbistatin-treated cell before the onset of motion. (B) Average of forces in the cell in function of time, for control (*blue*) and blebbistatin-treated (*red*) cell. (C) Average of force on each region along the contour are plotted in function of their distance from the cell center, before (*magenta*) and after (*cyan*) stable shape acquisition for (C) one example cell and for (B) cells together (n = 3). R corresponds to the Pearson coefficient correlation.

5.4.2 Mapping of switches in contractility-inhibited cells

Contractility-inhibited cells showed dramatically reduced traction forces, but exhibited small edge fluctuations and eventually polarized, albeit with a delay and without maintaining a constant shape. We next tested how inhibition of traction and abnormalities in polarization are related to switches between protrusion and retraction. Mapping switches and plotting switch distribution in function of the distance from the cell center (figure 5.13) revealed that in blebbistatin-treated cells, in contrast to control cells during fluctuation, PR and RP switches were found at the same locations and nearly at the same distance from the cell center. This is not surprising as it simply demonstrates in a different way that cell edge fluctuations were very small and the edge did not show persistent protrusion or retraction phases between switches. Thus, traction forces may not be necessary for the switch itself, but they may influence the amplitude of retraction after PR switch, and, indirectly, the amplitude of subsequent protrusion.

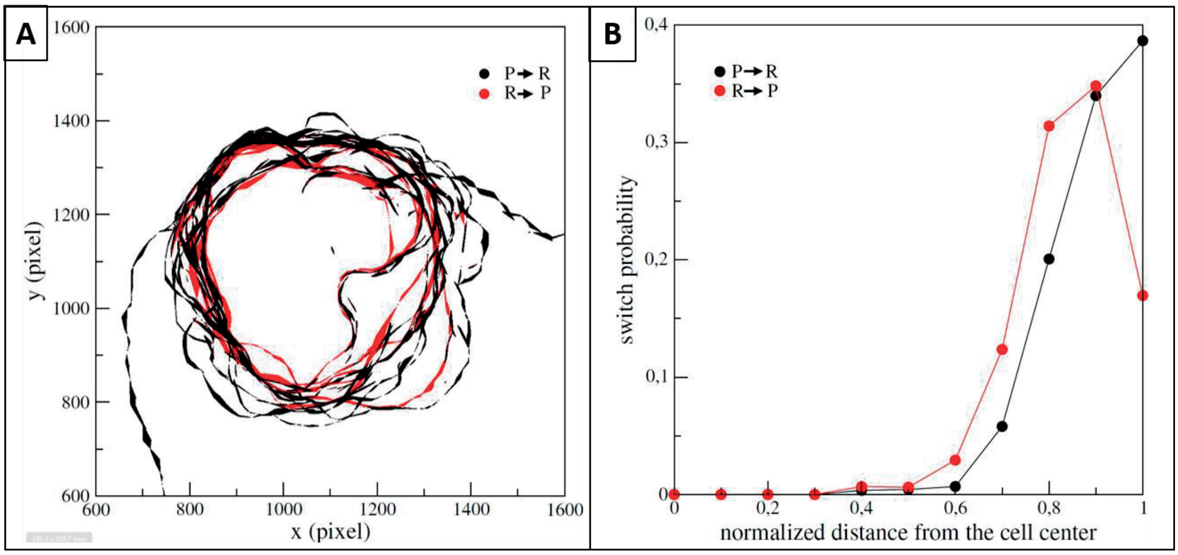

Figure 5.13: Switch mapping in contractility-inhibited cell. (A) Localization of PR (*black*) and RP (*red*) switches for blebbistatin-treated cell until the onset of motion (frame superimposed). (B) Switch probability as function of the normalized distance from the cell center in blebbistatin-treated cell until the onset of motion.

5.5 Manipulation of edge dynamics with external forces

5.5.1 External forces during cell fluctuation

As shown in the previous chapters, the process of switching from protrusion to retraction is correlated with a local increase of traction forces in the regions of the cell edge corresponding to the maximal distance of the edge from the cell center. In order to elucidate whether switches are induced by a local increased of traction force due to the increase of distance, or if increase of distance leads to switches through a mechanism independent of traction forces, we manipulated traction forces to test if traction force alone can induce switch.

For that, we applied local force at the cell edge by placing a micropipette inside the gel near the protruding region. Micropipette deformed the gel pulling the cell edge together with the gel and thus effectively applying a local traction force between the cell edge and the substrate. In most cases, the cell edge initially moved a small distance outward together with the deformed gel, but then, after 10-15 seconds, started retracting, indicating that external force induced protrusion-retraction switch (fig 5.14). A small delay between the application of the force and the onset of retraction suggested that retraction was not a trivial result of immediate detachment of the cell edge at the moment of force application, but indeed a consequence of force increase.

This experiment suggests that switches from protrusion to retraction could be induced by a local increase of forces, and thus distance-sensing could work through traction force increase. However, protrusion-retraction switches were also occurring naturally in the cells during these experiments, which made quantification of the results difficult.

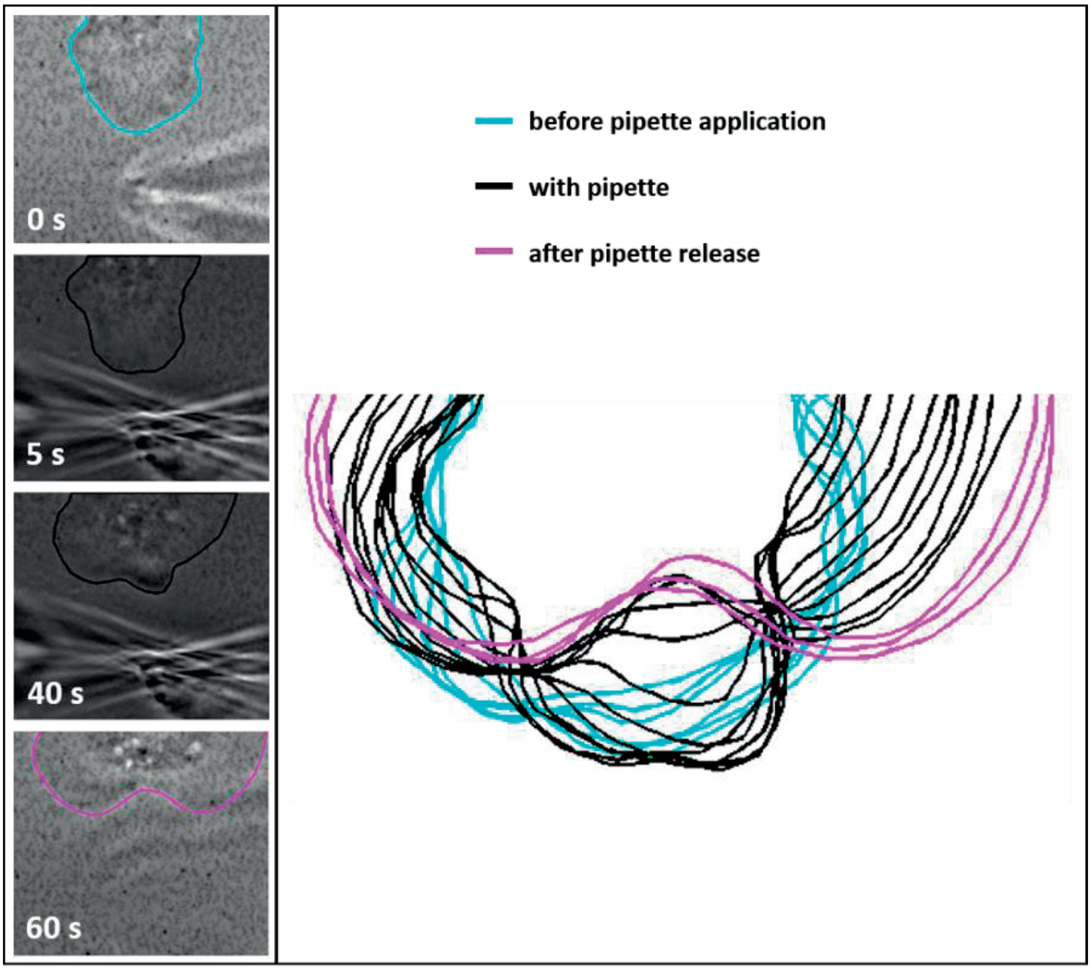

Figure 5.14: Induced external force on polyacrylamide gel. A micropipette was inserted inside the gel close to the cell edge in order to deform it and apply a force at this part of the cell. Cell contours are overlapped on the phase contrast image and plotted all together with colors corresponding to the cell position before pipette application on the gel (*cyan*), during force application by the pipette (*black*) and after the release of the pipette (*magenta*). Interval between contours was 5 seconds.

5.5.2 External forces on contractility-inhibited cells

We tested if external force could induced protrusion-retraction switch in blebbistatin-treated cells that lack significant internal forces and do not display prominent edge fluctuations. By pulling the gel with the micropipette, we observed local retraction at the region nearest to the pipette application (5 out of 9 applications) (fig 5.15), suggesting that increase of force led to a retraction event. No retraction was observed at the same time at the edge regions located at the opposite side of the cell with respect to the pipette application site or orthogonally to this site. This was in contrast to control cells that exhibited continuous edge fluctuations prior to polarization making it somewhat difficult to distinguish intrinsic retraction and the retraction induced by external force. Thus, blebbistatin-treated cells presented a clear case to demonstrate initiation of retraction by application of local force. This experiment proves that switching from protrusion to retraction could be induced by a local increase of traction force even when the cell is unable to develop strong endogenous traction.

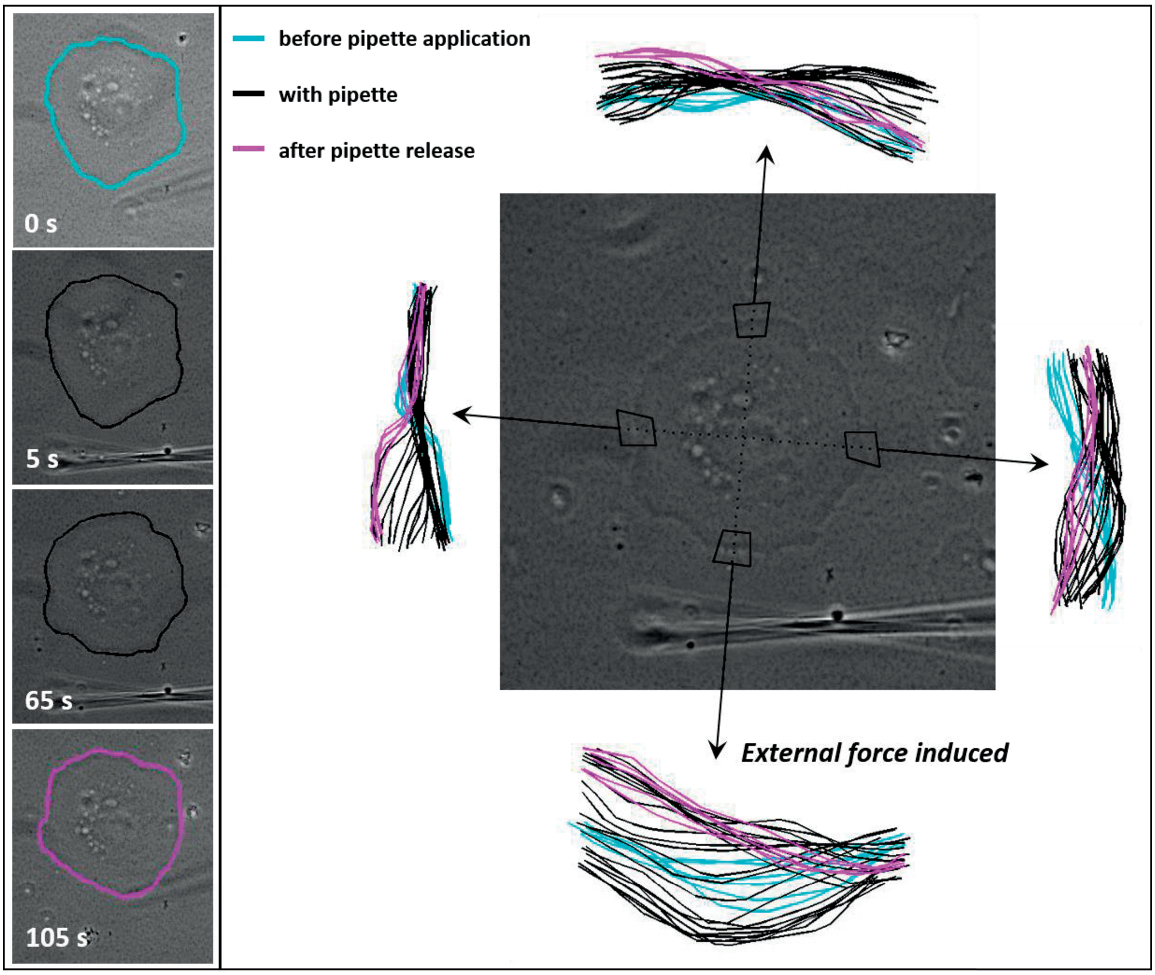

Figure 5.15: Induced external force on polyacrylamide gel for contractility-inhibited cell. A micropipette was inserted inside the gel close to the cell edge in order to deform it and apply a force at this part of the cell. Cell contours are plotted for the region of the applied force and the three other regions (opposite and orthogonal to the site of force application) with colors corresponding to the cell position before pipette application on the gel (*cyan*), during force application by the pipette (*black*) and after the release of the pipette (*magenta*). Interval between contours was 5 seconds.

5.5 Conclusion

In this chapter, we have shown that traction forces increase with the distance from the cell center, that local increase of force often coincides with the onset of retraction during polarization on the soft substrate and protrusion-retraction fluctuation on the rigid substrate, that maximal force positions coincide with protrusion-retraction switches, that inhibition of contractility suppresses both traction forces and cell edge dynamics, and that retraction of the edge could be initiated by local external force. These results indicate that distance-dependent protrusion-retraction switches are, at least in part, mediated by the increase of traction forces.

Chapter 3

6) Contact angle at the leading edge controls switching process

Protrusion depends on the actin polymerization which has to overcome membrane tension to push the membrane forward. Actin polymerization and membrane tension are believed to be antagonistic forces that define the protrusion rate at the leading edge. Resistance to actin protrusion is a product of membrane tension and mean local curvature (Laplace’s law); thus, it depends on the local geometry of the membrane interface. In our recent work (Gabella et al.), we found that the protrusion rate does not correlate with membrane tension, but, instead, strongly correlates with cell roundness. We explained these findings by considering the leading edge as a triple interface between the substrate, membrane, and extracellular medium. In this model, the contact angle between the membrane and the substrate determines the load on actin polymerization and, therefore, the protrusion rate.

6.1 Shape of the protruding edge

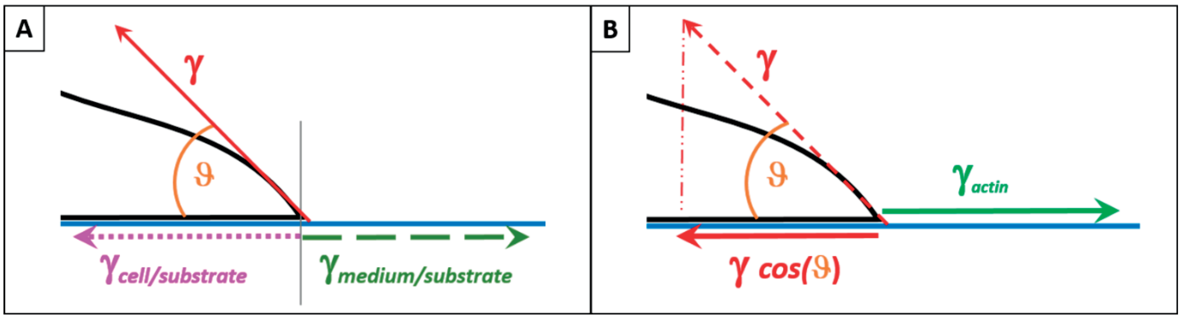

Figure 6.1: Contact angle of the cell edge. A) The interfacial tension between the cell and the substrate surface $\gamma_{cell/substrate}$ and between the medium and the substrate surface $\gamma_{medium/substrate}$ are opposite and both oriented along the substrate surface. The membrane tension γ, which correspond to the interfacial tension between the apical membrane and the medium, is directed according to the contact angle (ϑ) formed by the membrane and the substrate at the leading edge B) Actin polymerization creates a tension against the cell membrane, which is oriented parallel to the substrate surface. Effective resistance to actin tension is given by the projection of γ on the substrate surface $\gamma\ cos(\vartheta)$.

By likening the cell to a liquid droplet, we can apply a simplified model of force balance inspired by Young-Laplace equation, considering the cell edge as a triple interface. The interfacial tension between the cell and the substrate and between the extracellular medium and substrate are oriented along the surface opposite to each other (fig 6.1.A) and can be considered as constant values. Actin tension, corresponding to the force per unit length of the edge exerted by actin assembly against a narrow band of the membrane at the extremity of the protrusion, is also oriented along the surface (fig 6.1.B).

Regarding membrane tension, which correspond to the tension at the interface between the apical membrane of the protrusion and the extracellular medium, it is oriented according to the contact angle formed by the membrane with the substrate (fig 6.1.B). Resistance to actin polymerization is defined by the projection of membrane tension on the substrate surface. Thus, increasing contact angle is expected to decrease the effective resistance to actin polymerization resulting in the increase of protrusion rate, while decreasing contact angle is expected to increase the effective resistance resulting in the decrease of protrusion rate.

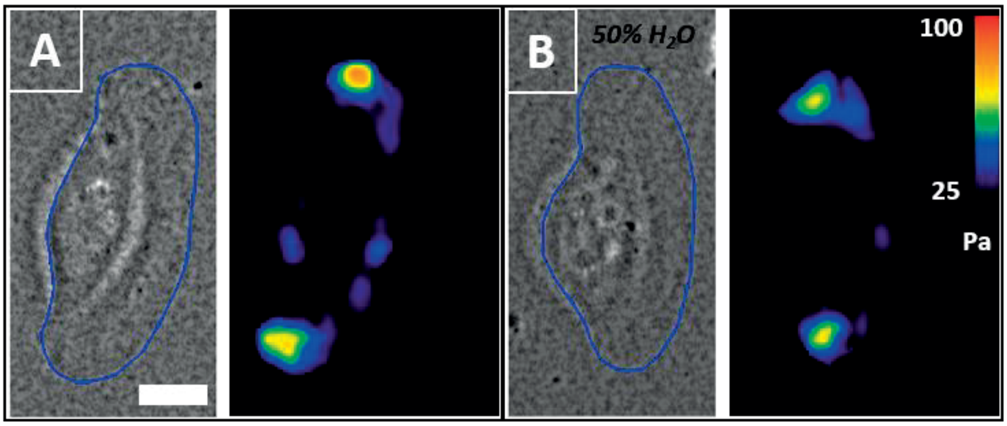

Figure 6.2: Traction forces of osmotically-treated cell. Phase contrast and traction forces of cell (A) under normal condition and (B) in a medium with 50% of water. Scale bar = 5 µm.

Here, we propose a hypothesis that switches between protrusion and retraction can be induced by a decrease of the contact angle. When the cell edge extends, the protrusion becomes thinner and the contact angle at the extremity of the protrusion becomes smaller leading to the increase of resistance. Eventually, this may inhibit protrusion and induce a switch to retraction. Inversely, when the membrane retracts, the contact angle increases reducing the load against actin polymerization, and thus facilitating switch to protrusion. As the contact angle is expected to change with the extent of protrusion or retraction, this hypothesis could explain the dependence of switches on the distance from the cell center. In our recent work (Gabella et al.), we have speculated that approximating the cell shape with an ellipsoidal cap. Contact angle along the long cell axis is expected to be smaller than along the short axis and this could contribute to the protrusion-retraction switch at the lateral extremities of migrating keratocytes. In this work, contact angle was also manipulated with osmotically swelling and shrinking the cells resulting in the change of protrusion rate. No significant difference, however, was observed in traction force pattern upon osmotic treatment (fig 6.2), suggesting that alteration of tension balance due to contact angle may be confined to the tip of the leading edge and do not affect traction forces at the focal adhesions further away from the edge.

We evaluated the shape of vertical profile of the leading edge during protrusion-retraction oscillation using fluorescent displacement method. Cells were placed in a thin chamber containing fluorescent dye solution to produce shadow-like images, and the cell height was estimated from the difference of intensity between the cell and the background (Bottier et al., 2011). We observed that as the cell edge extended, the extremity of the protrusion became flatter as expected (fig 6.3) reducing the contact angle between the membrane and the substrate. When the protrusion switched to retraction contact angle increased again (fig 6.3).

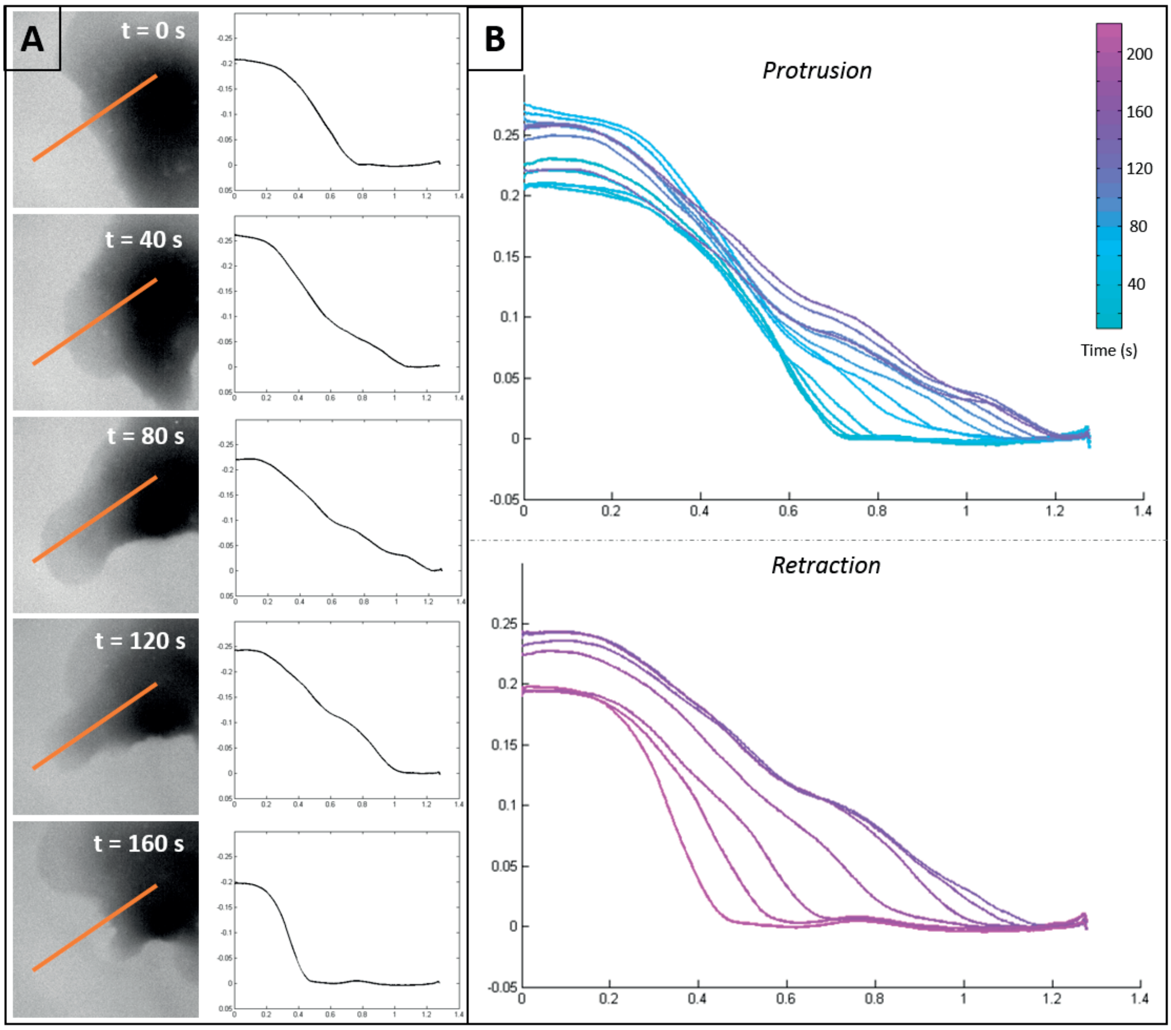

Figure 6.3: Cell protrusion shape. A) Fluorescence-displacement image of a protruding-retracting cell edge and the height profile of the protrusion-retraction event taken along the orange line. B) Same height profile are plotted together in function of time (colorbar) for the protrusion phase (to*p*) and the retraction phase (*bottom*). Horizontal axis: position along the orange line; vertical axis: fluorescence intensity.

6.2 Modification of contact angle using substrate topography

We manipulated contact angle to test if it indeed controls the switch from protrusion to retraction. Osmotic swelling or shrinking of the cell is expected to change the global cell shape and contact angle around the entire edge but would not necessarily change the distribution of protrusion-retraction switches. We decided to manipulate the contact angle locally by using substrate topography rather than cell shape alteration. Influence of the substrate topography on the dynamics of triple interface was described in wetting phenomena as pinning: in this characteristic behavior edge of the liquid droplet is drawn to the ridges of the surface, because at the ridge unbalanced forces arise that trap the edge at the ridge (Kalinin et al., 2009). Based on the same principle, we hypothesized that protrusion dynamics will be modified when it reaches a boundary where substrate orientation changes. During protrusion on a flat substrate, the forces at the edge are balanced (fig 6.4.A). When the substrate orientation changes, the forces become unbalanced because the tension at the medium/substrate interface is no longer aligned with other tensions (fig 6.4.B). This is expected to halt the protrusion: the cell would need to increase contact angle between the apical membrane and the substrate to pass the ridge. Pause in protrusion may also increase probability of a switch to retraction. Similarly, during retraction substrate ridge may be expected to increase probability of a switch to protrusion.

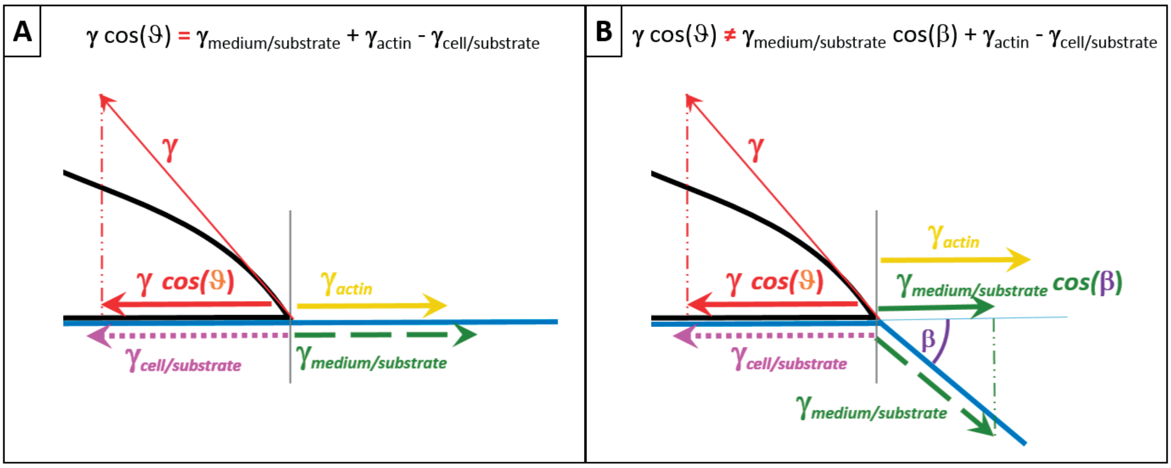
A
$\gamma \cos(\vartheta) = \gamma_{medium/substrate} + \gamma_{actin} - \gamma_{cell/substrate}$
γ
$\gamma \cos(\vartheta)$
γ_{actin}
$\gamma_{cell/substrate}$
$\gamma_{medium/substrate}$
B
$\gamma \cos(\vartheta) \neq \gamma_{medium/substrate} \cos(\beta) + \gamma_{actin} - \gamma_{cell/substrate}$
γ
γ_{actin}
$\gamma \cos(\vartheta)$
$\gamma_{medium/substrate} \cos(\beta)$
β
$\gamma_{cell/substrate}$
$\gamma_{medium/substrate}$

Figure 6.4: Force balance modification using topographical substrate. A) Protrusion on flat substrate: forces are balanced. B) When the orientation of the substrate is modified, the forces become unbalanced due to the change of alignment of the tension between the substrate and the extracellular medium $\gamma_{medium/substrate}$. The effective force is now related to the angle (β) between the flat substrate and the slope: $\gamma_{medium/substrate} \cos(\beta)$.

6.3 Effect of substrate topography on cell behavior and switch distribution

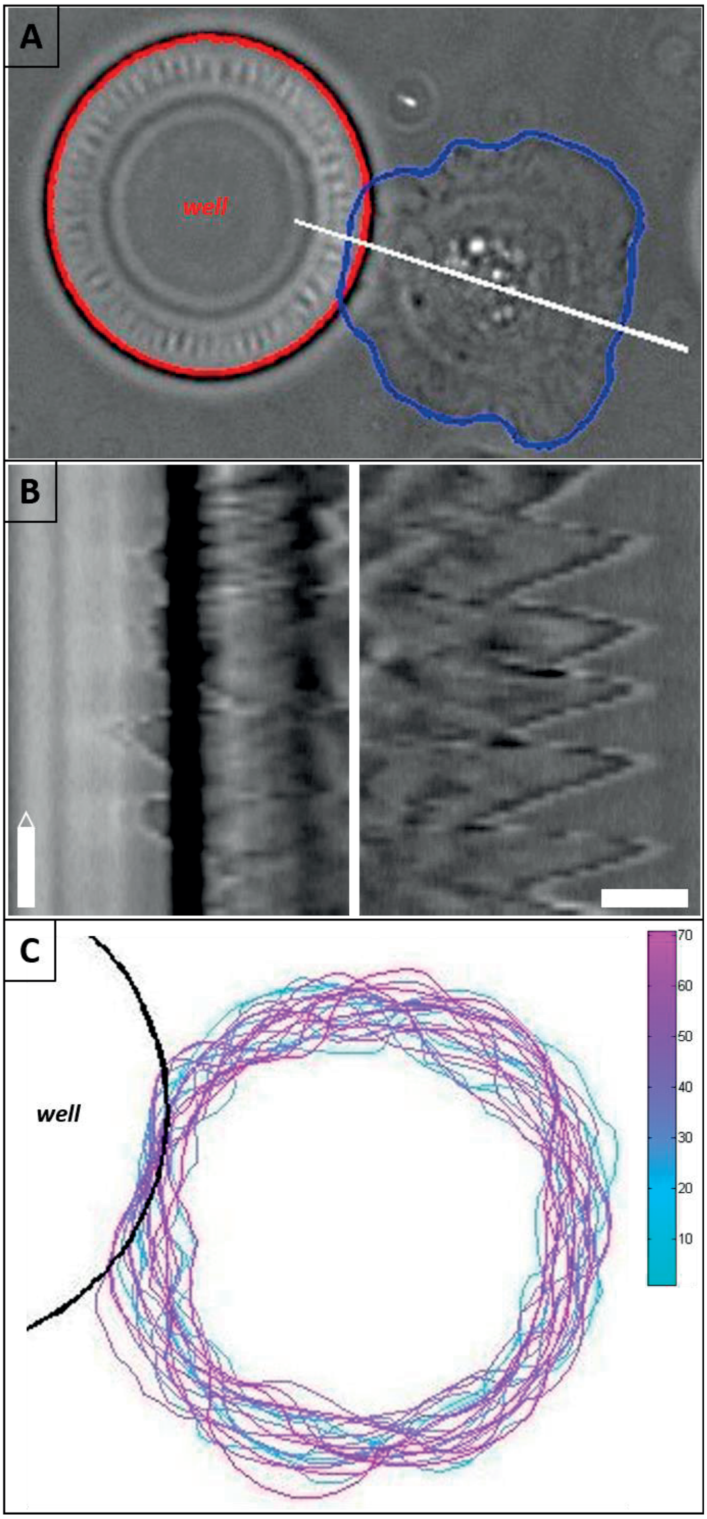

Figure 6.5: Cell fluctuation near topographic feature. A) Contour of the well (*red*) and contour of the cell (*blue*). B) Kymograph are taken along the white line (A) near the feature (*left*) and at the opposite side of the cell (*right*). C) Overlap of cell contours near the feature (black line). Colorbar correspond to the frame number (interval of 10 seconds between contours). Scale bar = 5 µm; time scale bar = 2 min.

We used photolithography and silicon molding to manufacture substrates with topographic features in the form of round hills or wells of the diameter of 50 µm and height or depth around 7-8 µm spaced by 50 µm (see Materials and Methods). We observed that substrate topography affected both polarizing and migrating cells. During polarization, it appeared that fluctuating edges of the cells could not cross the boundaries of substrate features. Superimposition of cell contours revealed that cell edge often paused at or near the boundary or crossed the boundary just for a very short distance before returning to it (fig 6.5). This behavior is similar to pinning as described for liquid droplets when the droplet edge is attracted to the boundary. To quantify the influence of the topographic feature on the occurrence of switches, we compared the number of switches per unit length of the cell edge near the feature and in the rest of the cell (see Materials and Methods). Consistent with the fact that the cell edge paused near the boundary, we have found approximately 1.5 times less switches of both types near the feature than in the rest of the cell edge.

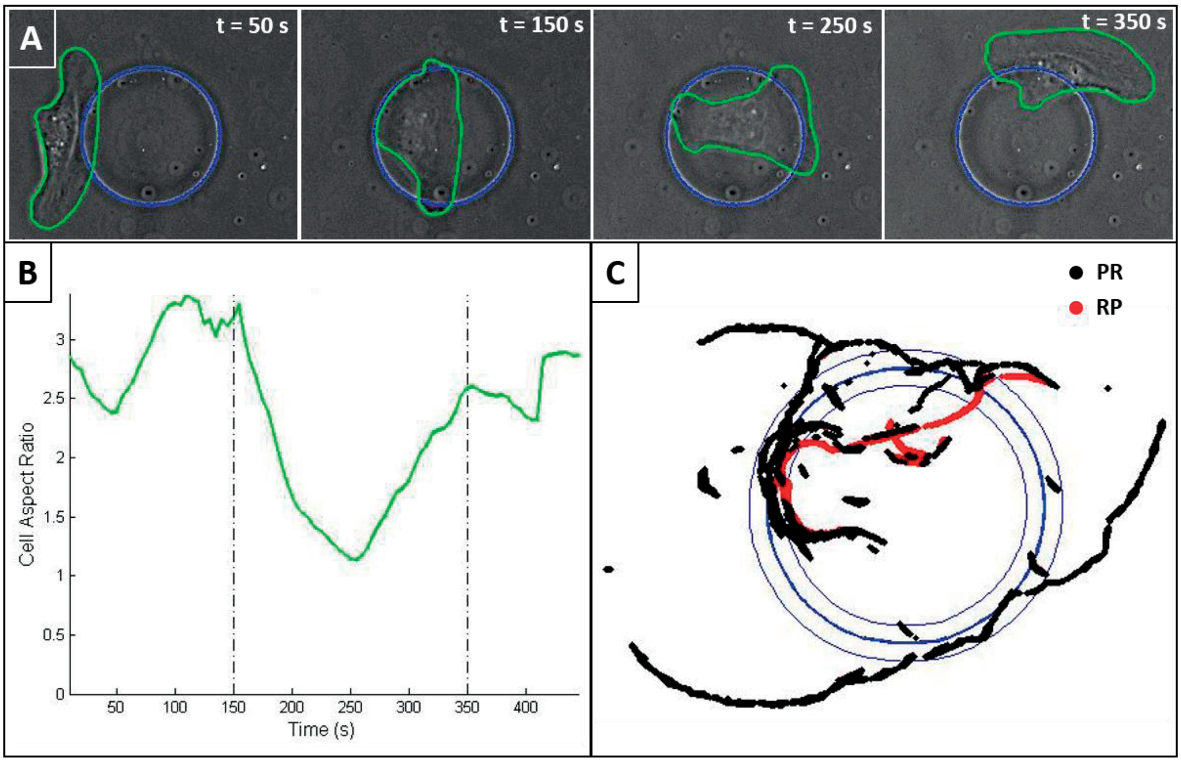

Figure 6.6: Polarized cell on topographic feature. A) Contour of the hill (*blue*) and contour of the cell (*red*). The shape of the migrating cell changes when it reaches the feature. B) Aspect ratio of the cell in function of time. The vertical lines delimit the time when the cell is on the hill. C) Mapping of protrusion to retraction (PR, *black*) and retraction to protrusion (PR, *red*) on the hill (blue lines). In order to quantify the number of switches per unit length of the cell edge near the feature and in the rest of the cell, the contour of the hill is enlarged and shrunk to define a region of interest around the feature. Diameter of the feature: 50 µm.

The cells that were already migrating were able to cross the feature boundaries without significant delay, but during crossing they changed the shape and generated new protrusions so that extremities of the cell often coincided with the boundary of the feature (fig 6.6.A and B). This suggested that protrusion-retraction switches that in migrating cells are localized at lateral extremities tended to coincide with the feature boundary. Switches from protrusion to retraction and from retraction to protrusion were both happening on or near the boundary (fig 6.6.C). In this case, approximately two times more of each switch type per unit edge length happened on or near the boundary than in the rest of the cell. Thus substrate features did not induce switches in completely new cell edge positions, but shifted the positions where the switches were already happening. The change of the shape of the cell was also apparent from examination of the dynamics of the cell aspect ratio during feature crossing: the cell adapted its shape to the shape of the substrate feature.

6.4 Conclusion

We found that tridimensional force balance at the cell edge affects the edge behavior. Using three-dimensional substrates, we could, depending on whether the cell was migrating or not, either promote or suppress switches at the sites where the substrate angle changed. We have also observed that tridimensional shape of the cell edge changed during natural protrusion-retraction cycles: the contact angle between the apical cell surface and the substrate decreased during protrusion and increased during retraction. These results indicate that tridimensional shape could be a part of feedback leading to cell-edge fluctuation and polarization. Note that in the case of substrate angle manipulation, feedback leads to the attraction of the cell edge to the substrate feature, thus suppressing edge fluctuation in the case of polarizing cells. Natural feedback due to the change of angle with the extent of protrusion is not expected to have such an effect, but rather promote edge fluctuation.

7) Conclusions and perspectives

In this thesis, we have investigated the mechanism of cell polarization focusing on cell edge dynamics in relation to traction forces and tridimensional shape of the edge. We have experimentally observed that protrusion-retraction switches universally happen at the maximal distance from the cell center independently of the orientation with respect to the overall motion direction both during polarization and in directionally migrating cells. Computational model demonstrated that this distance sensitivity is sufficient for spontaneous emergence of cell polarity, motion and stable shape in the absence of any external directional cues. We focused on testing two physical hypotheses to explain protrusion-retraction switches and their distance sensitivity: that the switch from protrusion to retraction is triggered by the local increase of the traction force, and/or change of the force balance due to the variation of local tridimensional shape of the edge. We have observed the correlation between distance from the cell center and force magnitude and between the maximal forces and switches, as well as partial disorganization of switches upon inhibition of contractility and induction of switches by external force. This, together with the observation of actin dynamics, suggests that traction force increases with distance from the cell center, leading to detachment of the edge and initiation of retraction at a critical force level. Traction forces may be sufficient for distance-dependent switching, but are likely not the only mechanism. Investigating the second hypothesis about the origin of switches, we have demonstrated that edge shape changes in a predicted manner during protrusion-retraction cycles and that manipulating the force balance at the edge via substrate topography affects the edge dynamics and the distribution of switches, suggesting that switches may also happen in response to the edge shape changes.

Analysis of switches between protrusion and retraction represents a new way to study cell edge dynamics. Previous studies analyzing protrusion-retraction cycles and edge dynamics in polarized cells attempted to relate the rates of protrusion and retraction to various biochemical and biophysical parameters, such as actin assembly rate, small GTPase activity, orientation with respect to the cell motion direction or external gradient, etc. This research yielded important knowledge, but did not sufficiently explore common principles of control over cell edge dynamics, also because edge fluctuations and cell polarization were often studied as two unrelated phenomena. By focusing on a critical event in cell edge dynamics, switch in the direction of edge velocity, we were able to uncover a common denominator between the dynamics of fluctuating and migrating cells: dependence of the switch probability on the distance to the cell center.

Switch dependence on the distance represents a new type of feedback between the local cell dynamics and the cell shape. Surprisingly, this simple feedback was sufficient for spontaneous organization of edge activity into protruding and retracting parts, cell polarization, and for maintenance of this separation and the overall cell shape. Other types of feedback considered in cell polarization mechanism, such as signaling gradients or feedback from directional actin flow, somehow imply that the cell already has a direction or is even already moving, and therefore have trouble explaining initial polarization events needing significant external perturbation to initiate the process. Unlike these hypotheses, our distance-dependent mechanism works irrespective of whether the cell is moving or not and produces stable directionality from the initial completely random state.

The discovery of distance-sensitivity motivates the search for underlying mechanisms. Cell edge does not have a local capacity to measure the distance directly, it should be assisted by a kind of ruler, or a read-out parameter related to the distance. We focused on physical parameters that could be related to the distance, because, in any case, the switch from protrusion to retraction is ultimately a mechanical and physical event, and also because actin dynamics during switch suggested a sudden change in force balance.

We have measured traction forces exerted on the substrate during fluctuation and polarization and found a significant correlation between force and distance and also between forces and local protrusion-retraction switches. Previously, traction forces were measured with high precision and correlated to the local focal adhesion dynamics and to the durotaxis capacity in strongly adherent cells generating large forces (Plotnikov et al., 2012), but the relationship to the protrusion-retraction dynamics (which is not highly pronounced in these cells) was not investigated. Another study (Ji et al., 2008) inferred internal forces in cell edge fluctuation from actin dynamics, but the forces were not measured directly. Still another recent study (Barnhart et al., 2015) related overall traction force fluctuation to motility initiation, but the forces in the individual protrusion-retraction cycles were not documented. Our study is the first, to our knowledge, to directly follow traction force evolution during protrusion-retraction and the entire polarization process. Discovered relationship between force and linear distance is not trivial; previous study instead suggested that the traction forces scale with the cell area (Oakes et al., 2014). However, other studies observed force-distance correlation by looking at the cell in fixed geometries on patterned substrate (Rape et al., 2011) and proposed a dynamic force-distance relationship based on force-probing in microplate assay (Étienne et al., 2015). Our study suggests that in the context of cell polarization force-distance relationship may mediate self-organization of edge activity and the emergence of stable migratory shape.

Another part of force balance at the dynamic cell edge concerns membrane tension and actin polymerization forces. The magnitude of resistance from membrane to actin assembly is considered by most researchers as double membrane tension (Keren, 2011) (Lieber et al., 2013), to account for apical and ventral membrane. This does not provide any freedom for local modulation of membrane resistance or potential relationship between resistance and distance. In contrast, we consider membrane tension as a part of a tridimensional force balance at the edge (Gabella et al.), meaning that resistance could be modulated through the edge shape, e.g. propagation and flattening of protrusion would increase resistance, resulting in a feedback from the distance. We have observed such flattening, and also have modulated edge dynamics via three-dimensional geometry of the substrate. Three-dimensional force balance in the context of cell spreading, overall shape and traction forces was considered in several recent studies ((Burnette et al., 2014) (Fouchard et al., 2014) (Álvarez-González et al., 2015)) underscoring the emergent importance of the third dimension in cell mechanics. It remains to be determined to what extent this three-dimensional force balance is contributed by membrane tension and actomyosin-dependent traction.

Our study thus elucidated novel important principles helping to understand the mechanism of cell polarization, but also posed intriguing questions for the follow-up research. Distance-sensing principle works in keratocyte cell geometry characterized by extension orthogonal to the motion direction, but it remains to be investigated how it could be adapted to other geometries and to what extend it indeed works in other cell types. This would require both the analysis of the edge dynamics and the computational work. Preliminary computational results (Franck Raynaud, personal communication) suggest that by modifying the definition of the center in the computational model, many different types of cell geometry could be reproduced.

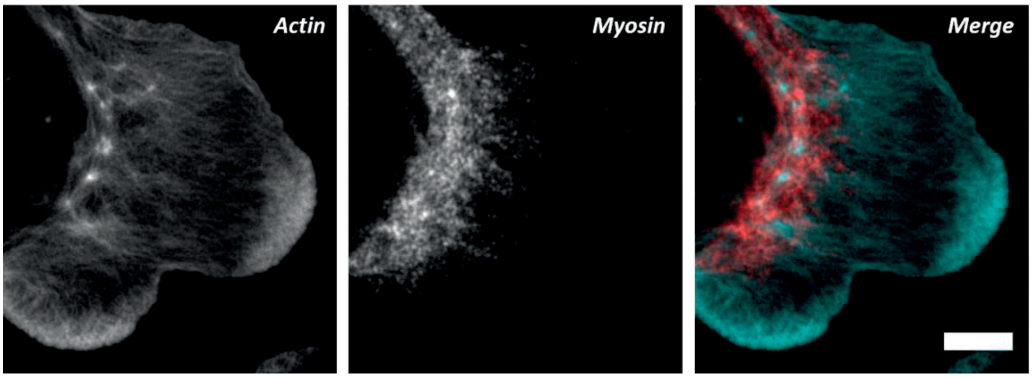

Figure 7.1: Actomyosin organization in cell protrusion. Scale bar = 5 µm.

Another intriguing problem is why the traction forces indeed scale with the distance. Telescopic collapse of actin network during retraction suggests contractile elements connected in series, but in this case force output would not depend on the number of elements, and, consequently, the length of the assembly, but only on the force output of one element. To understand how telescopic contraction is combined with length-dependent force output, it would be necessary to investigate the structure and dynamic rearrangement of actin and myosin II in relation to the traction force during protrusion retraction cycles. Figure 7.1 presents a static high-resolution fluorescent image of actin and myosin distribution in protruding region of the cell during fluctuation. This gives a sense of possible configurations that could be expected, like linear chains of myosin assemblies along the protrusion axis and actin filaments criss-crossing these chains, hinting on a possible telescopic collapse by filament alignment parallel to the edge.

Finally, cytoskeletal dynamics and traction force measurement could be combined with three-dimensional substrates and dynamic measurement of the cell vertical profile to evaluate the contribution of tridimensional shape to the force balance and protrusion-retraction switches.

Bibliography

Alberts B., A.J., J. Lewis, M. Raff, K. Roberts, and P. Walter (2002). Molecular Biology of the Cell. 4th ed. Garland Science.

Allard, J., and Mogilner, A. (2013). Traveling waves in actin dynamics and cell motility. Current opinion in cell biology *25*, 107-115.

Álvarez-González, B., Meili, R., Bastounis, E., Firtel, Richard A., Lasheras, Juan C., and del Álamo, Juan C. (2015). Three-Dimensional Balance of Cortical Tension and Axial Contractility Enables Fast Amoeboid Migration. Biophysical Journal *108*, 821-832.

Ambühl, M.E., Brepsant, C., Meister, J.J., Verkhovsky, A.B., and Sbalzarini, I.F. (2012). High-resolution cell outline segmentation and tracking from phase-contrast microscopy images. Journal of Microscopy *245*, 161-170.

Anderson, K.I., and Cross, R. (2000). Contact dynamics during keratocyte motility. Current Biology *10*, 253-260.

Barnhart, E., Lee, K.-C., Allen, G.M., Theriot, J.A., and Mogilner, A. (2015). Balance between cell−substrate adhesion and myosin contraction determines the frequency of motility initiation in fish keratocytes. Proceedings of the National Academy of Sciences *112*, 5045-5050.

Barnhart, E.L., Lee, K.-C., Keren, K., Mogilner, A., and Theriot, J.A. (2011). An Adhesion-Dependent Switch between Mechanisms That Determine Motile Cell Shape. PLoS Biol *9*, e1001059.

Bear, J.E., Rawls, J.F., and Saxe, C.L. (1998). SCAR, a WASP-related Protein, Isolated as a Suppressor of Receptor Defects in Late Dictyostelium Development. The Journal of Cell Biology *142*, 1325-1335.

Beningo, K.A., and Wang, Y.-L. (2002). Flexible substrata for the detection of cellular traction forces. Trends in Cell Biology *12*, 79-84.

Bottier, C., Gabella, C., Vianay, B., Buscemi, L., Sbalzarini, I.F., Meister, J.-J., and Verkhovsky, A.B. (2011). Dynamic measurement of the height and volume of migrating cells by a novel fluorescence microscopy technique. Lab on a Chip *11*, 3855-3863.

Boulant, S., Kural, C., Zeeh, J.-C., Ubelmann, F., and Kirchhausen, T. (2011). Actin dynamics counteract membrane tension during clathrin-mediated endocytosis. Nat Cell Biol *13*, 1124-1131.

Burnette, D.T., Shao, L., Ott, C., Pasapera, A.M., Fischer, R.S., Baird, M.A., Der Loughian, C., Delanoe-Ayari, H., Paszek, M.J., Davidson, M.W.*, et al.* (2014). A contractile and counterbalancing adhesion system controls the 3D shape of crawling cells. The Journal of Cell Biology *205*, 83-96.

Burton, K., and Taylor, D.L. (1997). Traction forces of cytokinesis measured with optically modified elastic substrata. Nature *385*, 450-454.

Carlier, M.-F., Pernier, J., and Avvaru, B.S. (2013). Control of actin filament dynamics at barbed ends by WH2 domains: From capping to permissive and processive assembly. Cytoskeleton *70*, 540-549.

Carlier, M.-F., Wiesner, S., Le Clainche, C., and Pantaloni, D. (2003). Actin-based motility as a self-organized system: mechanism and reconstitution in vitro. Comptes Rendus Biologies *326*, 161-170.

Carlier, M.F., Jean, C., Rieger, K.J., Lenfant, M., and Pantaloni, D. (1993). Modulation of the interaction between G-actin and thymosin beta 4 by the ATP/ADP ratio: possible implication in the regulation of actin dynamics. Proceedings of the National Academy of Sciences of the United States of America *90*, 5034-5038.

Carlier, M.F.a.D.P. (1986). Direct evidence for ADP-Pi-F-actin as the major intermediate in ATP-actin polymerization. Rate of dissociation of Pi from actin filaments. Biochemistry *25*, 7789-7792.

Casella, J.F., Maack, D.J., and Lin, S. (1986). Purification and initial characterization of a protein from skeletal muscle that caps the barbed ends of actin filaments. Journal of Biological Chemistry *261*, 10915-10921.

Castrillon, D.H., and Wasserman, S.A. (1994). Diaphanous is required for cytokinesis in Drosophila and shares domains of similarity with the products of the limb deformity gene. Development *120*, 3367-3377.

Chesarone, M.A., DuPage, A.G., and Goode, B.L. (2010). Unleashing formins to remodel the actin and microtubule cytoskeletons. Nat Rev Mol Cell Biol *11*, 62-74.

Cramer, L.P. (2010). Forming the cell rear first: breaking cell symmetry to trigger directed cell migration. Nat Cell Biol *12*, 628-632.

Cramer, L.P. (2013). Mechanism of cell rear retraction in migrating cells. Current Opinion in Cell Biology *25*, 591-599.

Cross, R.A., and McAinsh, A. (2014). Prime movers: the mechanochemistry of mitotic kinesins. Nat Rev Mol Cell Biol *15*, 257-271.

Dayel, M.J., Akin, O., Landeryou, M., Risca, V., Mogilner, A., and Mullins, R.D. (2009). In Silico Reconstitution of Actin-Based Symmetry Breaking and Motility. PLoS Biology *7*, e1000201.

Dembo, M., and Wang, Y. (1999). Stresses at the cell-to-substrate interface during locomotion of fibroblasts. Biophys J *76*, 2307 - 2316.

Derry, J.M.J., Ochs, H.D., and Francke, U. (1994). Isolation of a novel gene mutated in Wiskott-Aldrich syndrome. Cell *78*, 635-644.

Dominguez, R., Freyzon, Y., Trybus, K.M., and Cohen, C. (1998). Crystal Structure of a Vertebrate Smooth Muscle Myosin Motor Domain and Its Complex with the Essential Light Chain: Visualization of the Pre–Power Stroke State. Cell *94*, 559-571.

du Roure, O., Saez, A., Buguin, A., Austin, R.H., Chavrier, P., Siberzan, P., and Ladoux, B. (2005). Force mapping in epithelial cell migration. Proceedings of the National Academy of Sciences of the United States of America *102*, 2390-2395.

Etienne-Manneville, S., and Hall, A. (2002). Rho GTPases in cell biology. Nature *420*, 629-635.

Étienne, J., Fouchard, J., Mitrossilis, D., Bufi, N., Durand-Smet, P., and Asnacios, A. (2015). Cells as liquid motors: Mechanosensitivity emerges from collective dynamics of actomyosin cortex. Proceedings of the National Academy of Sciences *112*, 2740-2745.

Euteneuer, U., and Schliwa, M. (1984). Persistent, directional motility of cells and cytoplasmic fragments in the absence of microtubules. Nature *310*, 58-61.

Fouchard, J., Bimbard, C., Bufi, N., Durand-Smet, P., Proag, A., Richert, A., Cardoso, O., and Asnacios, A. (2014). Three-dimensional cell body shape dictates the onset of traction force generation and growth of focal adhesions. Proceedings of the National Academy of Sciences *111*, 13075-13080.

Fournier, M.F., Sauser, R., Ambrosi, D., Meister, J.-J., and Verkhovsky, A.B. (2010). Force transmission in migrating cells. The Journal of Cell Biology *188*, 287-297.

Fujiwara, I., Takahashi, S., Tadakuma, H., Funatsu, T., and Ishiwata, S.i. (2002). Microscopic analysis of polymerization dynamics with individual actin filaments. Nat Cell Biol *4*, 666-673.

Gabella, C., Bertseva, E., Bottier, C., Piacentini, N., Bornert, A., Jeney, S., Forró, L., Sbalzarini, Ivo F., Meister, J.-J., and Verkhovsky, Alexander B. (2014). Contact Angle at the Leading Edge Controls Cell Protrusion Rate. Current Biology *24*, 1126-1132.

Gardel, M., Sabass, B., Ji, L., Danuser, G., Schwarz, U., and Waterman, C. (2008). Traction stress in focal adhesions correlates biphasically with actin retrograde flow speed. J Cell Biol *183*, 999 - 1005.

Giannone, G., Dubin-Thaler, B.J., Rossier, O., Cai, Y., Chaga, O., Jiang, G., Beaver, W., Döbereiner, H.-G., Freund, Y., Borisy, G*., et al.* (2007). Lamellipodial Actin Mechanically Links Myosin Activity with Adhesion-Site Formation. Cell *128*, 561-575.

Gremm, D., and Wegner, A. (2000). Gelsolin as a calcium-regulated actin filament-capping protein. European Journal of Biochemistry *267*, 4339-4345.

Grimm, H.P., Verkhovsky, A.B., Mogilner, A., and Meister, J.-J. (2003). Analysis of actin dynamics at the leading edge of crawling cells: implications for the shape of keratocyte lamellipodia. European Biophysics Journal *32*, 563-577.

Harris, A.K., Stopak, D., and Wild, P. (1981). Fibroblast traction as a mechanism for collagen morphogenesis. Nature *290*, 249-251.

Higgs, H.N. (2005). Formin proteins: a domain-based approach. Trends in Biochemical Sciences *30*, 342-353.

Hoffmann, M., and Schwarz, U. (2013). A kinetic model for RNA-interference of focal adhesions. BMC Systems Biology *7*, 2.

Houk, Andrew R., Jilkine, A., Mejean, Cecile O., Boltyanskiy, R., Dufresne, Eric R., Angenent, Sigurd B., Altschuler, Steven J., Wu, Lani F., and Weiner, Orion D. (2012). Membrane Tension Maintains Cell Polarity by Confining Signals to the Leading Edge during Neutrophil Migration. Cell *148*, 175-188.

Humphries, M.J. (2000). Integrin Structure. Biochemical Society Transactions *28*, 311-340.

Isenberg, G., Aebi, U., and Pollard, T.D. (1980). An actin-binding protein from Acanthamoeba regulates actin filament polymerization and interactions. Nature *288*, 455-459.

Ji, L., Lim, J., and Danuser, G. (2008). Fluctuations of intracellular forces during cell protrusion. Nat Cell Biol *10*, 1393-1400.

Kaksonen, M., Toret, C.P., and Drubin, D.G. (2006). Harnessing actin dynamics for clathrin-mediated endocytosis. Nat Rev Mol Cell Biol *7*, 404-414.

Kalinin, Y.V., Berejnov, V., and Thorne, R.E. (2009). Contact Line Pinning by Microfabricated Patterns: Effects of Microscale Topography. Langmuir *25*, 5391-5397.

Kardon, J.R., and Vale, R.D. (2009). Regulators of the cytoplasmic dynein motor. Nat Rev Mol Cell Biol *10*, 854-865.

Keren, K. (2011). Cell motility: the integrating role of the plasma membrane. European Biophysics Journal *40*, 1013-1027.

Keren, K., Pincus, Z., Allen, G.M., Barnhart, E.L., Marriott, G., Mogilner, A., and Theriot, J.A. (2008). Mechanism of shape determination in motile cells. Nature *453*, 475-480.

Kim, S.A., Tai, C.-Y., Mok, L.-P., Mosser, E.A., and Schuman, E.M. (2011). Calcium-dependent dynamics of cadherin interactions at cell–cell junctions. Proceedings of the National Academy of Sciences *108*, 9857-9862.

Kozlov, M.M., and Mogilner, A. (2007). Model of Polarization and Bistability of Cell Fragments. Biophysical Journal *93*, 3811-3819.

Lee, J. (2007). The Use of Gelatin Substrates for Traction Force Microscopy in Rapidly Moving Cells. In Methods in Cell Biology (Academic Press), pp. 295-312.

Lee, J., Ishihara, A., Theriot, J.A., and Jacobson, K. (1993). Principles of locomotion for simple-shaped cells. Nature *362*, 167-171.

Lee, J., Leonard, M., Oliver, T., Ishihara, A., and Jacobson, K. (1994). Traction forces generated by locomoting keratocytes. The Journal of Cell Biology *127*, 1957-1964.

Lieber, Arnon D., Schweitzer, Y., Kozlov, Michael M., and Keren, K. (2015). Front-to-Rear Membrane Tension Gradient in Rapidly Moving Cells. Biophysical Journal *108*, 1599-1603.

Lieber, Arnon D., Yehudai-Resheff, S., Barnhart, Erin L., Theriot, Julie A., and Keren, K. (2013). Membrane Tension in Rapidly Moving Cells Is Determined by Cytoskeletal Forces. Current Biology *23*, 1409-1417.

Lo, C.-M., Wang, H.-B., Dembo, M., and Wang, Y.-l. (2000). Cell Movement Is Guided by the Rigidity of the Substrate. Biophysical Journal *79*, 144-152.

Lock, J.G., Wehrle-Haller, B., and Strömblad, S. (2008). Cell–matrix adhesion complexes: Master control machinery of cell migration. Seminars in Cancer Biology *18*, 65-76.

Ma, L., Rohatgi, R., and Kirschner, M.W. (1998). The Arp2/3 complex mediates actin polymerization induced by the small GTP-binding protein Cdc42. Proceedings of the National Academy of Sciences of the United States of America *95*, 15362-15367.

Mabuchi, I. (1983). An actin-depolymerizing protein (depactin) from starfish oocytes: properties and interaction with actin. The Journal of Cell Biology *97*, 1612-1621.

Machesky, L.M., Atkinson, S.J., Ampe, C., Vandekerckhove, J., and Pollard, T.D. (1994). Purification of a cortical complex containing two unconventional actins from Acanthamoeba by affinity chromatography on profilin-agarose. The Journal of Cell Biology *127*, 107-115.

Machesky, L.M., and Insall, R.H. (1999). Signaling to Actin Dynamics. The Journal of Cell Biology *146*, 267-272.

Maciver, S.K. (1998). How ADF/cofilin depolymerizes actin filaments. Current Opinion in Cell Biology *10*, 140-144.

Maiuri, P., Rupprecht, J.-F., Wieser, S., Ruprecht, V., Bénichou, O., Carpi, N., Coppey, M., De Beco, S., Gov, N., Heisenberg, C.-P*., et al.* (2015). Actin Flows Mediate a Universal Coupling between Cell Speed and Cell Persistence. Cell *161*, 374-386.

Marcy, Y., Prost, J., Carlier, M.-F., and Sykes, C. (2004). Forces generated during actin-based propulsion: A direct measurement by micromanipulation. Proceedings of the National Academy of Sciences of the United States of America *101*, 5992-5997.

Marée, A.F.M., Jilkine, A., Dawes, A., Grieneisen, V.A., and Edelstein-Keshet, L. (2006). Polarization and Movement of Keratocytes: A Multiscale Modelling Approach. Bulletin of Mathematical Biology *68*, 1169-1211.

Markey, F., Lindberg, U., and Eriksson, L. (1978). Human platelets contain profilin, a potential regulator of actin polymerisability. FEBS Letters *88*, 75-79.

Martin, S.G. (2009). Microtubule-dependent cell morphogenesis in the fission yeast. Trends in Cell Biology *19*, 447-454.

Mazzarello, P. (1999). A unifying concept: the history of cell theory. Nat Cell Biol *1*, E13-E15.

Miki, H., Miura, K., and Takenawa, T. (1996). N-WASP, a novel actin-depolymerizing protein, regulates the cortical cytoskeletal rearrangement in a PIP2-dependent manner downstream of tyrosine kinases. The EMBO Journal *15*, 5326-5335.

Miki, H., Suetsugu, S., and Takenawa, T. (1998). WAVE, a novel WASP-family protein involved in actin reorganization induced by Rac. The EMBO Journal *17*, 6932-6941.

Mockrin, S.C., and Korn, E.D. (1980). Acanthamoeba profilin interacts with G-actin to increase the rate of exchange of actin-bound adenosine 5'-triphosphate. Biochemistry *19*, 5359-5362.

Mogilner, A., and Oster, G. (1996). Cell motility driven by actin polymerization. Biophysical Journal *71*, 3030-3045.

Moon, A.G., and Tranquillo, R.T. (1993). Fibroblast-populated collagen microsphere assay of cell traction force: Part 1. Continuum model. AIChE Journal *39*, 163-177.

Mostowy, S., and Cossart, P. (2012). Septins: the fourth component of the cytoskeleton. Nat Rev Mol Cell Biol *13*, 183-194.

Mseka, T., and Cramer, Louise P. (2011). Actin Depolymerization-Based Force Retracts the Cell Rear in Polarizing and Migrating Cells. Current Biology *21*, 2085-2091.

Mullins, R.D., Heuser, J.A., and Pollard, T.D. (1998). The interaction of Arp2/3 complex with actin: Nucleation, high affinity pointed end capping, and formation of branching networks of filaments. Proceedings of the National Academy of Sciences of the United States of America *95*, 6181-6186.

Mullins, R.D., and Pollard, T.D. (1999). Rho-family GTPases require the Arp2/3 complex to stimulate actin polymerizationin Acanthamoeba extracts. Current Biology *9*, 405-415.

Oakes, Patrick W., Banerjee, S., Marchetti, M.C., and Gardel, Margaret L. (2014). Geometry Regulates Traction Stresses in Adherent Cells. Biophysical Journal *107*, 825-833.

Oliver, T., Dembo, M., and Jacobson, K. (1999). Separation of Propulsive and Adhesive Traction Stresses in Locomoting Keratocytes. The Journal of Cell Biology *145*, 589-604.

Park, J.S., Chu, J.S., Tsou, A.D., Diop, R., Tang, Z., Wang, A., and Li, S. (2011). The Effect of Matrix Stiffness on the Differentiation of Mesenchymal Stem Cells in Response to TGF-β. Biomaterials *32*, 3921-3930.

Peskin, C.S., Odell, G.M., and Oster, G.F. (1993). Cellular motions and thermal fluctuations: the Brownian ratchet. Biophysical Journal *65*, 316-324.

Picone, R., Ren, X., Ivanovitch, K.D., Clarke, J.D.W., McKendry, R.A., and Baum, B. (2010). A Polarised Population of Dynamic Microtubules Mediates Homeostatic Length Control in Animal Cells. PLoS Biol *8*, e1000542.

Plotnikov, Sergey V., Pasapera, Ana M., Sabass, B., and Waterman, Clare M. (2012). Force Fluctuations within Focal Adhesions Mediate ECM-Rigidity Sensing to Guide Directed Cell Migration. Cell *151*, 1513-1527.

Pollard, T.D. (2003). The cytoskeleton, cellular motility and the reductionist agenda. Nature *422*, 741-745.

Pollard, T.D., and Borisy, G.G. (2003). Cellular Motility Driven by Assembly and Disassembly of Actin Filaments. Cell *112*, 453-465.

Ponti, A., Machacek, M., Gupton, S., Waterman-Storer, C., and Danuser, G. (2004). Two distinct actin networks drive the protrusion of migrating cells. Science *305*, 1782 - 1786.

Porter, M.E. (1996). Axonemal dyneins: assembly, organization, and regulation. Current Opinion in Cell Biology *8*, 10-17.

Quintin, S., Gally, C., and Labouesse, M. (2008). Epithelial morphogenesis in embryos: asymmetries, motors and brakes. Trends in Genetics *24*, 221-230.

Raaijmakers, J.A., and Medema, R.H. (2014). Function and regulation of dynein in mitotic chromosome segregation. Chromosoma *123*, 407-422.

Raftopoulou, M., and Hall, A. (2004). Cell migration: Rho GTPases lead the way. Developmental Biology *265*, 23-32.

Rape, A.D., Guo, W.-h., and Wang, Y.-l. (2011). The regulation of traction force in relation to cell shape and focal adhesions. Biomaterials *32*, 2043-2051.

Ratheesh, A., and Yap, A.S. (2012). A bigger picture: classical cadherins and the dynamic actin cytoskeleton. Nat Rev Mol Cell Biol *13*, 673-679.

Raynaud, F., Ambuhl, M.E., Gabella, C., Bornert, A., Sbalzarini, I.F., Meister, J.-J., and Verkhovsky, A.B. (2016). Minimal model for spontaneous cell polarization and edge activity in oscillating, rotating and migrating cells. Nat Phys *advance online publication*.

Ridley, A.J. (1994). Membrane ruffling and signal transduction. BioEssays *16*, 321-327.

Ryan, G.L., Watanabe, N., and Vavylonis, D. (2012). A review of models of fluctuating protrusion and retraction patterns at the leading edge of motile cells. Cytoskeleton *69*, 195-206.

Safer, D., Golla, R., and Nachmias, V.T. (1990). Isolation of a 5-kilodalton actin-sequestering peptide from human blood platelets. Proceedings of the National Academy of Sciences of the United States of America *87*, 2536-2540.

Schaub, S., Meister, J.-J., and Verkhovsky, A.B. (2007). Analysis of actin filament network organization in lamellipodia by comparing experimental and simulated images. Journal of Cell Science *120*, 1491-1500.

Servant, G., Weiner, O.D., Herzmark, P., Balla, T., Sedat, J.W., and Bourne, H.R. (2000). Polarization of Chemoattractant Receptor Signaling During Neutrophil Chemotaxis. Science *287*, 1037-1040.

Svitkina, T.M., and Borisy, G.G. (1999). Arp2/3 Complex and Actin Depolymerizing Factor/Cofilin in Dendritic Organization and Treadmilling of Actin Filament Array in Lamellipodia. The Journal of Cell Biology *145*, 1009-1026.

Svitkina, T.M., Verkhovsky, A.B., McQuade, K.M., and Borisy, G.G. (1997). Analysis of the Actin–Myosin II System in Fish Epidermal Keratocytes: Mechanism of Cell Body Translocation. The Journal of Cell Biology *139*, 397-415.

Symons, M., Derry, J.M.J., Karlak, B., Jiang, S., Lemahieu, V., McCormick, F., Francke, U., and Abo, A. (1996). Wiskott–Aldrich Syndrome Protein, a Novel Effector for the GTPase CDC42Hs, Is Implicated in Actin Polymerization. Cell *84*, 723-734.

Toyoshima, Y.Y., Kron, S.J., and Spudich, J.A. (1990). The myosin step size: measurement of the unit displacement per ATP hydrolyzed in an in vitro assay. Proceedings of the National Academy of Sciences of the United States of America *87*, 7130-7134.

Tse, J.R., and Engler, A.J. (2001). Preparation of Hydrogel Substrates with Tunable Mechanical Properties. In Current Protocols in Cell Biology (John Wiley & Sons, Inc.).

Tseng, Q., Wang, I., Duchemin-Pelletier, E., Azioune, A., Carpi, N., Gao, J., Filhol, O., Piel, M., Thery, M., and Balland, M. (2011). A new micropatterning method of soft substrates reveals that different tumorigenic signals can promote or reduce cell contraction levels. Lab on a Chip *11*, 2231-2240.

Vallotton, P., Danuser, G., Bohnet, S., Meister, J.-J., and Verkhovsky, A.B. (2005). Tracking Retrograde Flow in Keratocytes: News from the Front. Molecular Biology of the Cell *16*, 1223-1231.

Verkhovsky, A.B. (2015). The mechanisms of spatial and temporal patterning of cell-edge dynamics. Current Opinion in Cell Biology *36*, 113-121.

Verkhovsky, A.B., Svitkina, T.M., and Borisy, G.G. (1997). Polarity sorting of actin filaments in cytochalasin-treated fibroblasts. Journal of Cell Science *110*, 1693-1704.

Verkhovsky, A.B., Svitkina, T.M., and Borisy, G.G. (1999). Self-polarization and directional motility of cytoplasm. Current Biology *9*, 11-S11.

Weber, A., Pennise, C.R., Babcock, G.G., and Fowler, V.M. (1994). Tropomodulin caps the pointed ends of actin filaments. The Journal of Cell Biology *127*, 1627-1635.

Wegner, A. (1976). Head to tail polymerization of actin. Journal of Molecular Biology *108*, 139-150.

Wein, R. (2015). CGAL User and Reference Manual 4.7 edn. CGAL Editorial Board.

Yam, P.T., Wilson, C.A., Ji, L., Hebert, B., Barnhart, E.L., Dye, N.A., Wiseman, P.W., Danuser, G., and Theriot, J.A. (2007). Actin–myosin network reorganization breaks symmetry at the cell rear to spontaneously initiate polarized cell motility. The Journal of Cell Biology *178*, 1207-1221.

Zaidel-Bar, R., Cohen, M., Addadi, L., and Geiger, B. (2004). Hierarchical assembly of cell–matrix adhesion complexes. Biochemical Society Transactions *32*, 416-420.

Zhang, K., and Chen, J. (2012). The regulation of integrin function by divalent cations. Cell Adhesion & Migration *6*, 20-29.

Zigmond, S.H. (1996). Signal transduction and actin filament organization. Current Opinion in Cell Biology *8*, 66-73.

Zigmond, S.H., Evangelista, M., Boone, C., Yang, C., Dar, A.C., Sicheri, F., Forkey, J., and Pring, M. (2003). Formin Leaky Cap Allows Elongation in the Presence of Tight Capping Proteins. Current Biology *13*, 1820-1823.

BORNERT Alicia
Status: single
Birth date: July 23th 1988
Nationality: French
Phone: (FR) +33 630 081 972

Route de la Maladière 8
1022 Chavannes-Près-Renens
(Switzerland)
alicia.bornert67@gmail.com
(CH) +41 766 084 221

Education

2012/2016	**Ph.D. candidate in Biotechnologies and Bioengineering** Ecole Polytechnique Fédérale de Lausanne (EPFL, Switzerland) Supervisor: Dr A.B. Verkhovsky Title: Protrusion-retraction switches and traction forces in spontaneous cell polarization
2009/2011	**Master in Cellular and Molecular Physiopathology** Medicine Faculty, University of Strasbourg (France)
2007/2009	**Bachelor in Cellular Biology and Physiology** University of Strasbourg (France)
2006	**High school certificate in Science**

Work experiences

2010/2011	**Master 2 internship, 1 year:** Laboratory of Cell Physics Institut de Science et d'Ingénierie Supramoléculaires (ISIS), and Institut de Génétique et de Biologie Moléculaire et Cellulaire (IGBMC), Strasbourg Supervisor: Dr Daniel RIVELINE Title: Roles of the Rho GTPases in directional cell motion.
2010	**Master 1 internship, 2 weeks:** Laboratory of Development and Physiopathology of the Intestine and Pancreas INSERM U682 Hautepierre, Strasbourg (France)
2009	**Master 1 internship, 2 weeks:** Laboratory of Cell Physics ISIS/IGBMC, Strasbourg (France)

Publications

- A. Bornert, N. Piacentini, F. Raynaud & A.B. Verkhovsky. *Protrusion-retraction transitions during cell polarization are induced by traction forces.* In preparation

- A. Bornert*, D. Caballero*, R. Voituriez & D. Riveline. *Protrusion fluctuations dynamics control long-term cell motion.* In preparation

- F. Raynaud, M. Ambühl, C. Gabella, A. Bornert, I.F. Sbalzarni, J.-J. Meister & A.B. Verkhovsky. *Minimal model for spontaneous cell polarization and edge activity in oscillating, rotating and migrating cells*. Nat Phys, 2016, *doi:10.1038/nphys3615*.

- C. Gabella, E. Bertseva, C. Bottier, N. Piacentini, A. Bornert, S. Jeney, L. Forrò, I.F. Sbalzarini, J.-J. Meister & A.B. Verkhovsky. *Contact Angle at the Leading Edge Controls Cell Protrusion Rate*. Current Biology, vol.24, issue 10, p.1126-1132, 2014.

- A. Bornert, N. Piacentini & A.B. Verkhovsky. *Traction force dynamics during cell polarization*. Poster presentation. The 2013 American Society for Cell Biology (ASCB) Annual Meeting, New Orleans, USA, December 14th - 18th 2013.

Skills

Biology: cell culture, immunostaining, transfection, pulldown assay, western blot
Microscopy: fluorescence and phase contrast (live cell imaging, time lapse), SEM, TFM
Microfabrication: silicon master, soft lithography, microcontact printing, surface functionalization
Informatics: - Common software: Microsoft Office, OpenOffice, Windows
- Analysis software: Matlab, ImageJ, Metamorph, VisiView, Origin

---

Others

Teaching Biology (2012/2014 Bachelor semester 1-2)
Genetic and genomic (2012/2013 Bachelor semester 5)
Languages French (mother tongue)
English (good skills, both written and oral)
Italian (good skills, both written and oral)
German (basic)
Leisure activities Sport (basket-ball, fitness), music (piano)
Diploma European first aid certificate obtained in 2004